

R-ED 11122

SCOUT
SYSTEM DESIGN
REPORT
SUPPLEMENT I
BASIC DATA

SCOUT PROJECT GROUP

PROPERTY FORM 602

U65-86047
ACCESSION NUMBER

140
THRU

1328
PAGES

NASA CR OR TMX OR AD NUMBER

CATEGORY

Honeywell
 Aeronautical Division

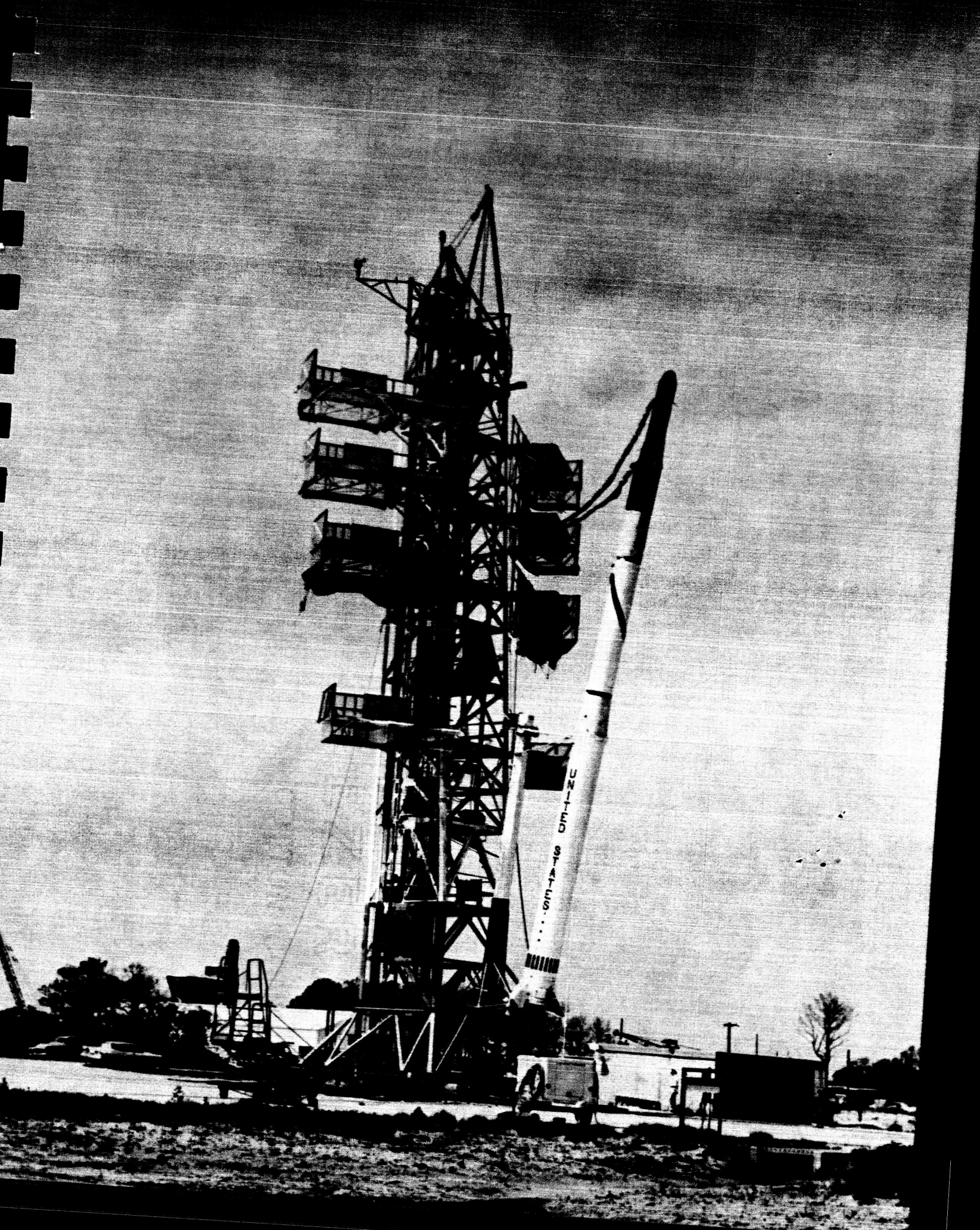
LOS ANGELES, CALIFORNIA

FOREWORD

This document is submitted to Chance Vought Corporation as a requirement of contract No. CV 300. This document constitutes the first of two supplements to the "SCOUT System Design Report" (R-ED 11117) published 3 January 1961. The previously published report, R-ED 11117, presented the methods and results of the system design of the SCOUT controls for the first three vehicles.

TABLE OF CONTENTS

	Page No.
FOREWORD	i
INTRODUCTION	x
I AERODYNAMICS OF FIRST THREE VEHICLES (20-Inch Diameter Fourth Stage)	I-1
II AERODYNAMICS OF FOURTH VEHICLE (25.7-Inch Diameter Fourth Stage and Nose Cone)	II-1
III WEIGHTS AND INERTIA OF FIRST THREE VEHICLES (20-Inch Diameter Fourth Stage)	III-1
IV WEIGHTS AND INERTIA OF FOURTH VEHICLE (25.7-Inch Diameter Fourth Stage)	IV-1
V STRUCTURE OF FIRST THREE VEHICLES (20-Inch Diameter Fourth Stage)	V-1
VI STRUCTURE OF FOURTH VEHICLE (25.7-Inch Diameter Fourth Stage)	VI-1
VII ENGINE THRUST	VII-1
VIII CONTROL MEMBERS	VIII-1
IX FLIGHT PROFILE	IX-1



LIST OF ILLUSTRATIONS

Figure No.		Page No.
i-1	SCOUT Body Dimensions and Nomenclature	-xii-
I-1	First-Step Rigid-Body Lift Coefficient Vs Mach Number	I-2
I-2	First-Step Zero-Lift Drag Coefficient Vs Mach Number	I-3
I-3	First-Step Coefficient of Drag Due to Lift Vs Mach Number	I-4
I-4	First-Step Rigid-Body Center-of-Pressure Location Vs Mach Number	I-5
I-5	First-Step Rigid-Body Normal Force Coefficient and Center of Pressure Vs Mach Number for Body Alone	I-6
I-6	Nose Cone Normal Force Coefficient Due to Angle of Attack Vs Mach Number	I-7
I-7	First-Step Rigid-Body Pitch Damping Coefficient Vs Mach Number	I-8
I-8	First-Step Roll Damping Coefficient Vs Mach Number	I-9
I-9	First-Step Roll Moment Coefficient Due to Pitch and Yaw Angles of Attack	I-10
I-10	First-Stage Cylinder Lift Distribution Due to Angle of Attack	I-11
I-11	Fin Plus Carry-Over Lift Coefficient and Center of Pressure Vs Mach Number	I-12
I-12	Second-Stage Flare Lift Distribution Due to Angle of Attack	I-13
I-13	Second and Third-Stage Cylinder Lift Distribution Due to Angle of Attack	I-14
I-14	Fourth-Stage Cylinder and Flare Lift Distribution Due to Angle of Attack	I-15

Figure No.	Page No.
I-15 Nose Cone Lift Distribution Due to Angle of Attack	I-16
I-16 Second-Step Lift Coefficient Due to Angle of Attack Vs Mach Number	I-17
I-17 Second-Step Center-of-Pressure Location Vs Mach Number	I-18
II-1 Nose Cone Normal Force Coefficient Variation with Mach Number	II-2
II-2 Nose Cone Lift Distribution	II-3
II-3 Fourth-Stage Cylinder and Flare Lift Distribution	II-4
III-1 Weight Time History	III-2
III-2 First-Step Mass Vs Time	III-3
III-3 First-Step Pitch or Yaw Moment of Inertia Vs Time	III-4
III-4 First-Step Pitch or Yaw Moment of Inertia Vs Mass	III-5
III-5 First-Step Roll Moment of Inertia Vs Time	III-6
III-6 First-Step Center of Mass Vs Time	III-7
III-7 Second-Step Mass Vs Time	III-8
III-8 Second-Step Pitch or Yaw Moment of Inertia Vs Time	III-9
III-9 Second-Step Roll Moment of Inertia Vs Time	III-10
III-10 Second-Step Center of Mass Vs Time	III-11
III-11 Third-Step Mass Vs Time	III-12
III-12 Third-Step Pitch or Yaw Moment of Inertia Vs Time	III-13
III-13 Third-Step Roll Moment of Inertia Vs Time	III-14

Figure No.	Page No.
III-14 Third-Step Center of Mass Vs Time	III-15
III-15 Fourth-Step Mass Vs Time	III-16
III-16 Fourth-Step Pitch or Yaw Moment of Inertia Vs Time	III-17
III-17 Fourth-Step Roll Moment of Inertia Vs Time	III-18
III-18 Fourth-Step Center of Mass Vs Time	III-19
IV-1 First-Step Weight Vs Time	IV-2
IV-2 First-Step Pitch and Yaw Moment of Inertia Vs Time	IV-3
IV-3 First-Step Center-of-Mass Location Vs Time	IV-4
V-1 First-Step Bending-Mode Shapes and Frequencies at Launch	V-2
V-2 First-Step Bending-Mode Slopes at Launch	V-3
V-3 First-Step Stiffness Distribution of First and Second Stages	V-5
V-4 First-Step Stiffness Distribution of Third and Fourth Stages	V-6
V-5 First-Step Bending-Mode Shapes and Frequencies at the Transonic Condition	V-7
V-6 First-Step Bending -Mode Slopes at the Transonic Condition	V-8
V-7 First-Step Bending-Mode Shapes and Frequencies at the Maximum q Condition	V-10
V-8 First-Step Bending-Mode Slopes at the Maximum q Condition	V-11
V-9 First-Step Bending-Mode Shapes and Frequencies at Burnout	V-14

Figure No.	Page No.
V-10 First-Step Bending-Mode Slopes at Burnout	V-15
V-11 First-Step Mass Distribution at First-Stage Burnout	V-17
V-12 First-Step Propellant Mass Distribution at First-Stage Ignition	V-18
V-13 First-Step Torsion Mode Shapes at Launch	V-19
V-14 Second-Step Bending-Mode Shapes and Frequencies at Second-Stage Ignition	V-20
V-15 Second-Step Bending-Mode Slopes at Second-Stage Ignition	V-21
VI-1 First-Step Bending-Mode Shapes and Frequencies at Launch	VI-2
VI-2 First-Step Bending-Mode Slopes at Launch	VI-3
VI-3 First-Step Bending-Mode Shapes and Frequencies with 50 Percent Propellant Remaining	VI-9
VI-4 First-Step Bending-Mode Slopes with 50 Percent Propellant Remaining	VI-10
VI-5 First-Step Bending-Mode Shapes and Frequencies at Burnout	VI-16
VI-6 First-Step Bending-Mode Slopes at Burnout	VI-17
VII-1 First-Stage Motor (Algol) Thrust Vs Time	VII-2
VII-2 Second-Stage Motor (Castor) Thrust Vs Time	VII-3
VII-3 Third-Stage Motor (Antares) Thrust Vs Time	VII-4
VII-4 Fourth-Stage Motor (Altair) Thrust Vs Time	VII-5
VIII-1 First-Step Total Pitch Control Moment Vs Time	VIII-2

Figure No.	Page No.
VIII-2 First-Step Total Roll Control Moment Vs Time	VIII-3
VIII-3 Jet-Vane Lift Vs Time	VIII-4
VIII-4 Jet-Vane Roll Moment Vs Time	VIII-5
VIII-5 Jet-Vane Lift Coefficient Vs Deflection Two Seconds After Launch	VIII-6
VIII-6 Jet-Vane Lift Coefficient Vs Deflection 15 Seconds After Launch	VIII-7
VIII-7 Jet-Vane Lift Coefficient Vs Deflection 32 Seconds After Launch	VIII-8
VIII-8 Jet-Vane Hinge Moment Vs Deflection 4 Seconds After Launch	VIII-9
VIII-9 Jet-Vane Hinge Moment Vs Deflection 16 Seconds After Launch	VIII-10
VIII-10 Jet-Vane Hinge Moment Vs Deflection 34 Seconds After Launch	VIII-11
VIII-11 Aerodynamic Tip-Surface Normal-Force Coefficient Vs Mach Number	VIII-12
VIII-12 Aerodynamic Tip-Surface Roll Moment Coefficient Vs Mach Number	VIII-13
VIII-13 Aerodynamic Tip-Surface Normal-Force Coefficient Vs Deflection at Mach 0.8	VIII-14
VIII-14 Aerodynamic Tip-Surface Normal-Force Coefficient Vs Deflection at Mach 1.0	VIII-15
VIII-15 Aerodynamic Tip-Surface Normal-Force Coefficient Vs Deflection at Mach 1.2	VIII-16

Figure No.	Page No.
VIII-16 Aerodynamic Tip-Surface Normal-Force Coefficient Vs Deflection at Mach 2.0	VIII-17
VIII-17 Aerodynamic Tip-Surface Hinge Moment Coefficient Vs Deflection at Mach 0.8	VIII-18
VIII-18 Aerodynamic Tip-Surface Hinge Moment Coefficient Vs Deflection at Mach 1.0	VIII-19
VIII-19 Aerodynamic Tip-Surface Hinge Moment Coefficient Vs Deflection at Mach 1.2	VIII-20
VIII-20 Aerodynamic Tip-Surface Hinge Moment Coefficient Vs Deflection at Mach ≥ 2.0	VIII-21
VIII-21 Servo Actuator Control Valve Flow Vs Input Signal	VIII-22
IX-1 First-Step Mach Number Vs Time	IX-2
IX-2 First-Step Velocity Vs Time	IX-3
IX-3 First-Step Dynamic Pressure Vs Time	IX-4
IX-4 First and Second-Step Dynamic Pressure Vs Time	IX-5
IX-5 First-Step Altitude Vs Time	IX-6
IX-6 First-Step Flight Path Angle Vs Time	IX-7
IX-7 First-Step Angle of Attack Vs Time	IX-8
IX-8 Trajectory Plot Showing Stage Ignition, Burnout, and Coast	IX-9
IX-9 Vehicle Velocity Vs Time for the Entire Trajectory	IX-10

LIST OF TABLES

Table No..		Page No.
V-1	First-Step Bending-Mode Shape and Slope at Launch	V- 4
V-2	First-Step Bending -Mode Shape and Slope 17 Seconds After Launch	V- 9
V-3	First-Step Bending-Mode Shape and Slope 30.1 Seconds After Launch	V-12
V-4	First-Step Bending-Mode Shape and Slope 35.4 Seconds After Launch	V-13
V-5	First-Step Bending-Mode Shape and Slope at Burnout	V-16
VI-1	First-Step Bending-Mode Shapes at Launch	VI-4
VI-2	First-Step Bending-Mode Slope at Launch	VI-6
VI-3	First-Step Bending-Mode Shape with 50 Percent Propellant Remaining	VI-11
VI-4	First-Step Bending-Mode Slope with 50 Percent Propellant Remaining	VI-13
VI-5	First-Step Bending-Mode Shape at Burnout	VI-18
VI-6	First-Step Bending-Mode Slope at Burnout	VI-20

INTRODUCTION

This document presents the basic data used in the design of the control systems of the first three SCOUT vehicles, and also gives the data used to study control of the fourth vehicle.

FOURTH VEHICLE ANALYSIS

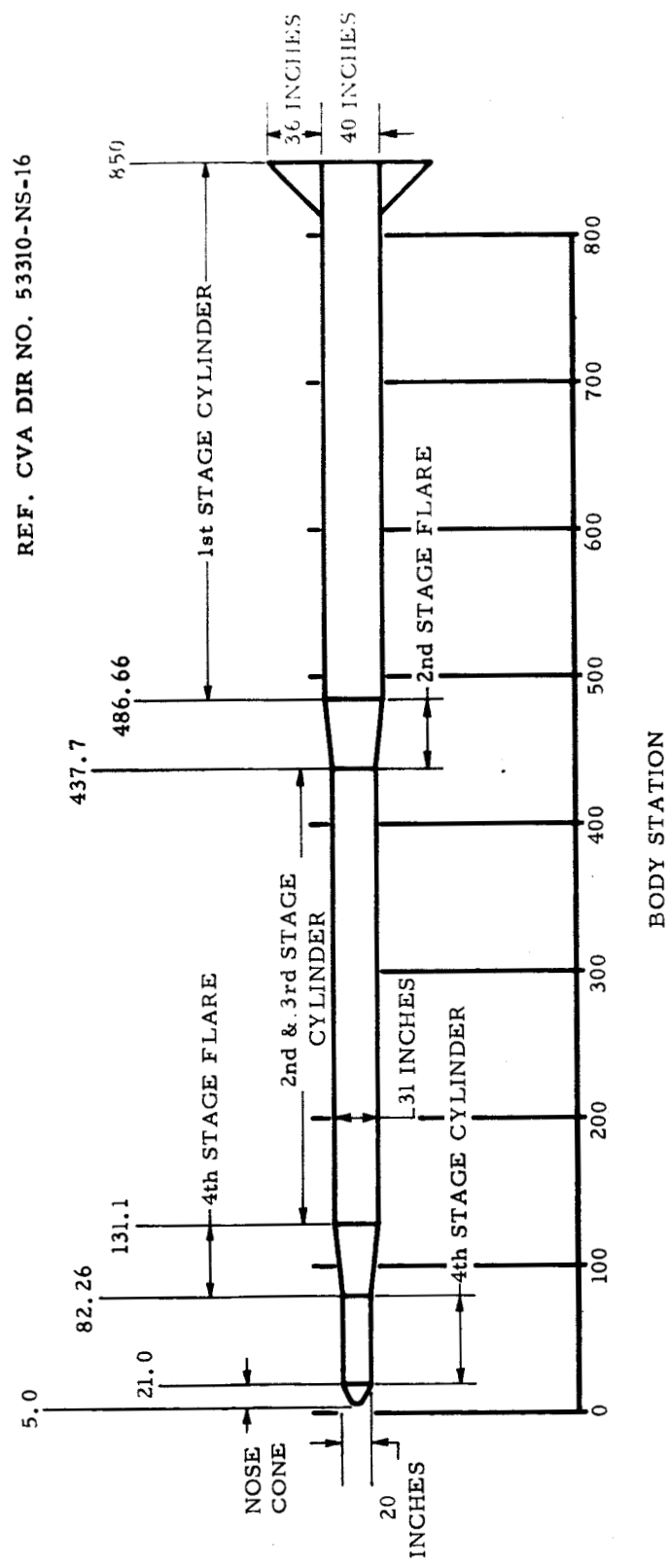
Per direction by NASA, the fourth vehicle analysis was based upon data from both the configuration of the first three vehicles and data supplied by NASA. Thus the fourth vehicle analysis does not exactly represent the fourth vehicle per se.

All data not listed explicitly for the fourth vehicle (25.7-inch diameter nose) is the same for both nose diameters. Body dimensions and nomenclature for the 20-inch diameter nose configuration are given in figure i-1.

SOURCE OF INFORMATION

The information contained in this document was obtained from various sources, and was the data available at the time of the control system design. Much of this data is now obsolete and has since been superseded. Data describing engine thrust, weight and inertia, and center of mass was obtained from NASA in a document received 2 November 1960. Jet-vane information was derived from an Aerojet preliminary letter of transmittal SRP: 5720:0821 dw dated 23 February 1960. Lift distributions were taken from CVA DIR No. 53310-NS-16, dated

8 June 1959. The original structural data was taken from CVA DIR No. 53480-NS-9 and DIR No. 53480-NS-9, Rev. A received 30 October and 2 November 1960, respectively. Where possible, references are included on the pertinent graphs.



R-ED 11122
-xii-

Figure i-1 SCOUT Body Dimensions and Nomenclature

SECTION I

**AERODYNAMICS OF FIRST THREE VEHICLES
(20-Inch Diameter Fourth Stage)**

**R - E D 11122
I-1**

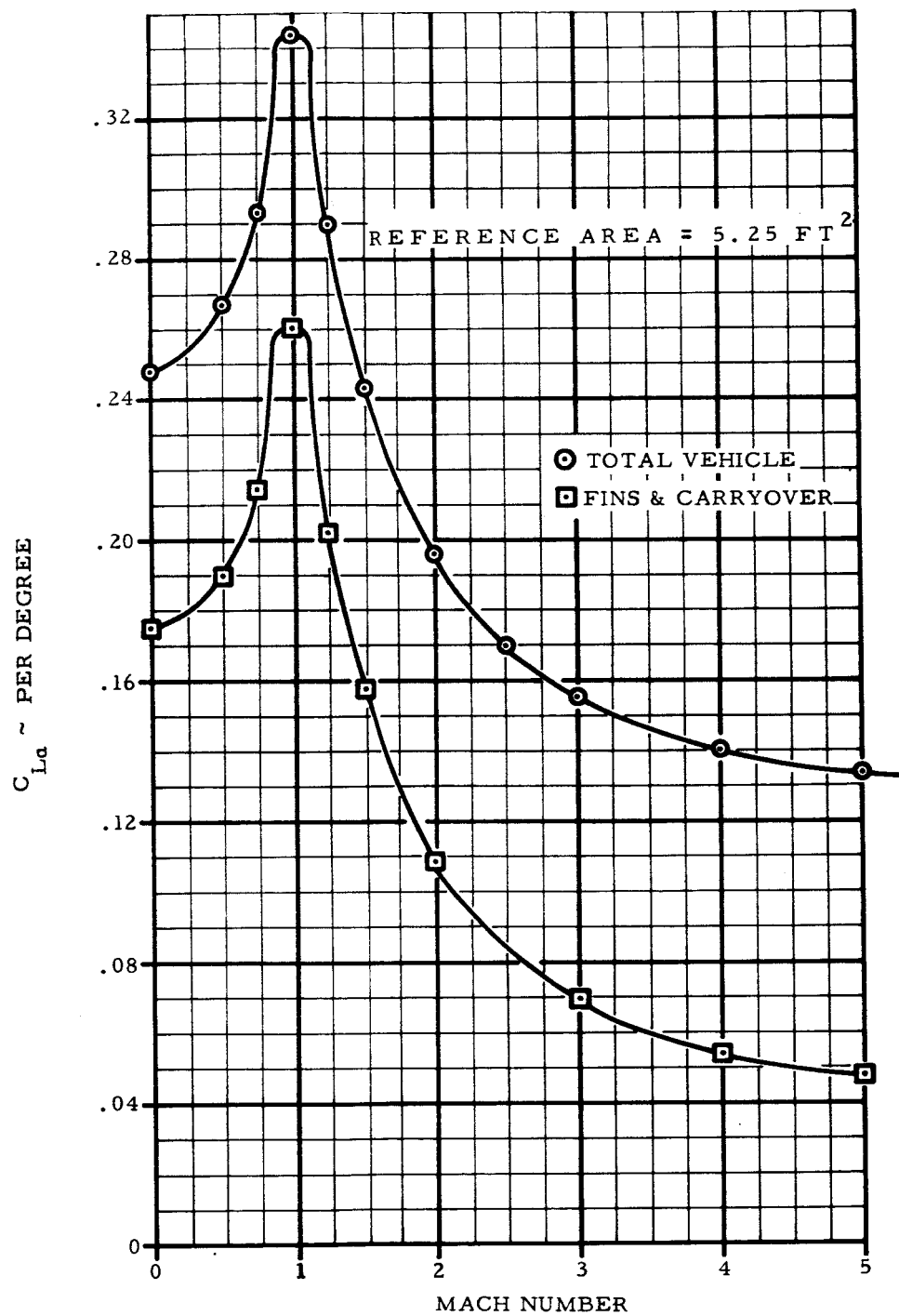


Figure I-1 First-Step Rigid-Body Lift Coefficient Vs Mach Number

R-ED 11122
I-2

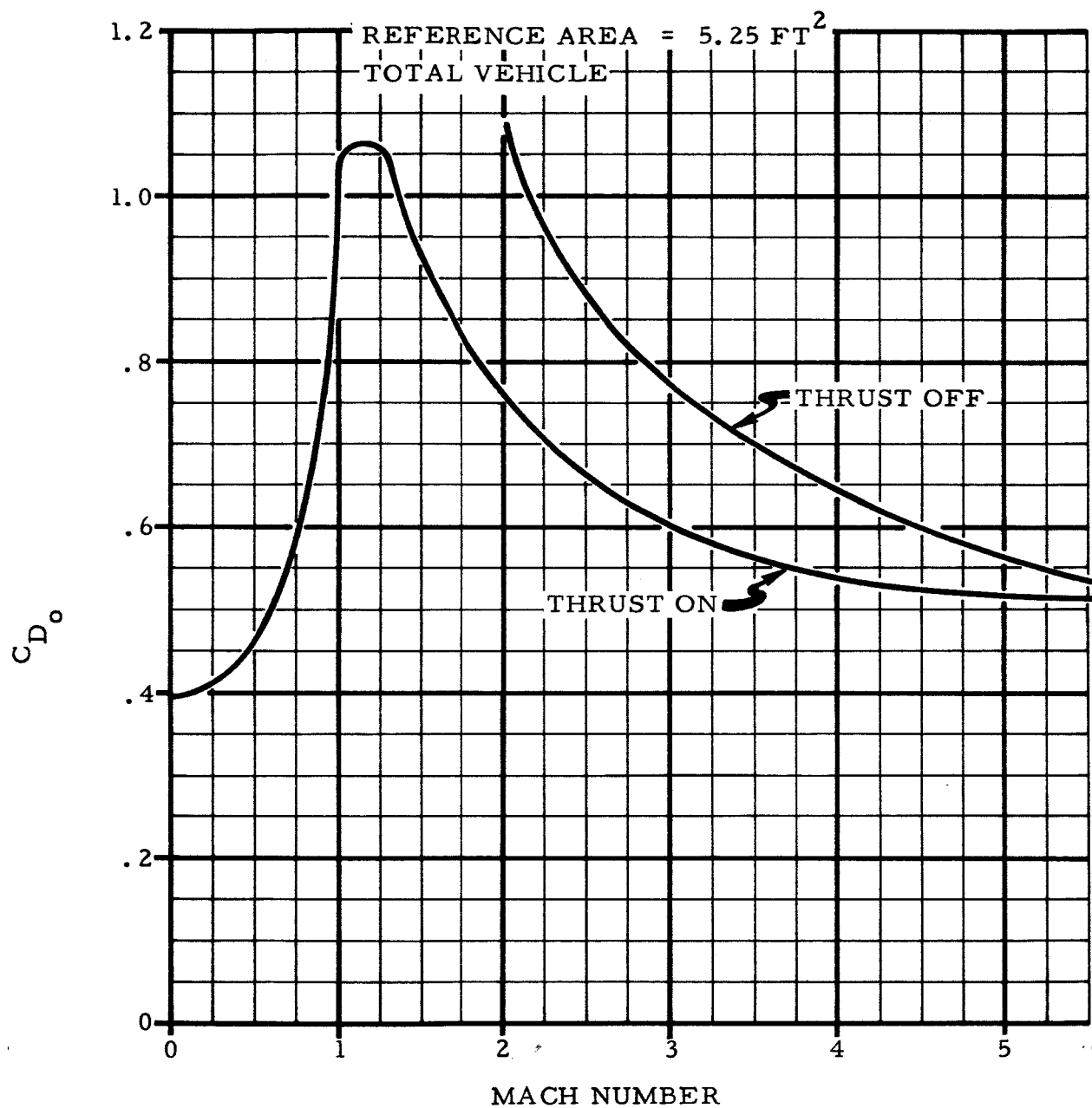


Figure I-2 First-Step Zero-Lift Drag Coefficient Vs Mach Number

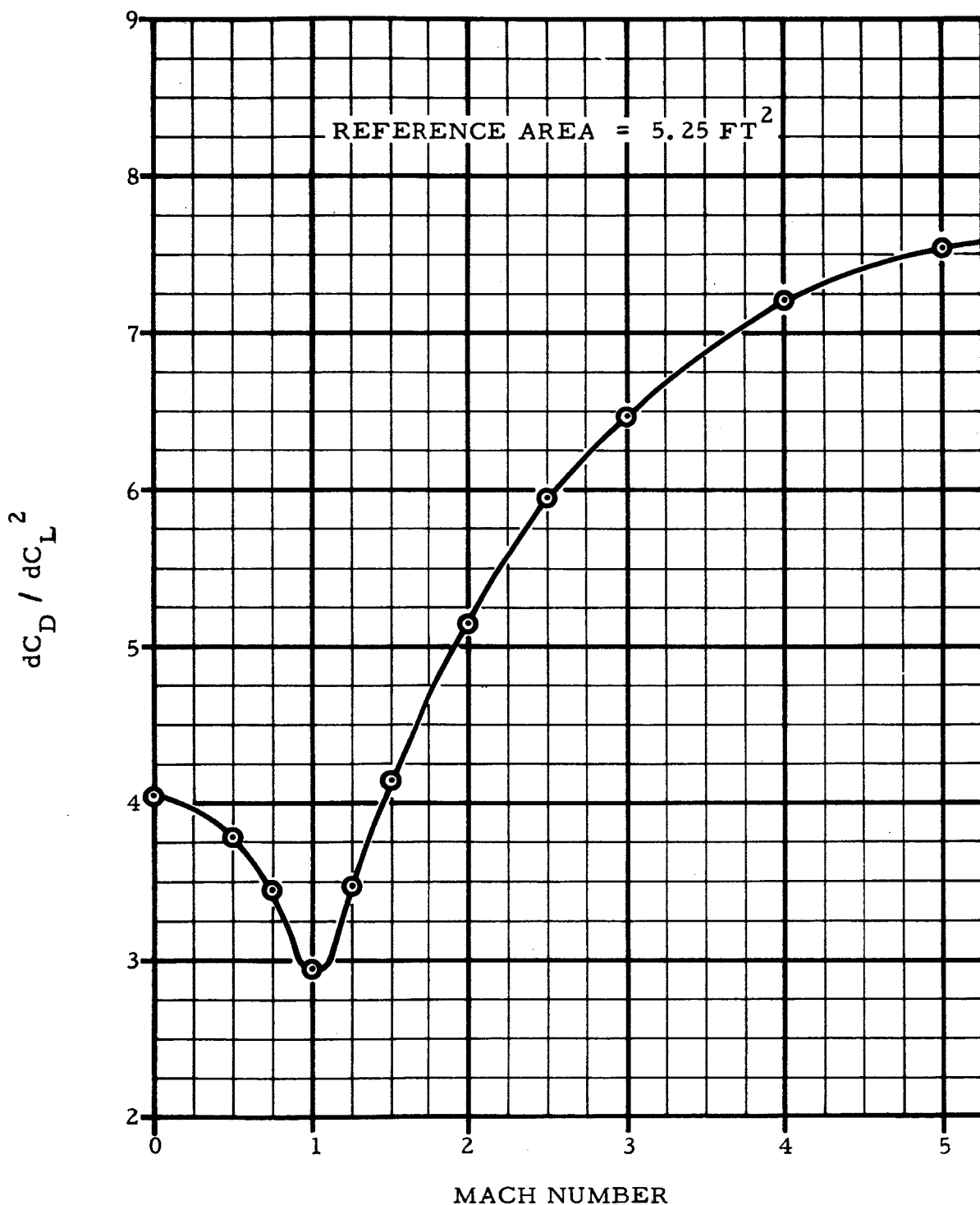


Figure I-3 First-Step Coefficient of Drag Due to Lift Vs Mach Number

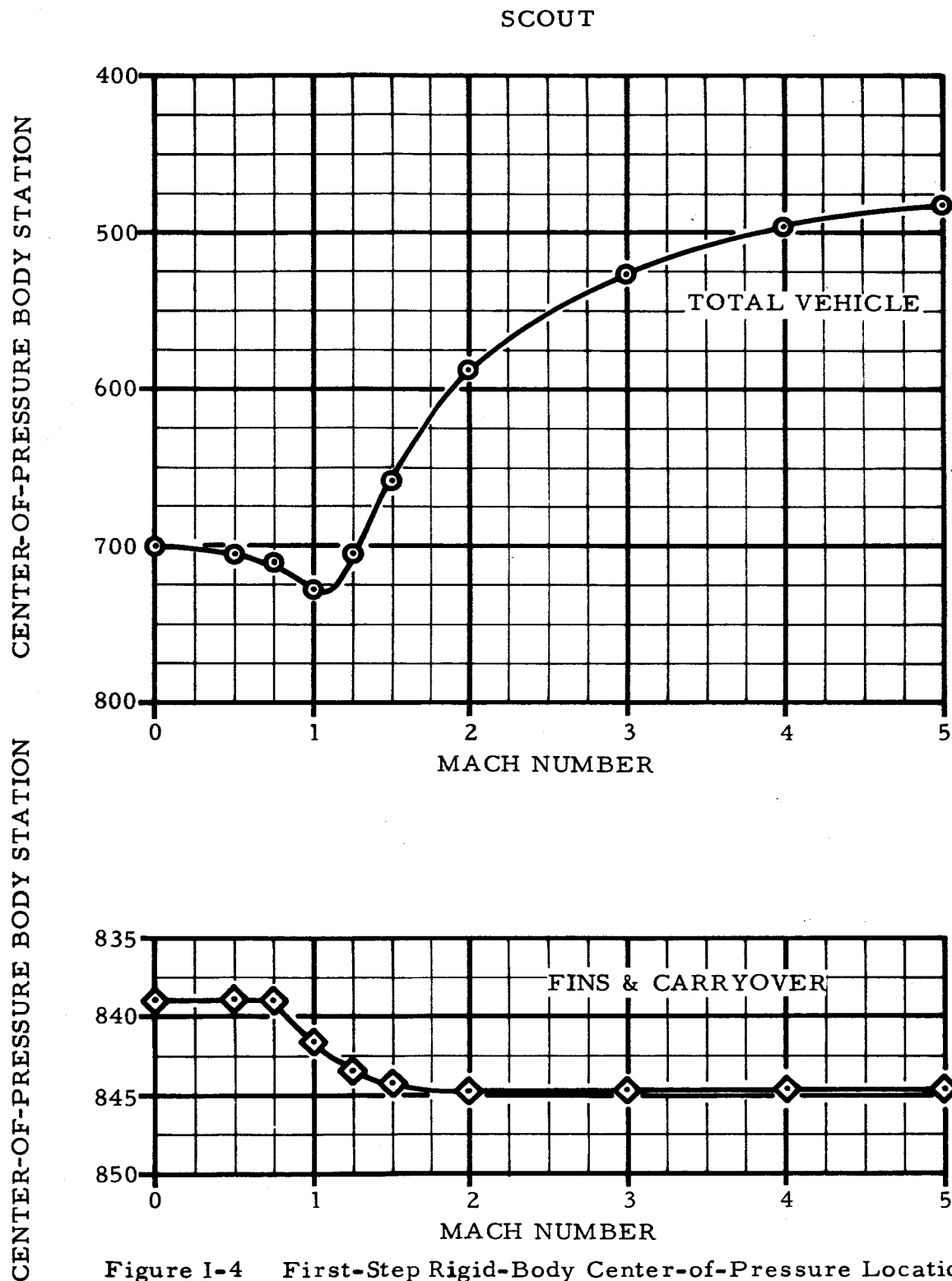
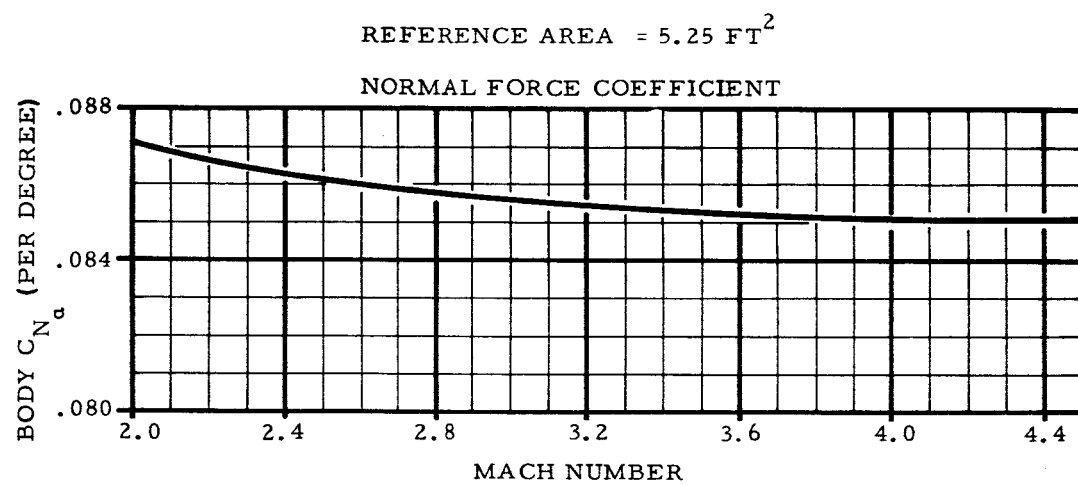


Figure I-4 First-Step Rigid-Body Center-of-Pressure Location Vs
Mach Number



REF. CVA DIR NO. 53310-NS-16A

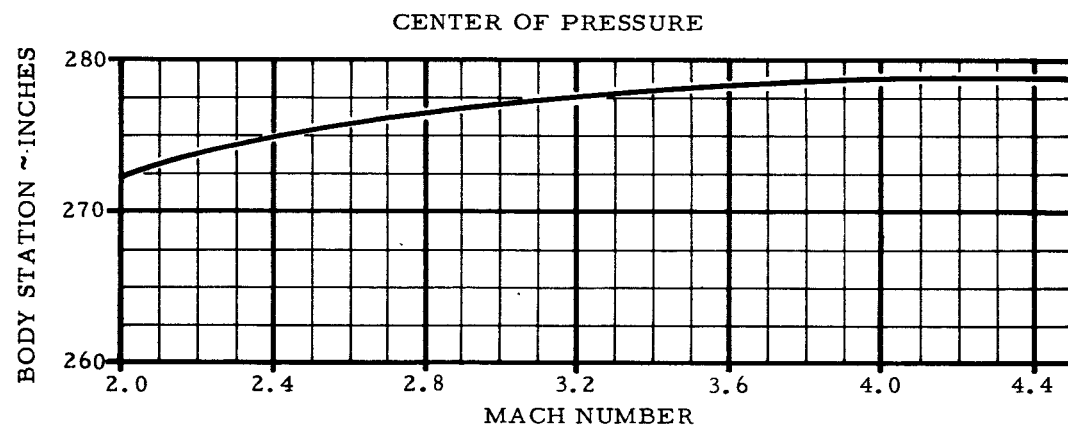


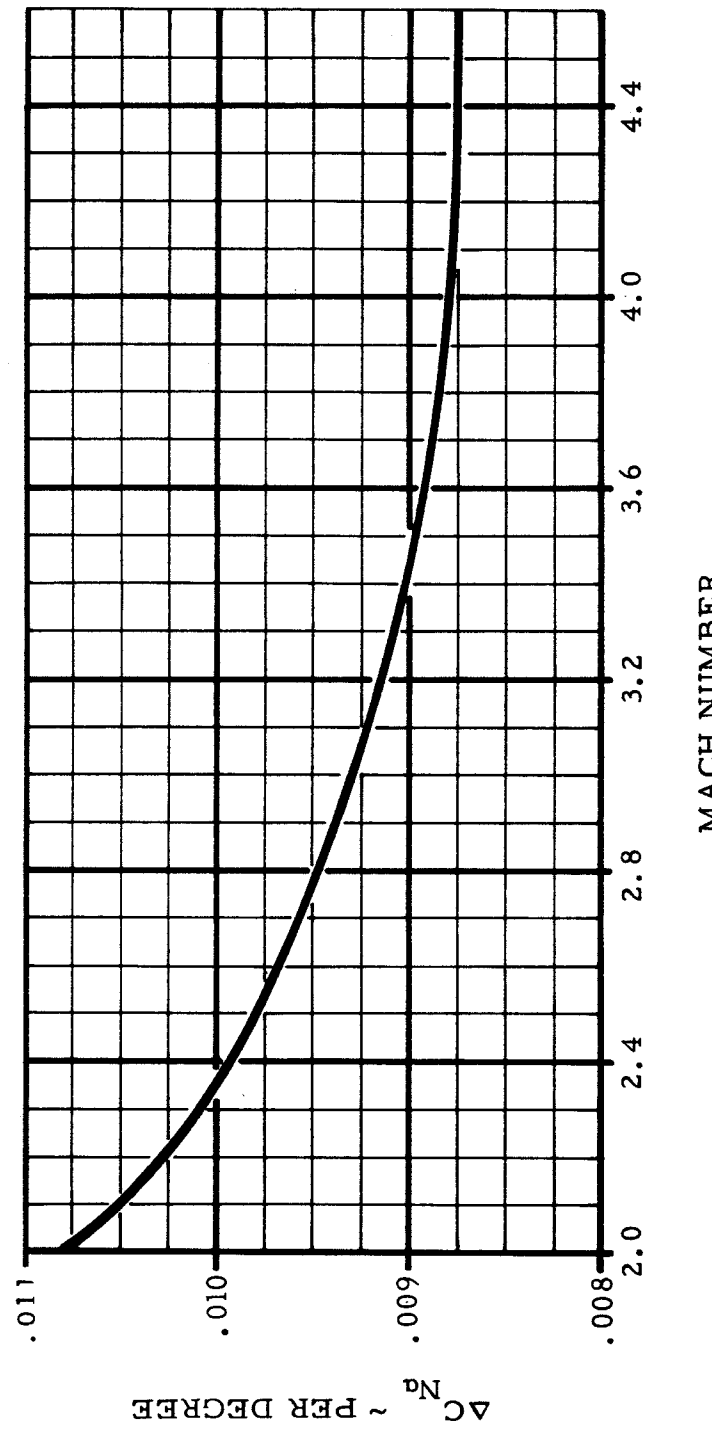
Figure I-5 First-Step Rigid-Body Normal Force Coefficient and Center of Pressure Vs Mach Number for Body Alone

R-ED 11122

I-6

REFERENCE AREA = 5.25 FT²

REF. CVA DIR NO. 53310-NS-16



MACH NUMBER

Figure I-6 Nose Cone Normal Force Coefficient Due to Angle of Attack
Vs Mach Number

$$-C_m q \frac{S \bar{c}^2}{2} \times \left(\frac{q}{v} \right) = \frac{FT-LB}{DEG/SEC}$$

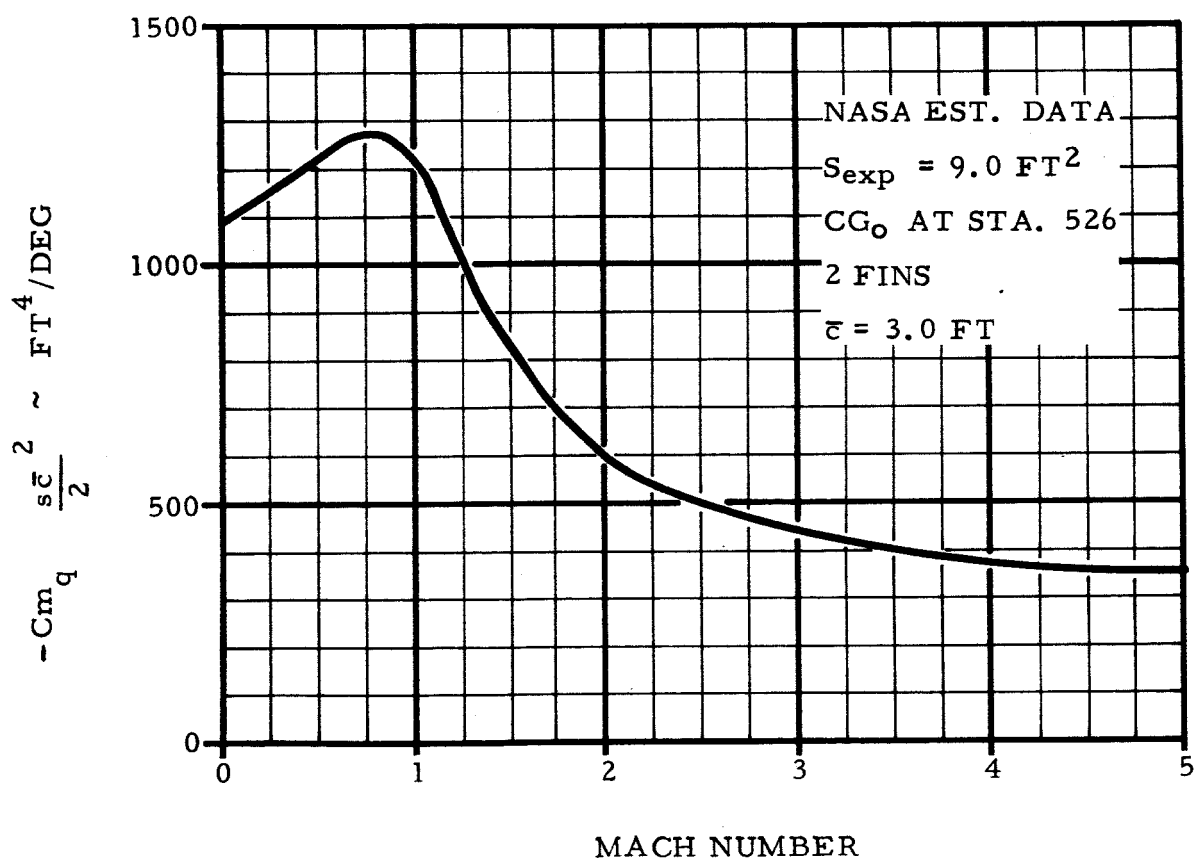
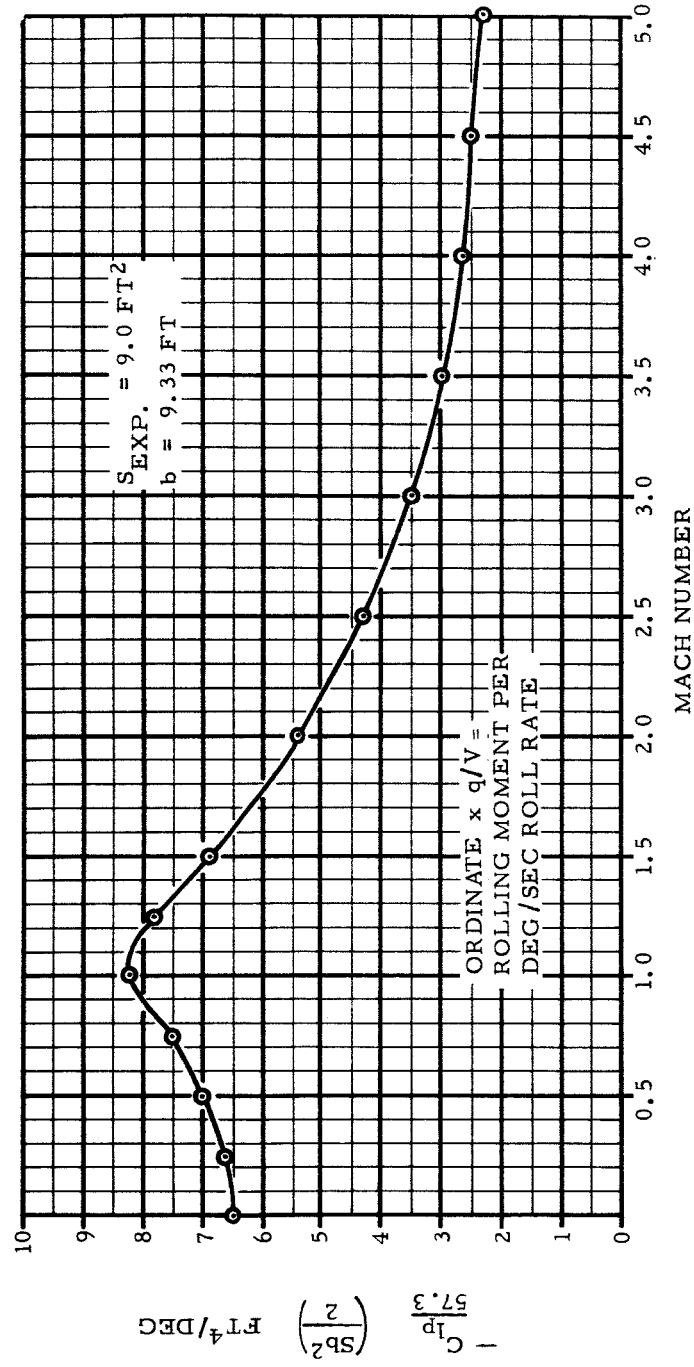


Figure I-7 First-Step Rigid-Body Pitch Damping Coefficient Vs Mach Number

Figure I-8 First-Step Roll Damping Coefficient Vs Mach Number



R-ED 11122
I-9

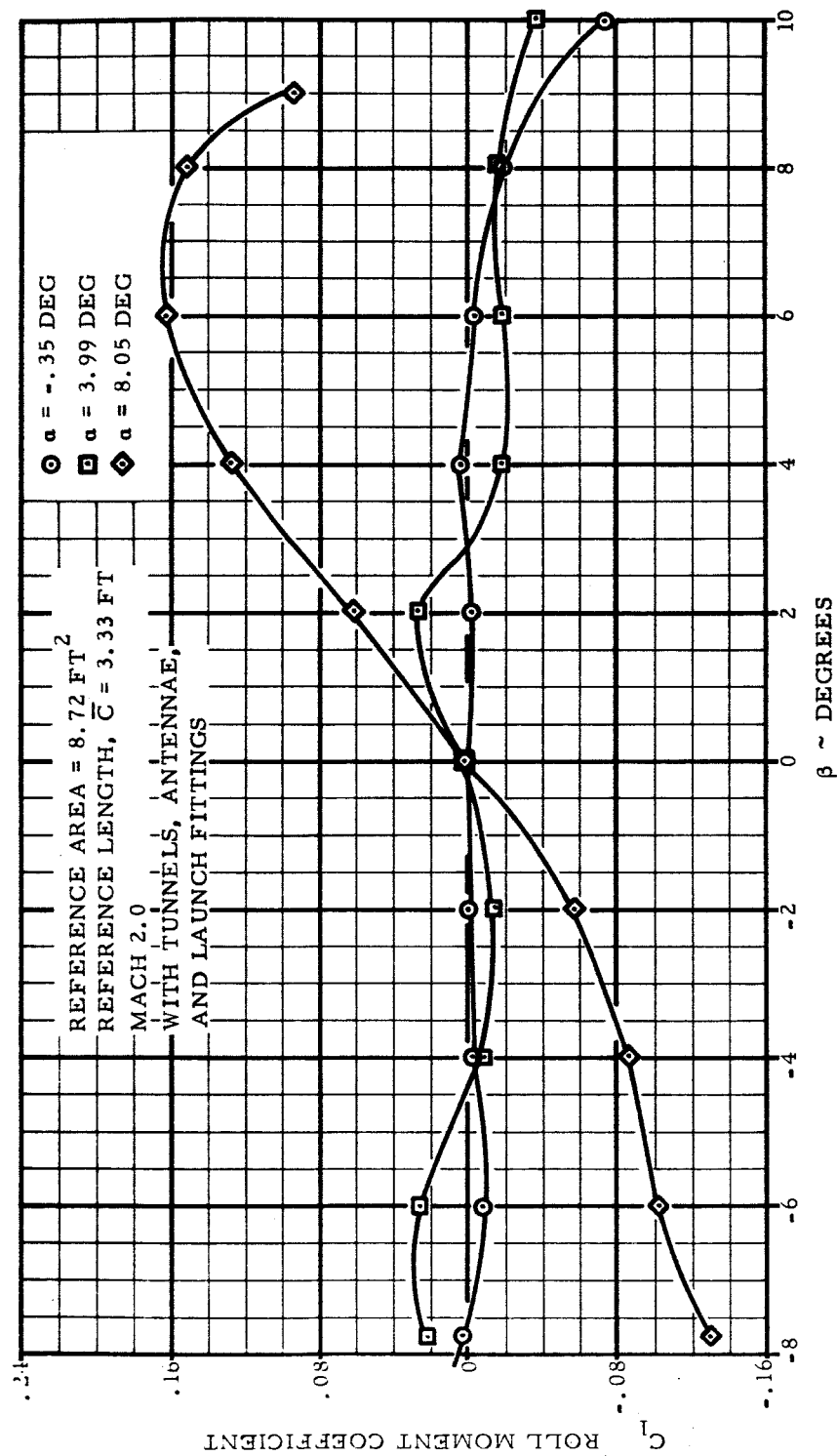
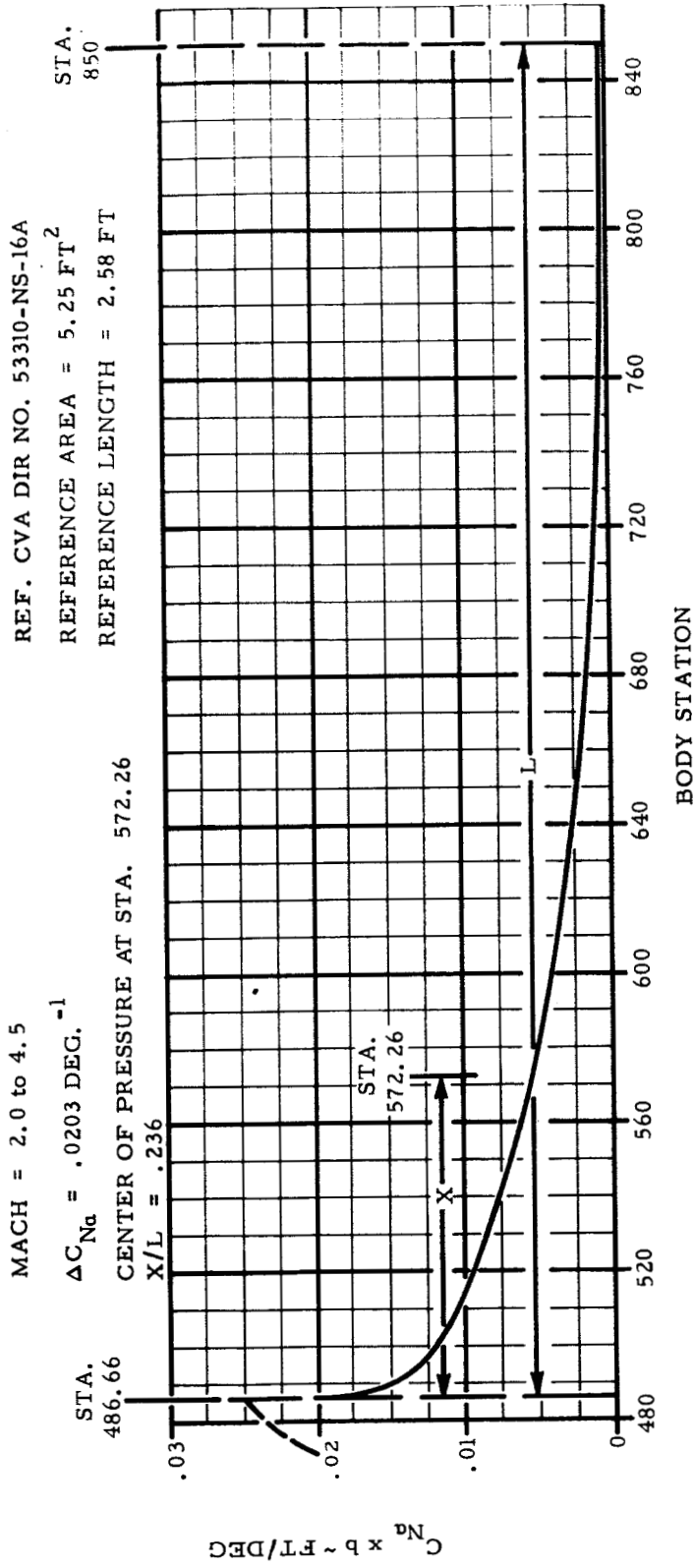


Figure 1-9 First-Step Roll Moment Coefficient Due to Pitch and Yaw Angles of Attack



R-ED 11122
I-11

Figure I-10 First-Stage Cylinder Lift Distribution Due to Angle of Attack

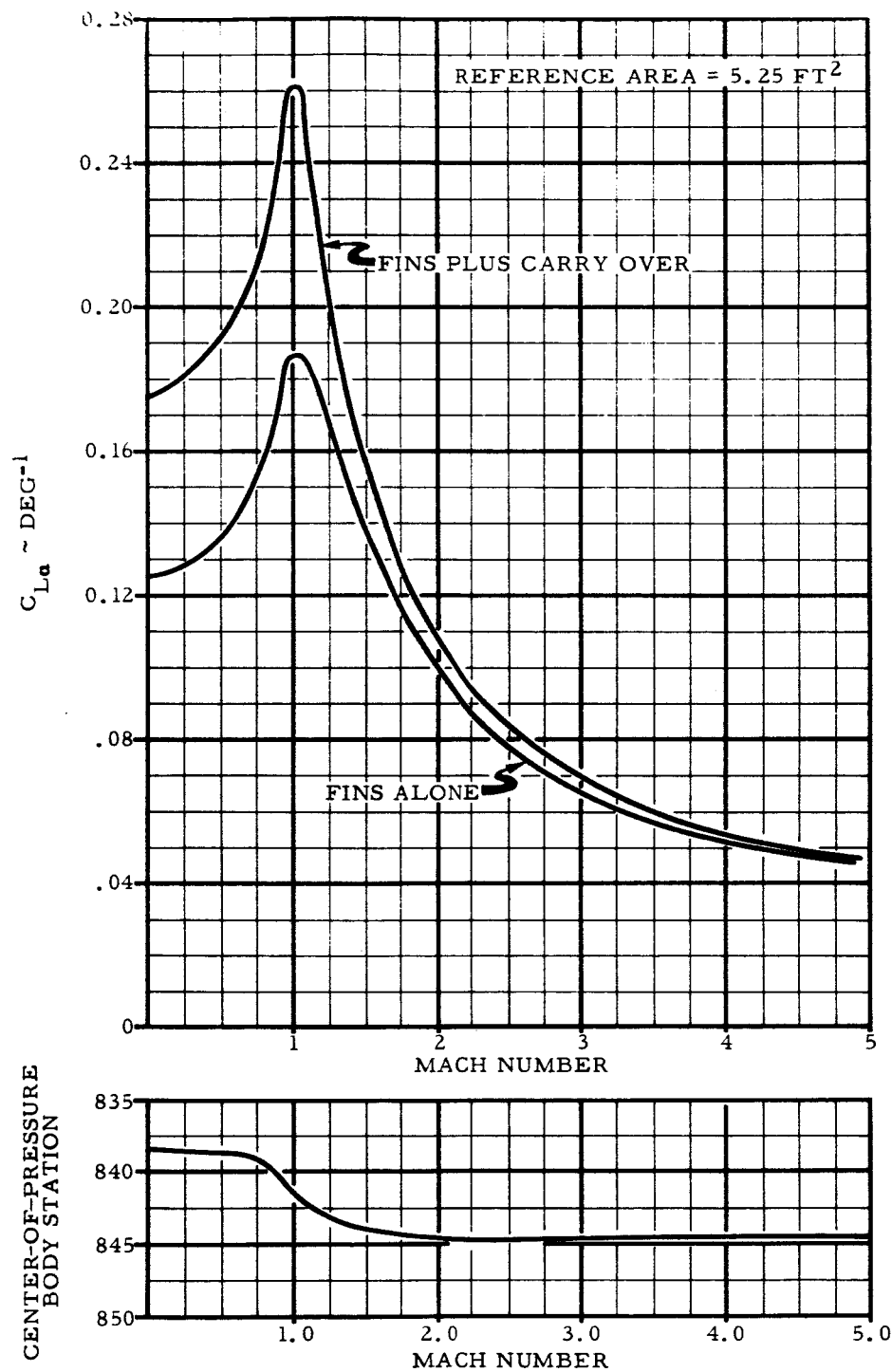


Figure I-11 Fin Plus Carry-Over Lift Coefficient and Center of Pressure Vs Mach Number

SCOUT

REFERENCE AREA = 5.25 FT^2

REF. CVA DIR NO. 53310-NS-16

REFERENCE LENGTH = 2.58 FT

CENTER OF PRESSURE AT STA. 470.4

$X/L = .669$

$$\Delta C_{Na} = .0106 \text{ DEG}^{-1}$$

MACH 2.0 TO 4.5

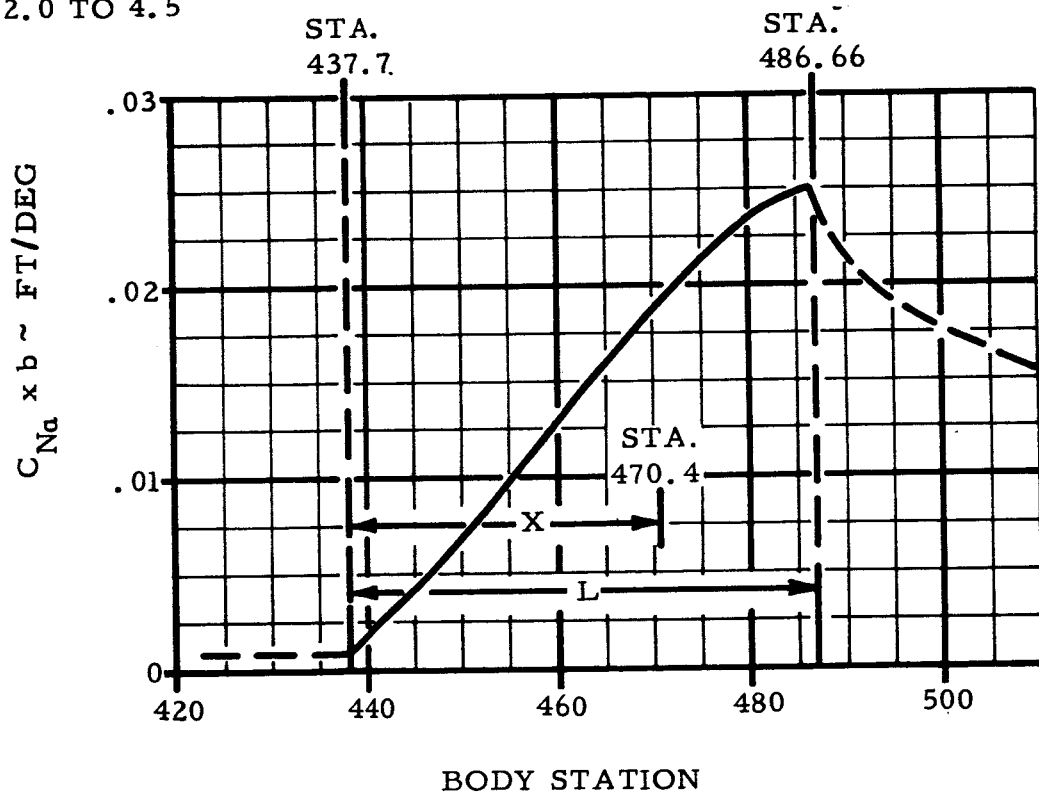
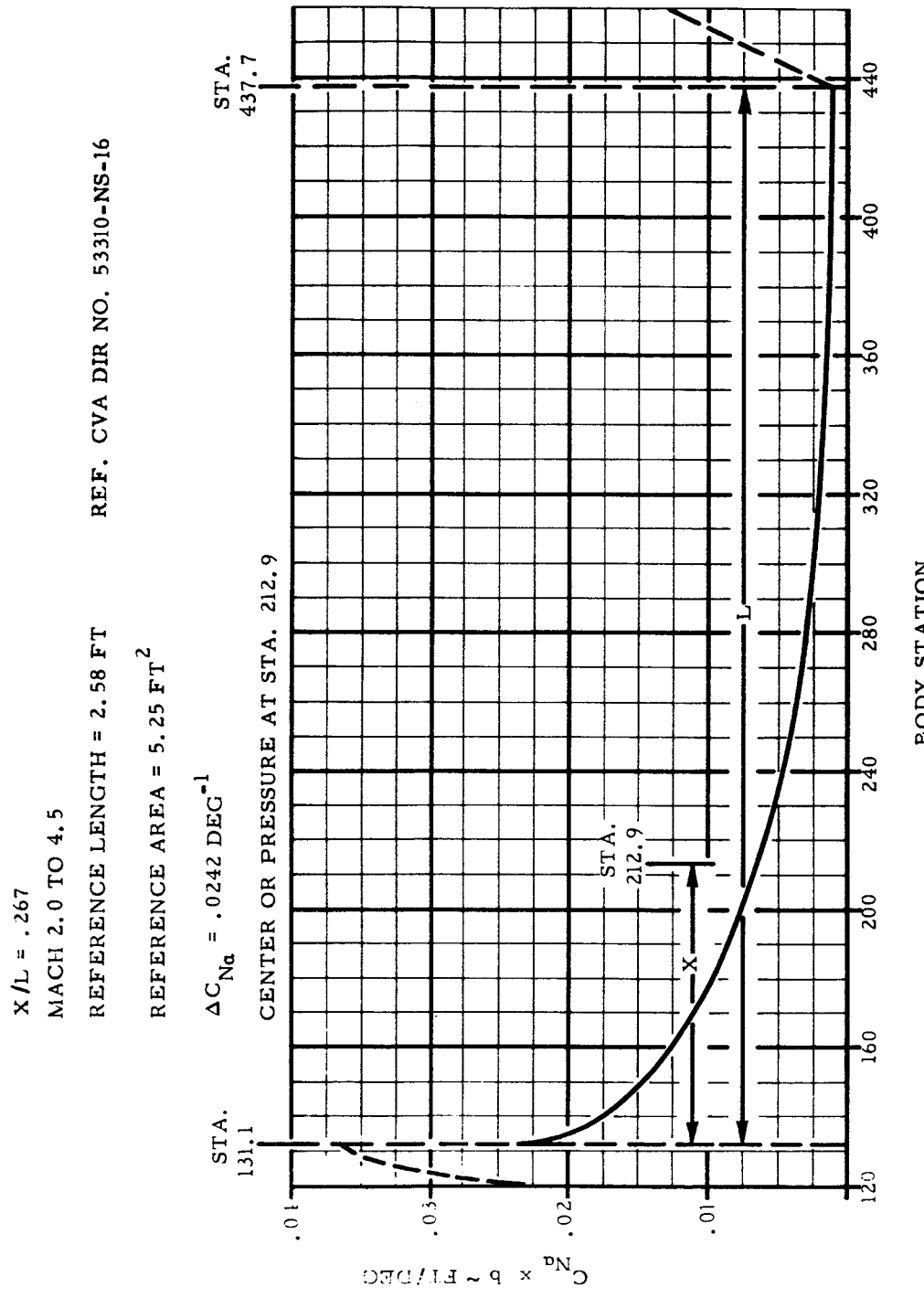


Figure I-12 Second-Stage Flare Lift Distribution Due to Angle of Attack

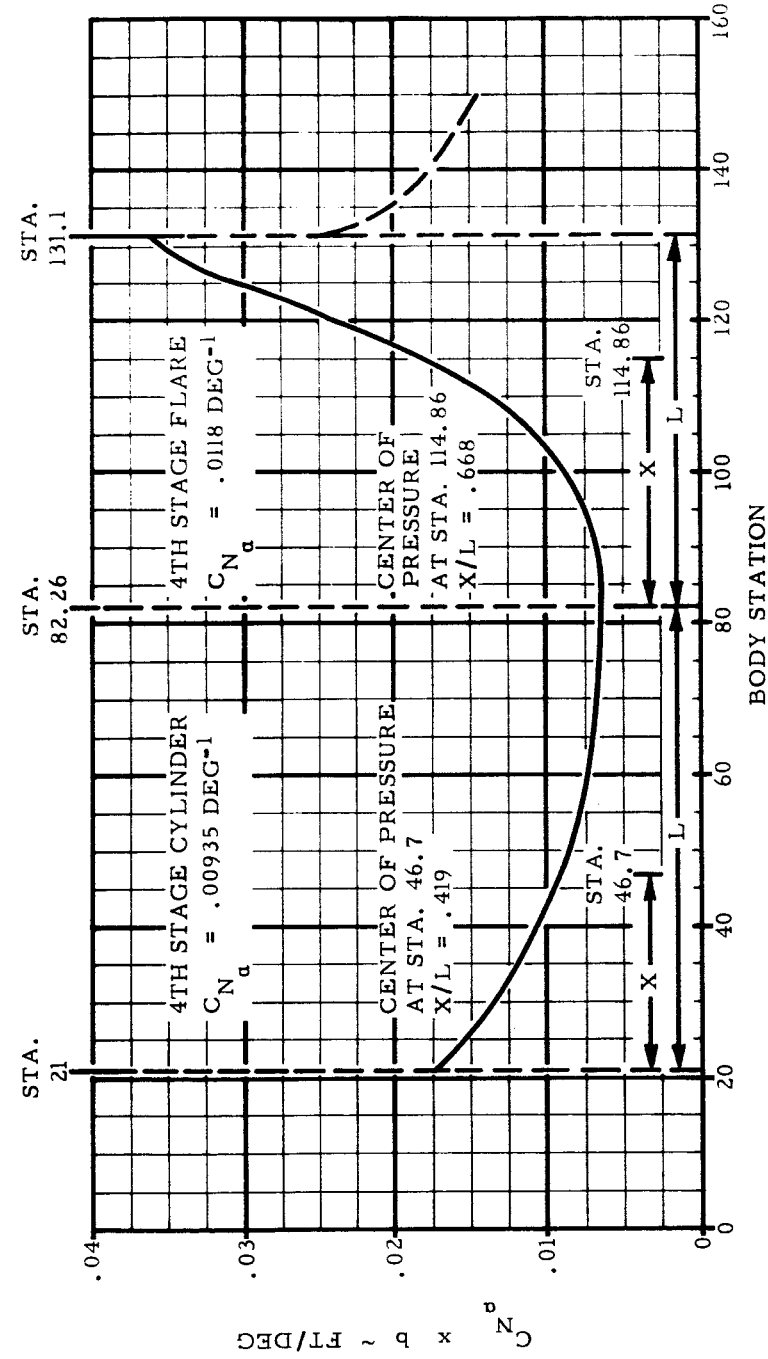


R-ED 11122
I-14

Figure I-13 Second and Third-Stage Cylinder Lift Distribution Due to Angle of Attack

$M_{\infty} = 2.0$ TO 4.5
 REFERENCE AREA $A = 5.25 \text{ ft}^2$
 REFERENCE LENGTH $L = 2.58 \text{ ft}^2$

REF. CVA DIR NO. 53310-NS-16



R-ED 11122
I-15

Figure I-14 Fourth-Stage Cylinder and Flare Lift Distribution Due to Angle of Attack

MACH 3.0

REF. CVA DIR NO. 53310-NS-16

$$\Delta C_{Na} = .00932 \text{ DEG.}^{-1}$$

CENTER OF PRESSURE AT STA. 15.4

$$X/L = .65$$

NOTE:

CENTER OF PRESSURE IS CONSTANT AT $X/L =$

.65 FOR $M = 2.0$ TO 4.5

REFERENCE AREA = 5.25 FT^2

REFERENCE LENGTH = 2.58 FT.

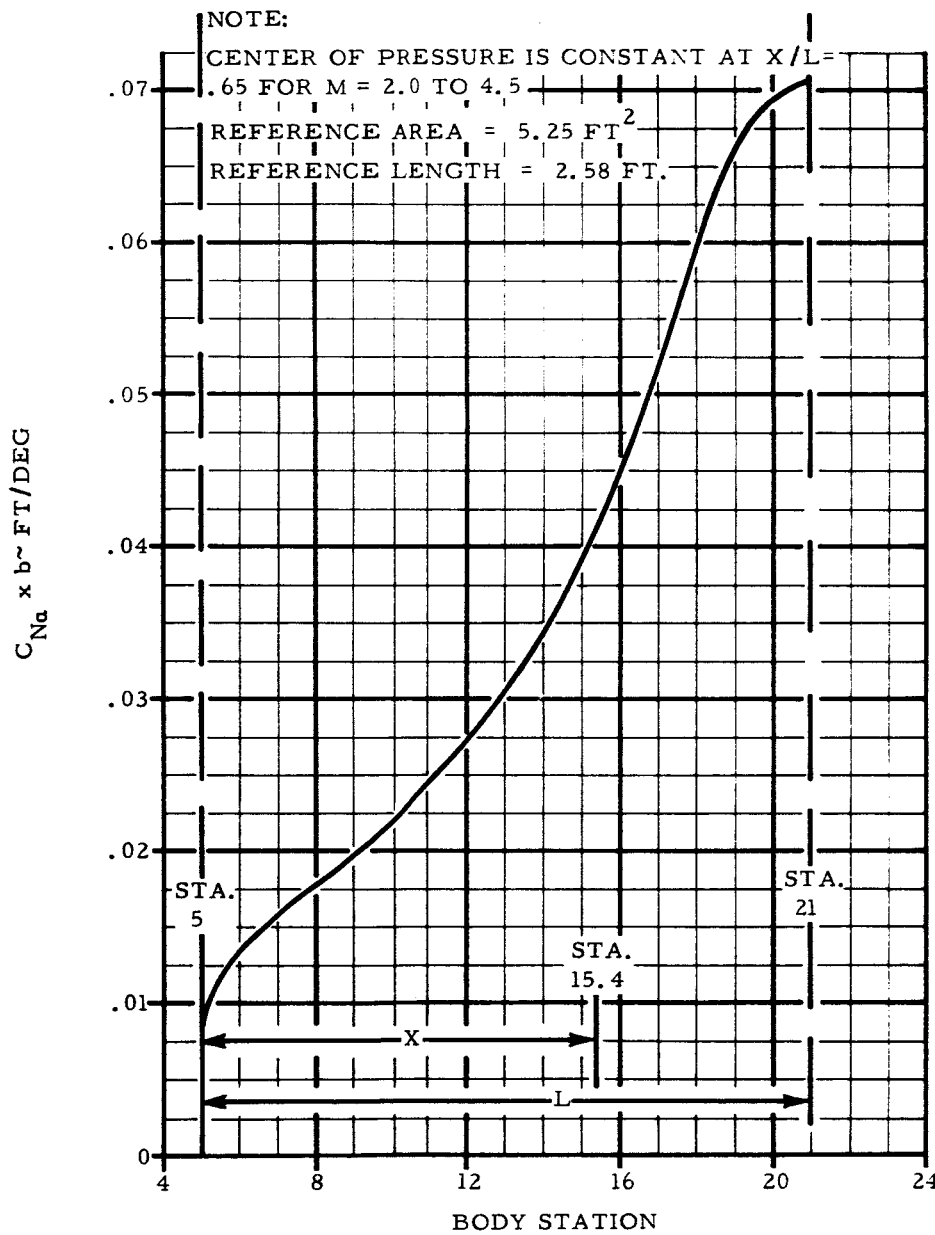


Figure I-15 Nose Cone Lift Distribution Due to Angle of Attack

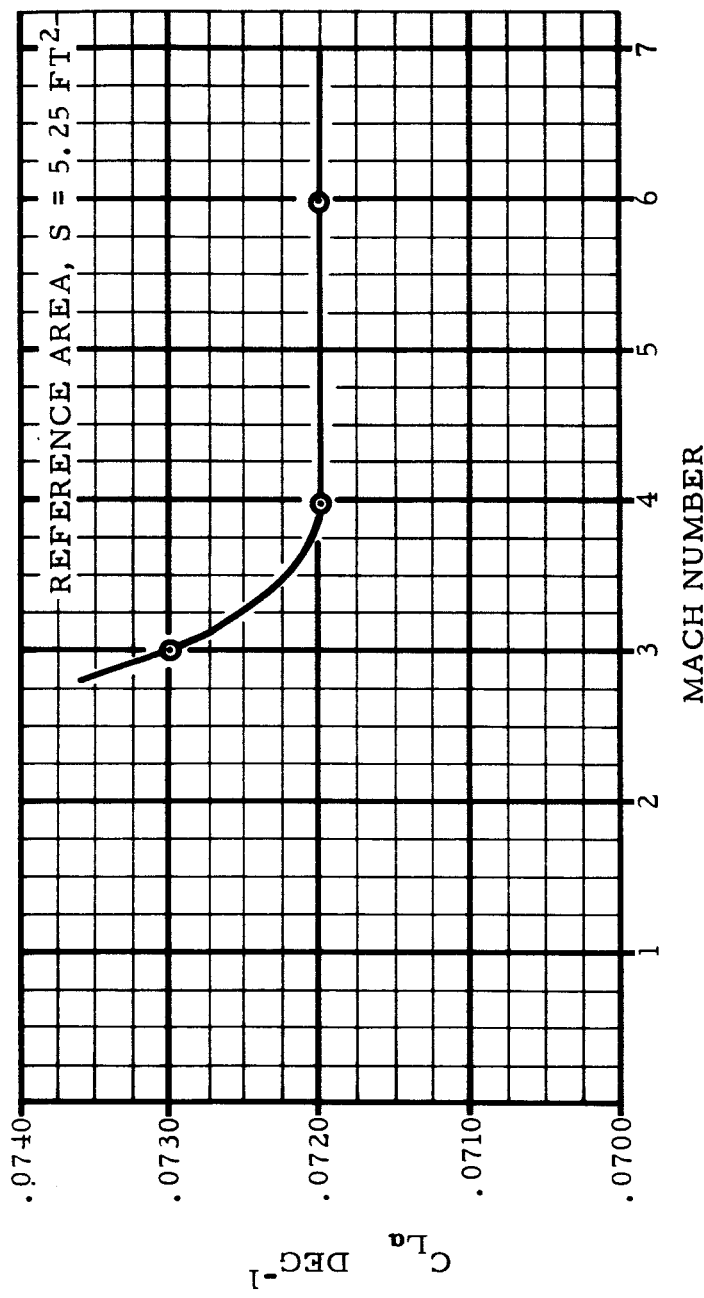
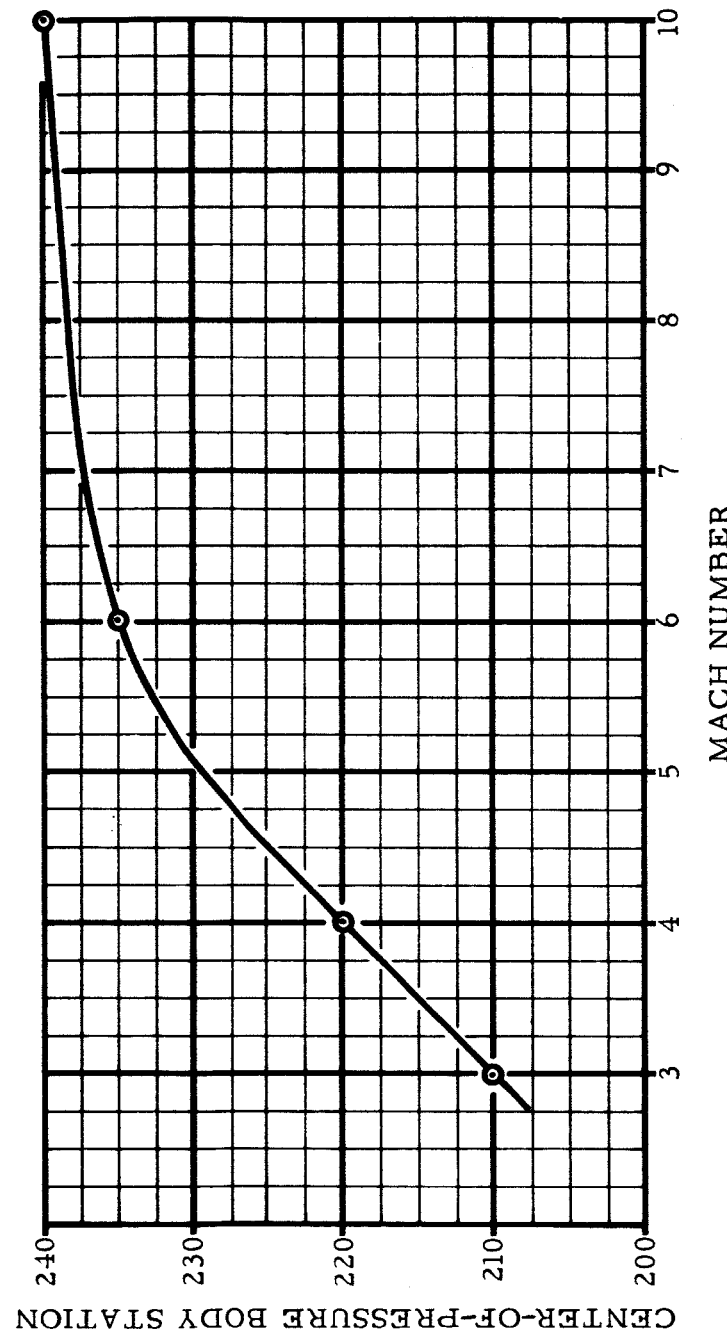


Figure I-16 Second-Step Lift Coefficient Due to Angle of Attack vs
Mach Number

Figure I-17 Second-Step Center-of-Pressure Location Vs Mach Number



SECTION II

AERODYNAMICS OF FOURTH VEHICLE
(25.7-Inch Diameter Fourth Stage And Nose Cone)

25.7-INCH DIAMETER NOSE

CVA DIR NO. 86250-AM-4

REFERENCE AREA = 5.25 FT²

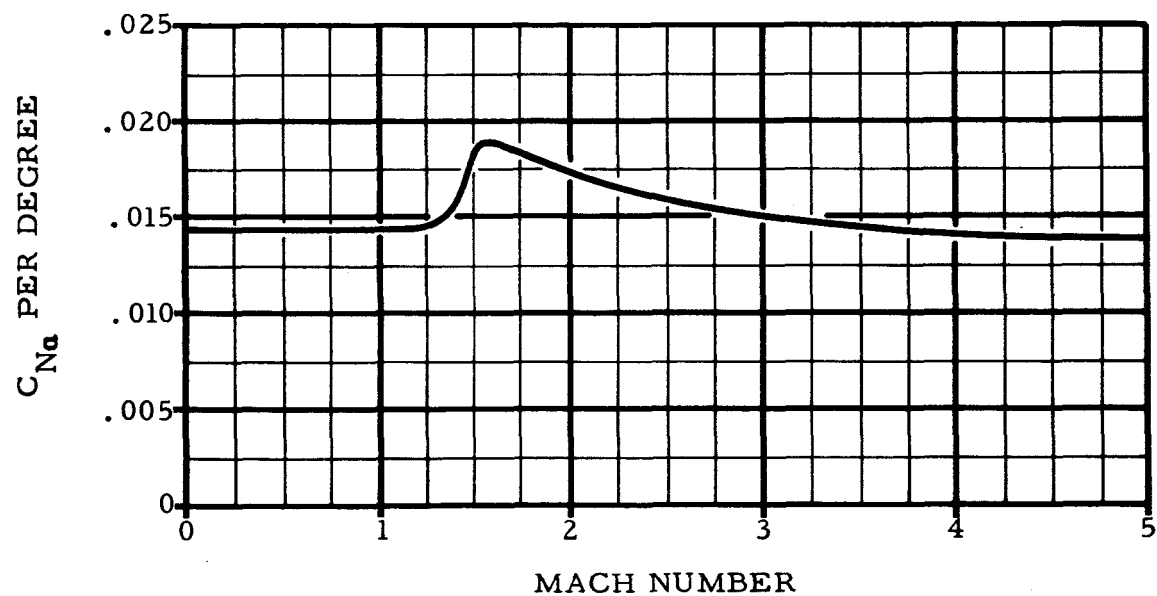


Figure II-1 Nose Cone Normal Force Coefficient Variation with Mach Number

NOTE:

25.7-INCH DIAMETER NOSE

CVA DIR NO. 86250-AM-4
MACH 3.0

1. $\Delta C_{Na} = .015$.
2. CENTER OF PRESSURE IS 7.49 INCHES FROM BASE OF CONE FOR MACH NUMBER OF 2.0 TO 5.0.
3. BASIC NOSE CONE IS 19 INCHES IN LENGTH.
TABLE SHOWS NOSE CONE STATION VARIATIONS.

BODY STATION

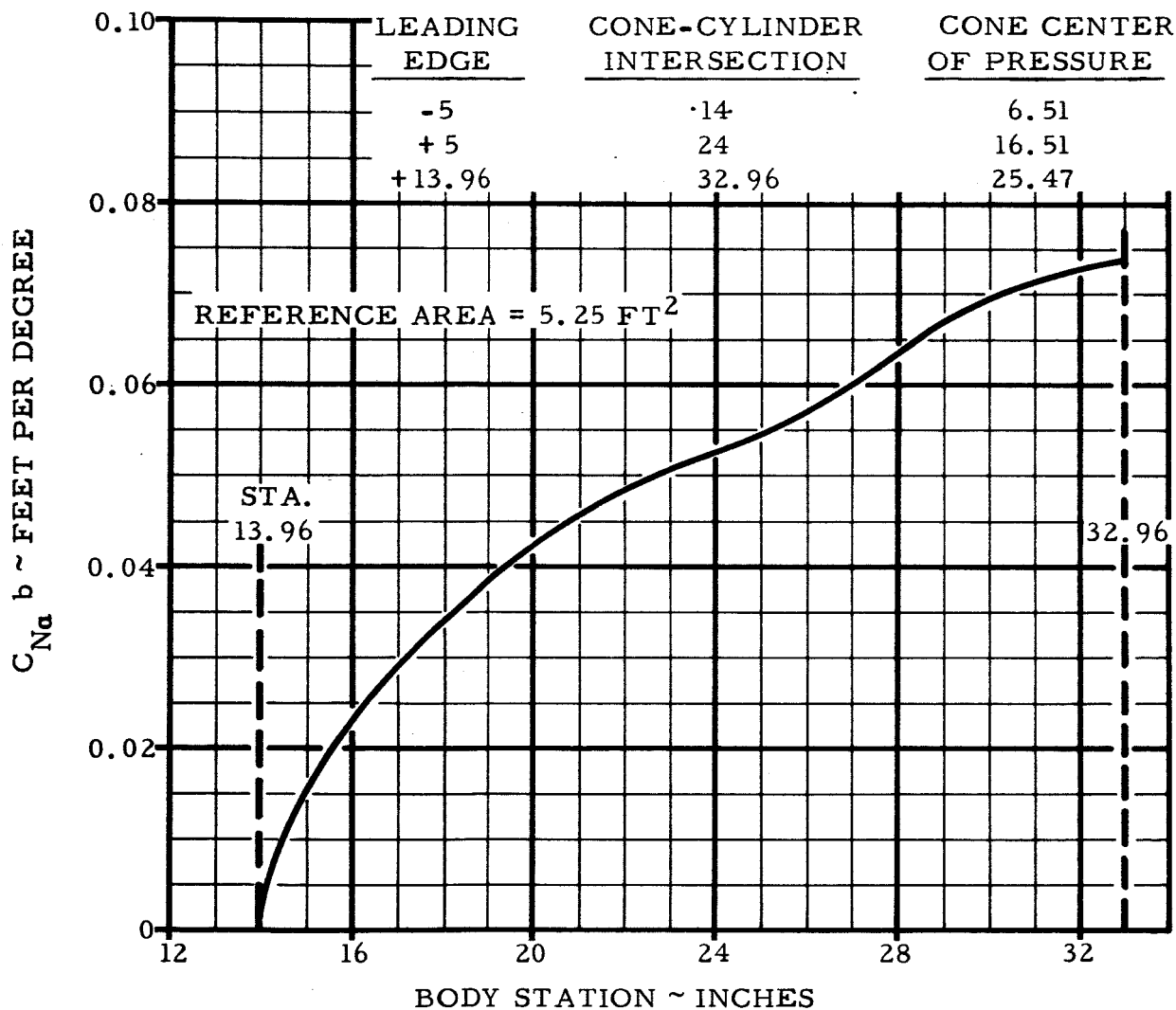
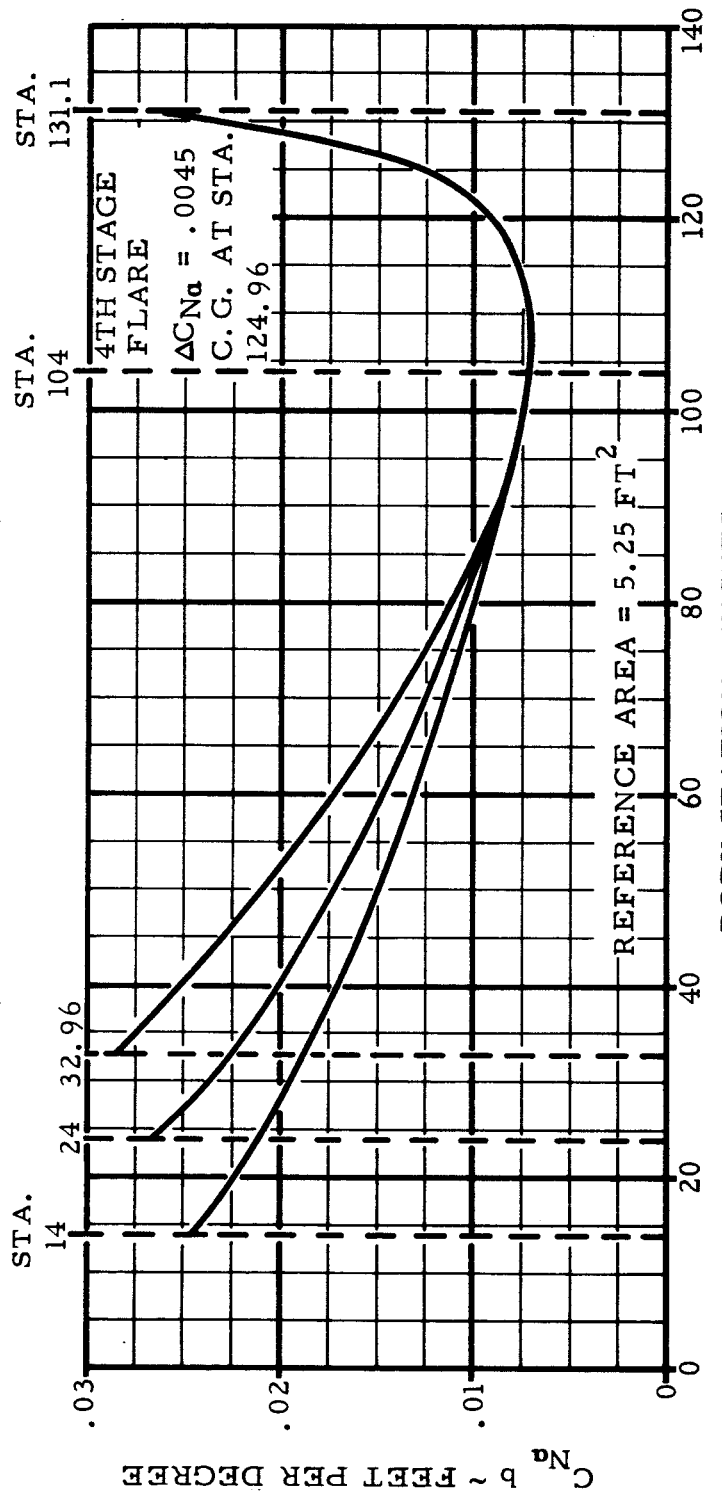


Figure II-2 Nose Cone Lift Distribution

CVA DIR NO. 86250-AM-4
MACH 2.0 TO 5.0

25.7-INCH DIAMETER NOSE

<u>NOSE STATION</u>	<u>ΔC_{Na}</u>	<u>CENTER-OF-PRESSURE BODY STATION</u>
-5	.0204	50.1
+5	.0189	55.5
+13.96	.0174	60.16



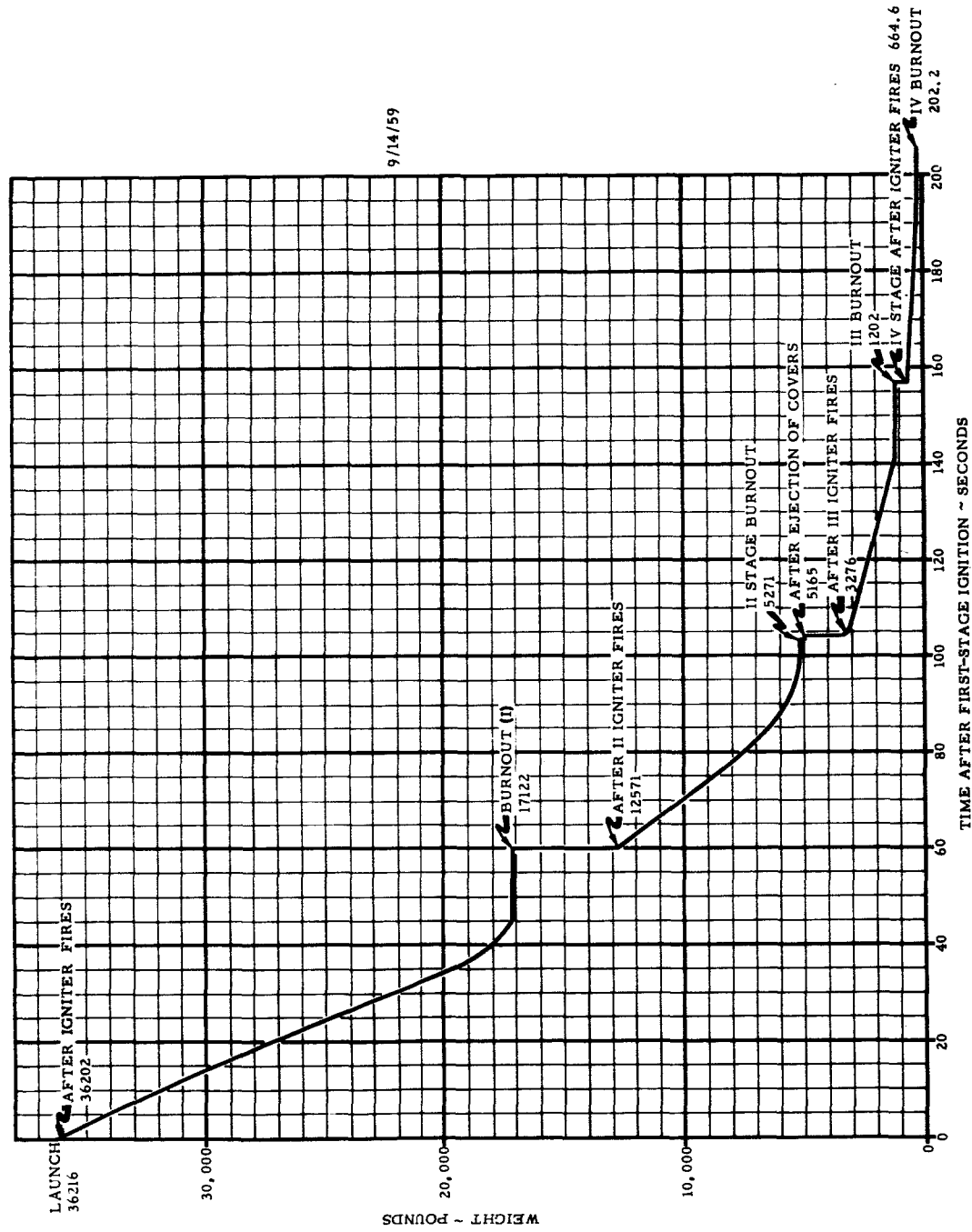
R-ED 11122
II-4

Figure II-3 Fourth-Stage Cylinder and Flare Lift Distribution

SECTION III

**WEIGHTS AND INERTIA OF FIRST THREE VEHICLES
(20-Inch Diameter Fourth Stage)**

Figure III-1 Weight Time History



R-ED 11122
III-2

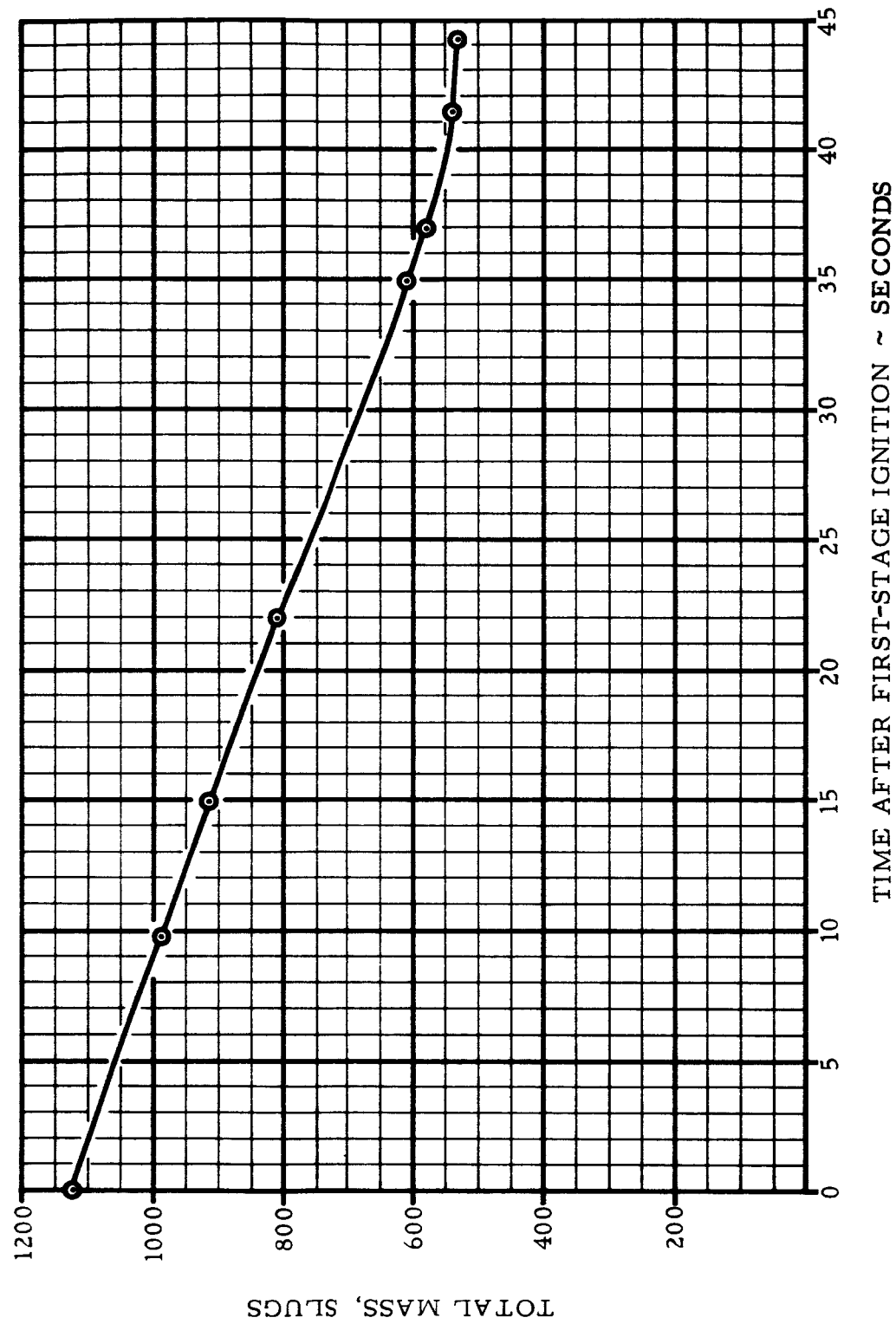


Figure III-2 First-Step Mass Vs Time

R-ED 11122
III-3

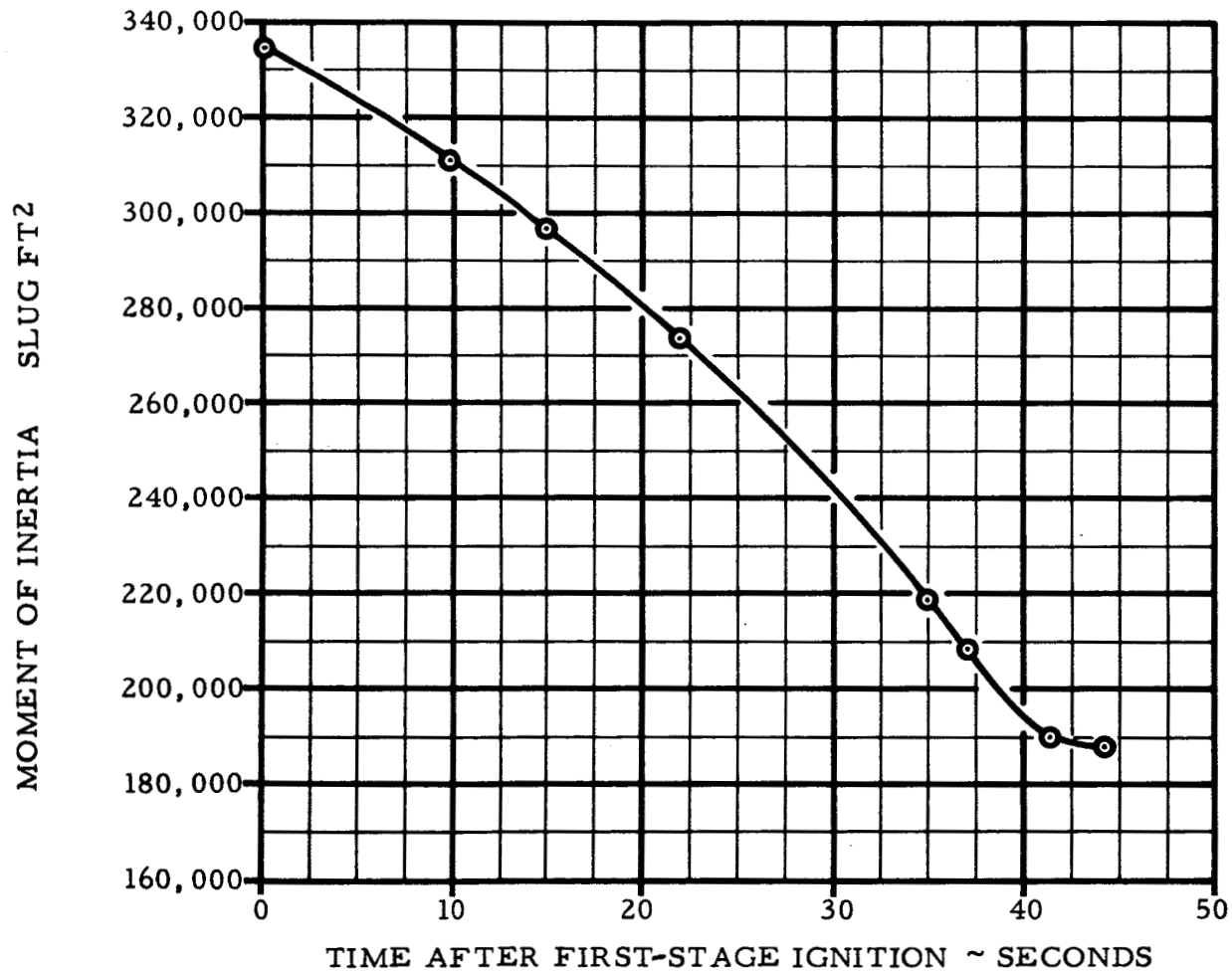


Figure III-3 First-Step Pitch or Yaw Moment of Inertia Vs Time

R-ED 11122
III-4

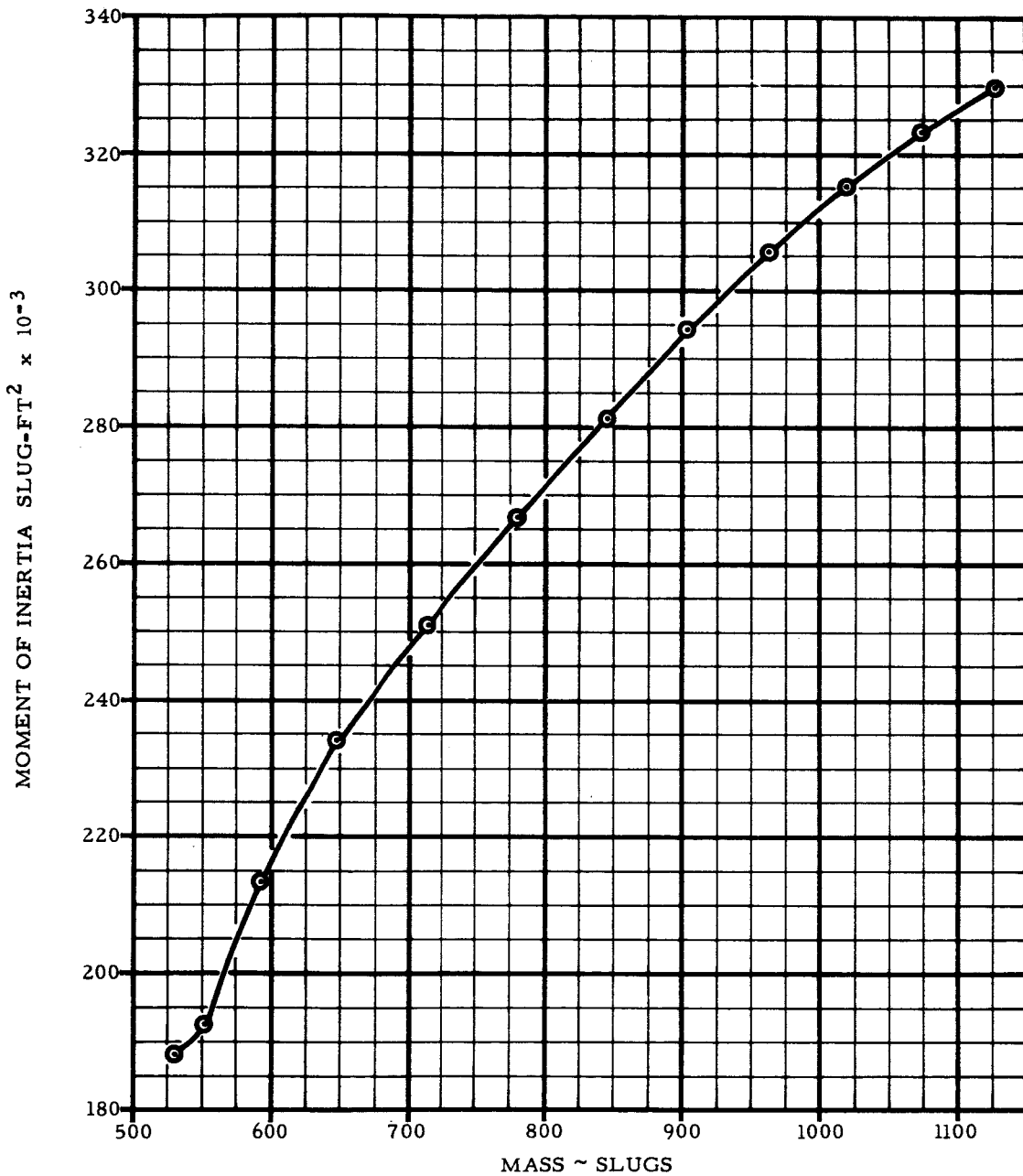


Figure III-4 First-Step Pitch or Yaw Moment of Inertia Vs Mass

R-ED 11122
III-5

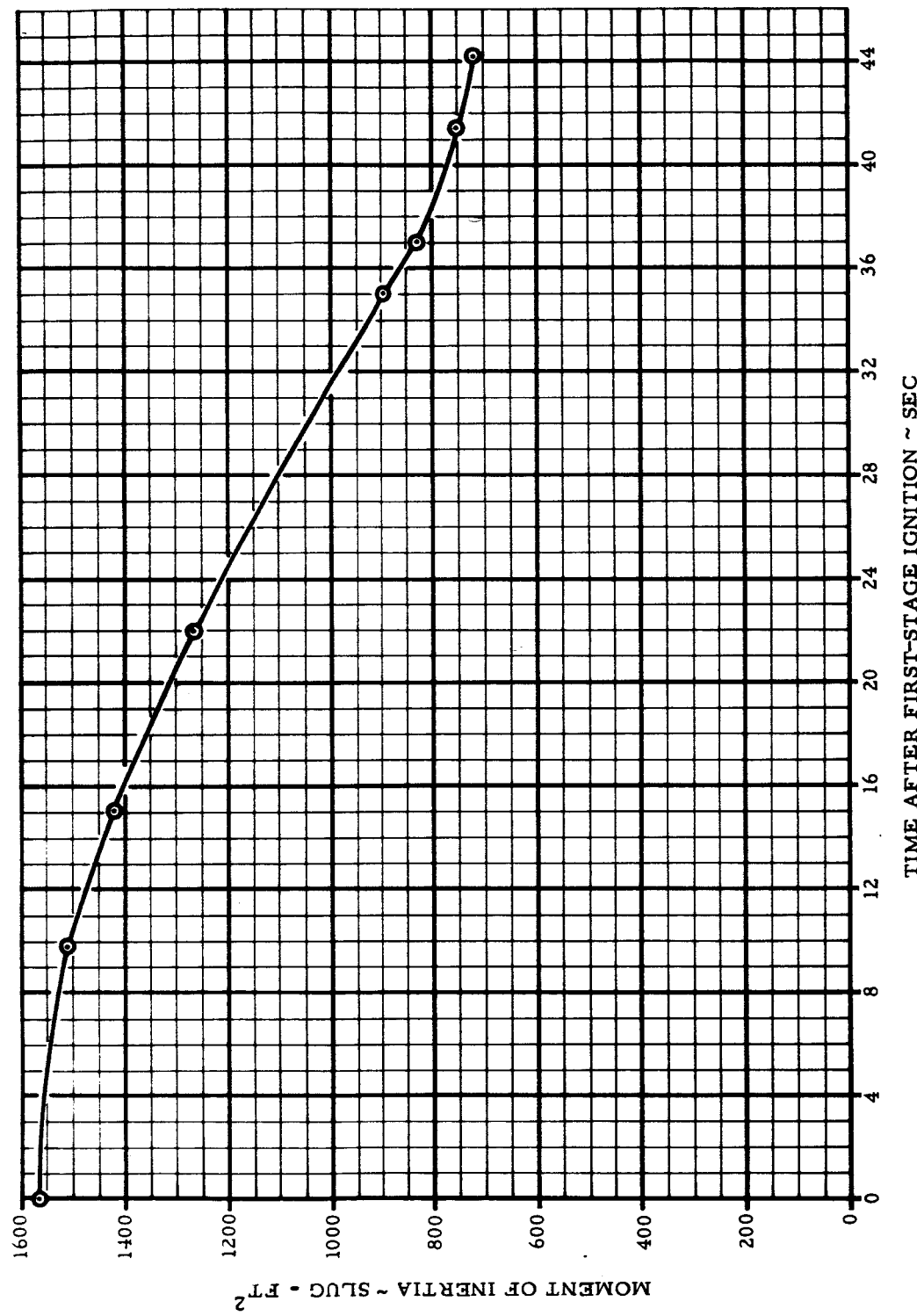


Figure III-5 First-Step Roll Moment of Inertia Vs Time

R-ED 11122
III-6

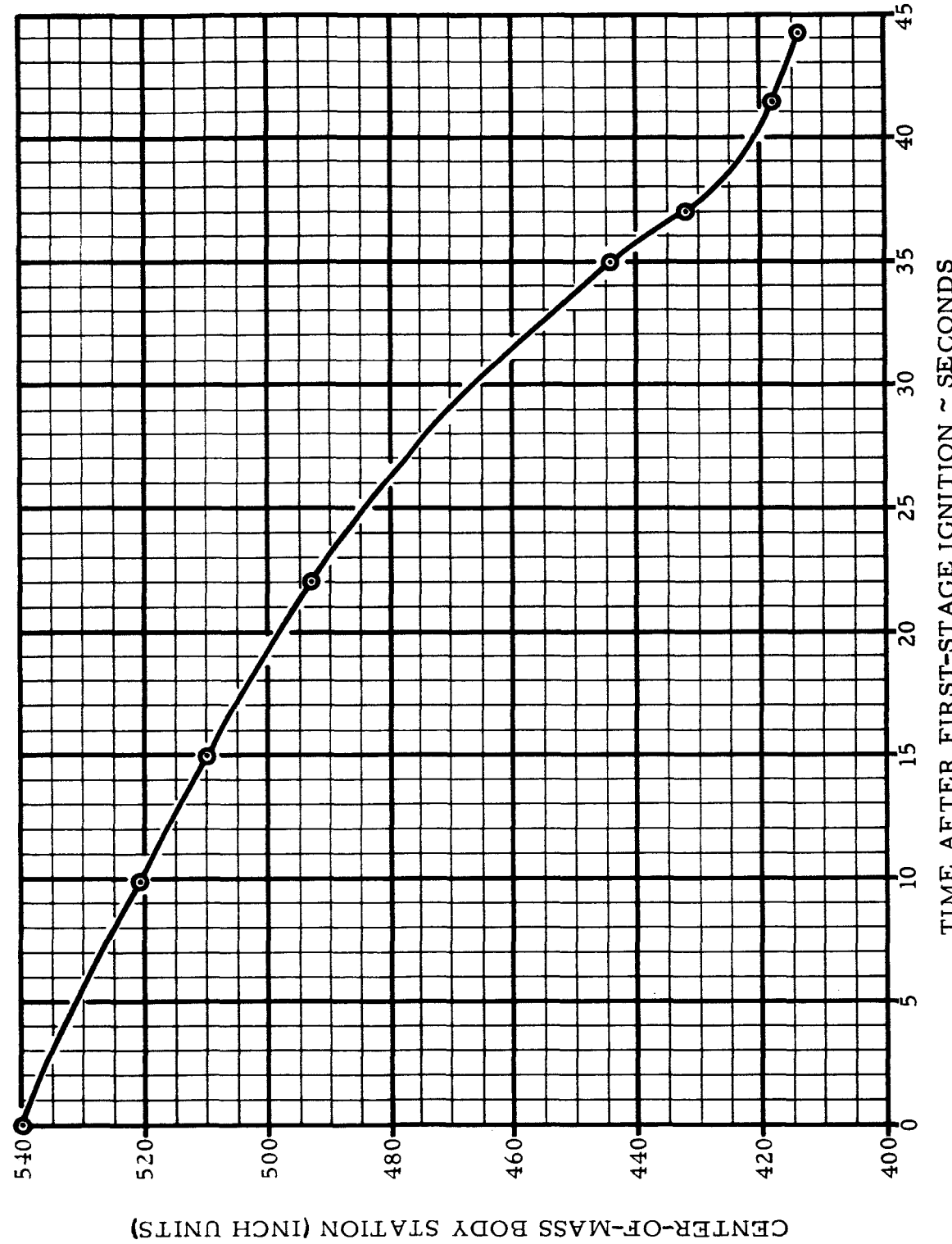


Figure III-6 First-Step Center of Mass Vs Time

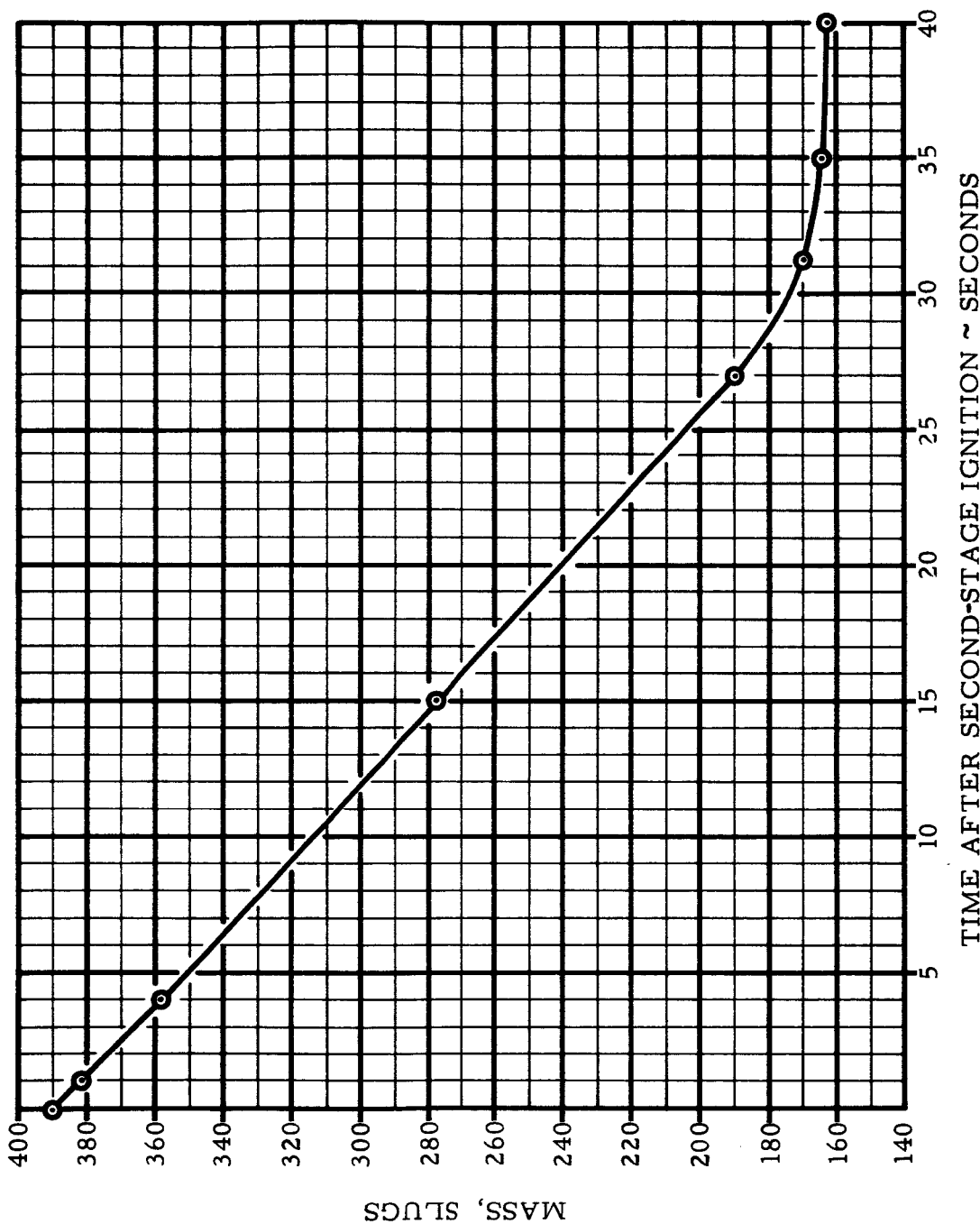


Figure III-7 Second-Step Mass Vs Time

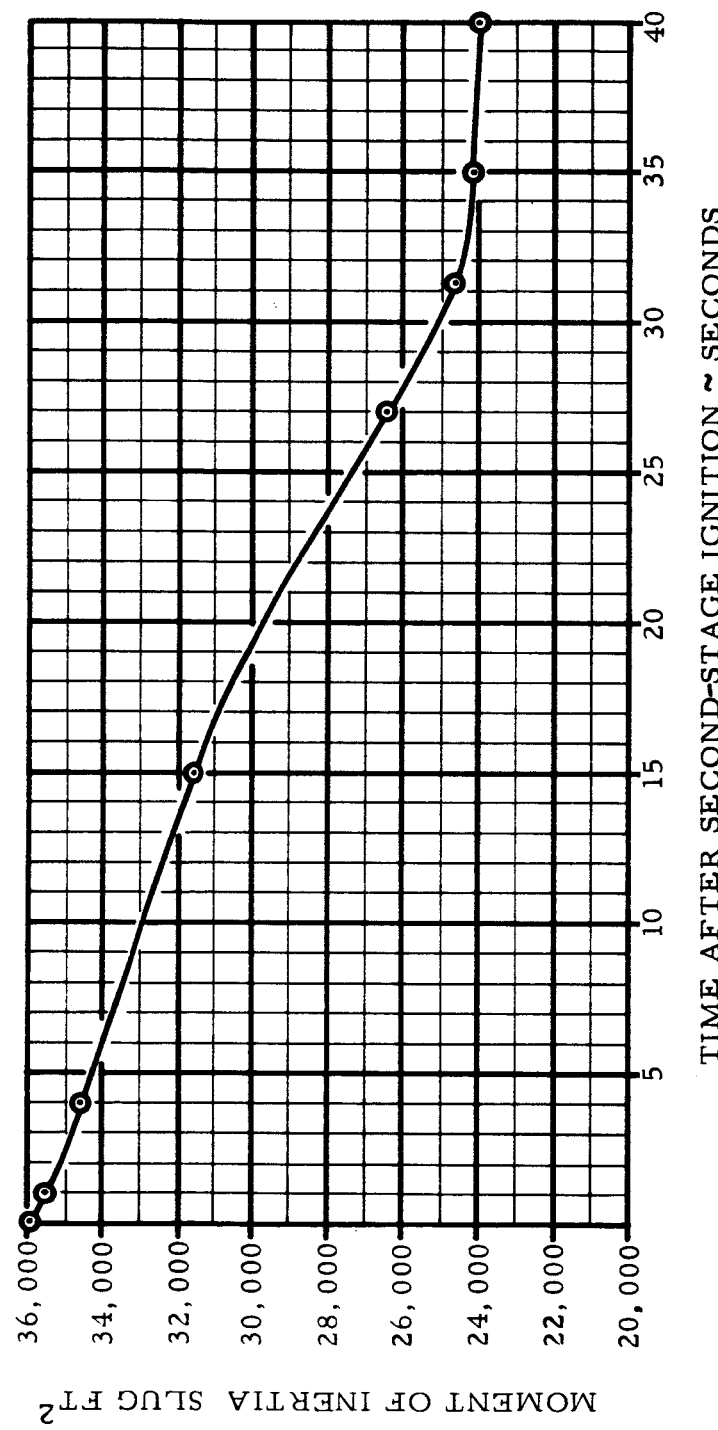


Figure III-8 Second-Step Pitch or Yaw Moment of Inertia Vs Time
III-9

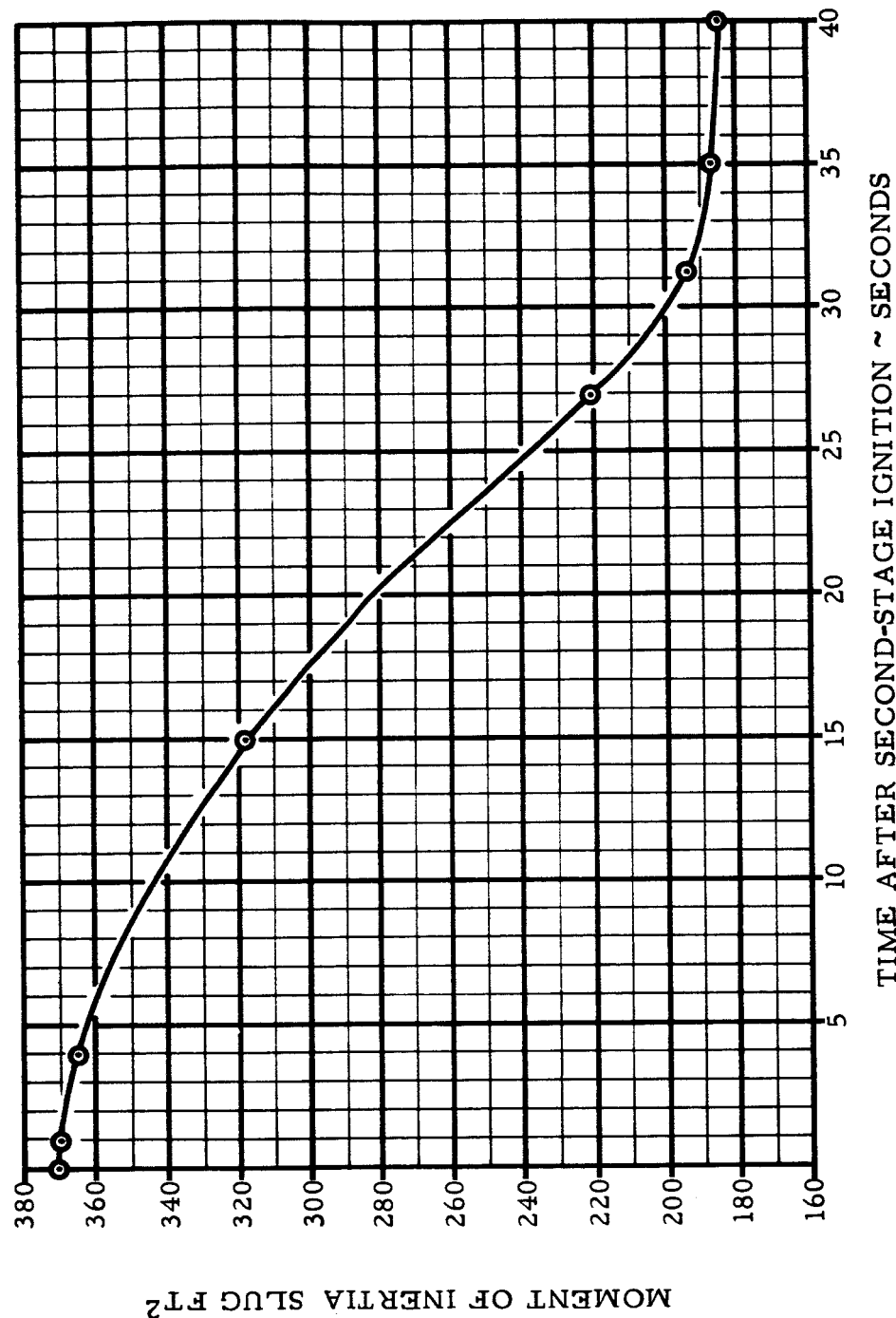


Figure III-9 Second-Step Roll Moment of Inertia Vs Time
III-10

R-ED 11122
III-10

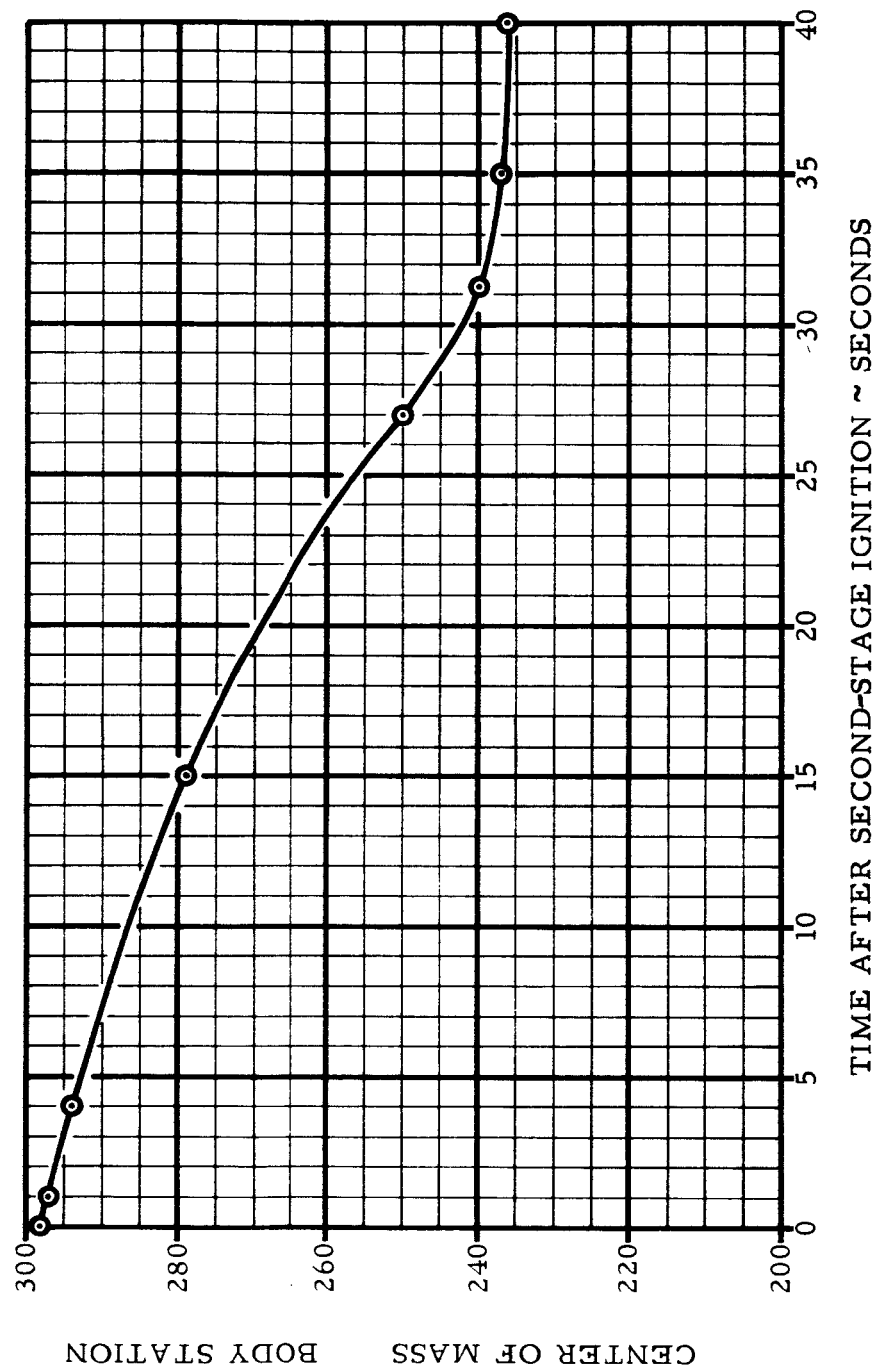


Figure III-10 Second-Step Center of Mass Vs Time

R-ED 11122
III-11

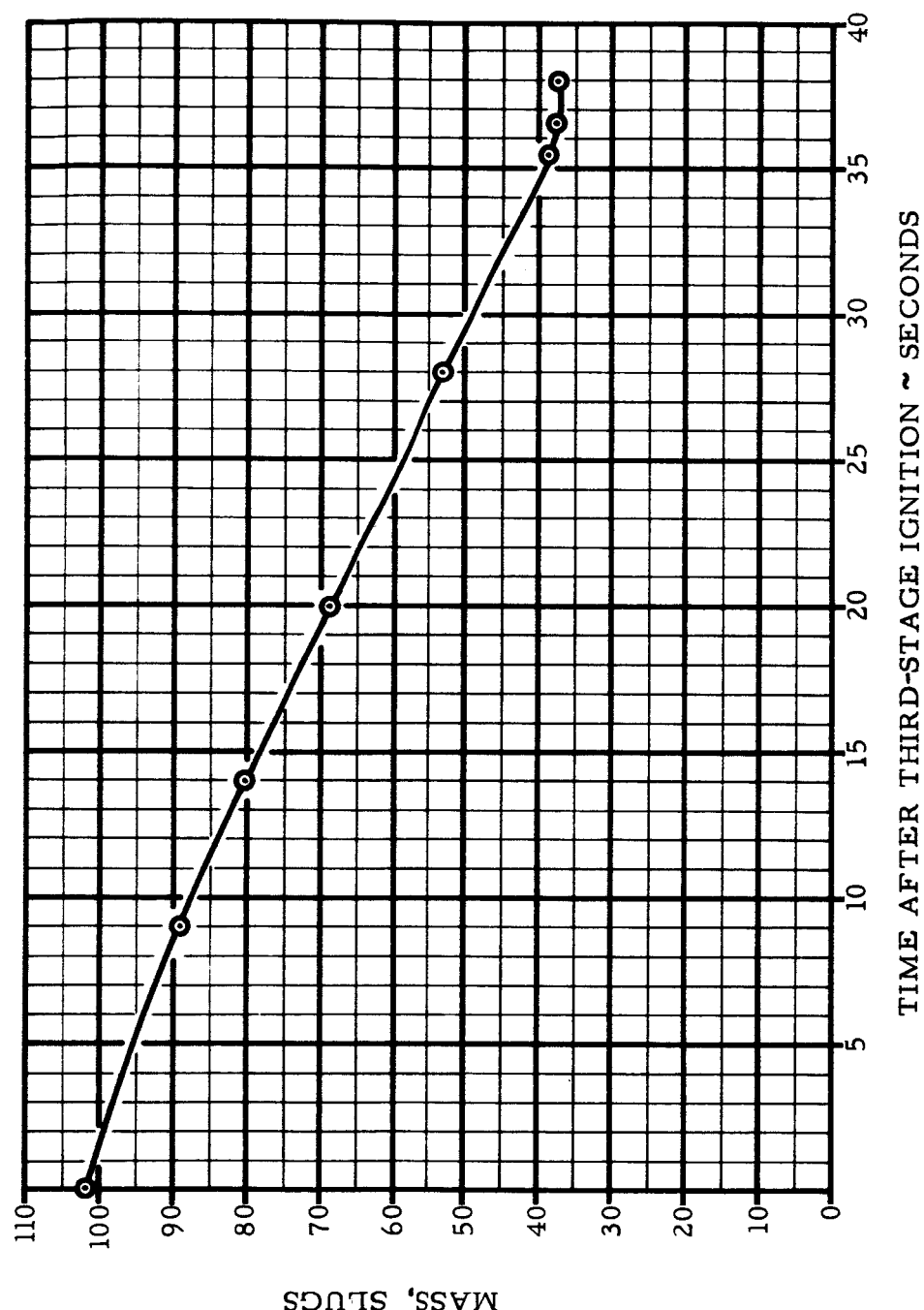


Figure III-11 Third-Step Mass Vs Time
III-12

R-ED 11122
III-12

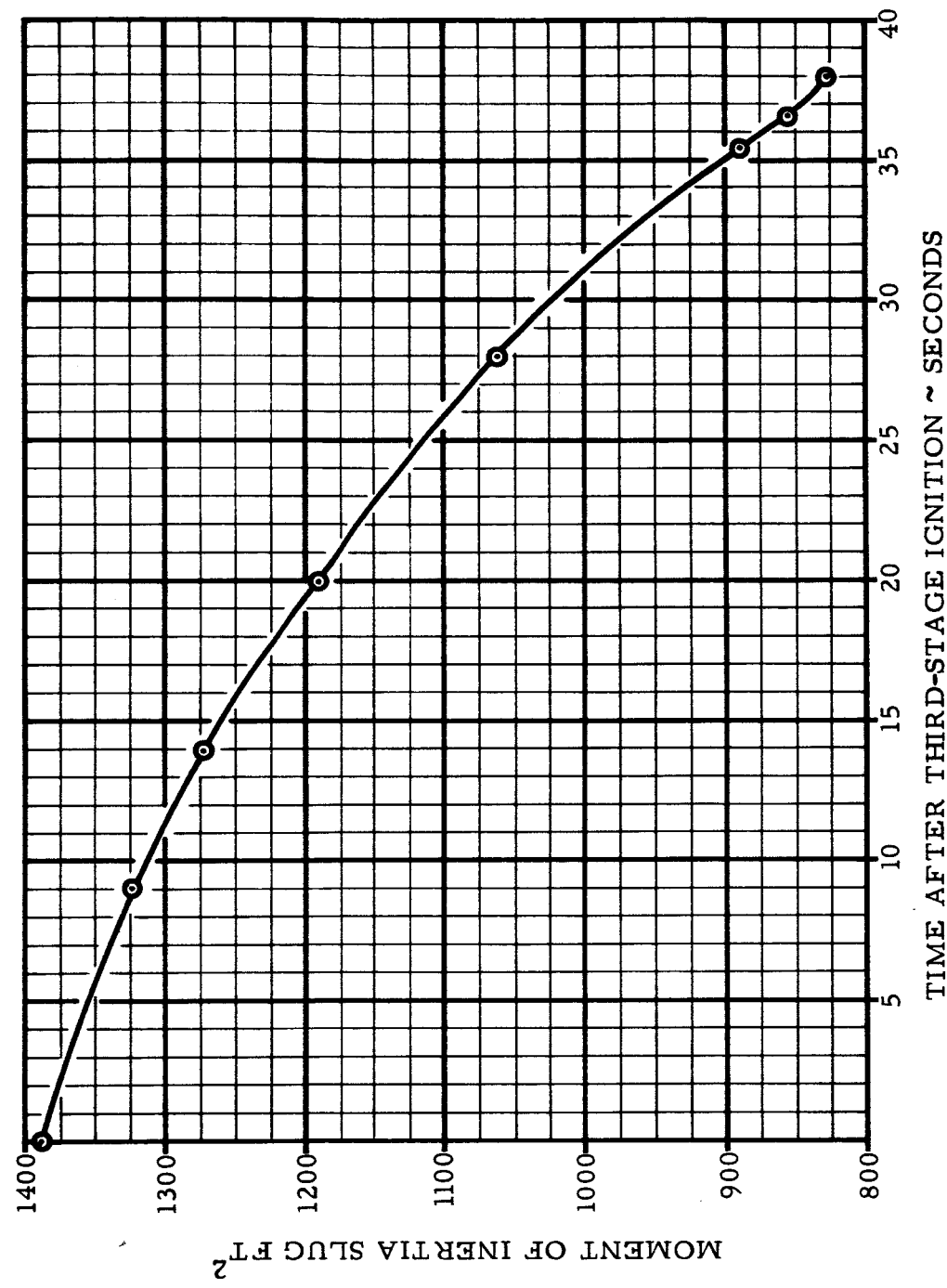
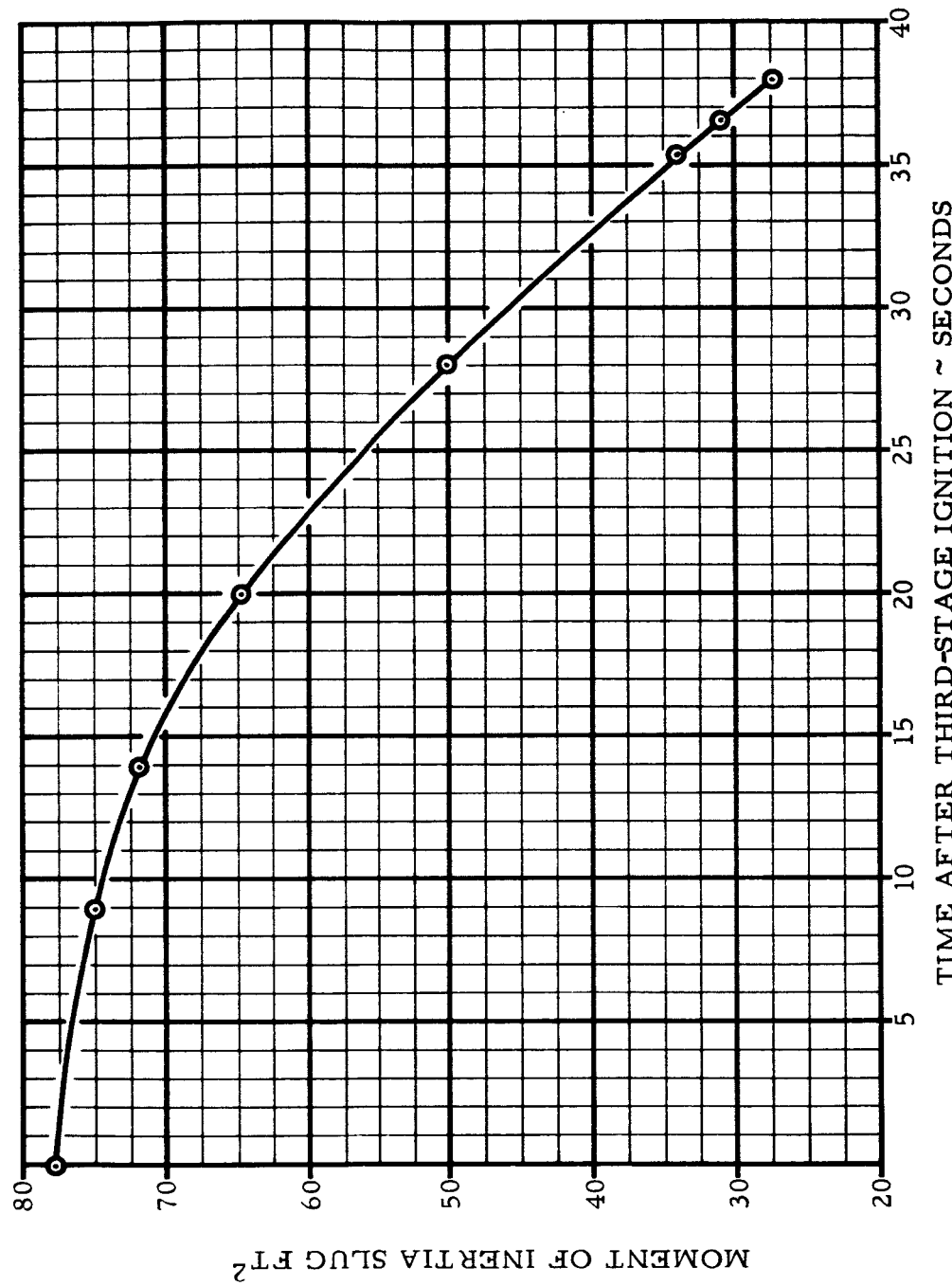


Figure III-12 Third-Step Pitch or Yaw Moment of Inertia Vs Time

R-ED 11122
III-13

Figure III-13 Third-Step Roll Moment of Inertia Vs Time



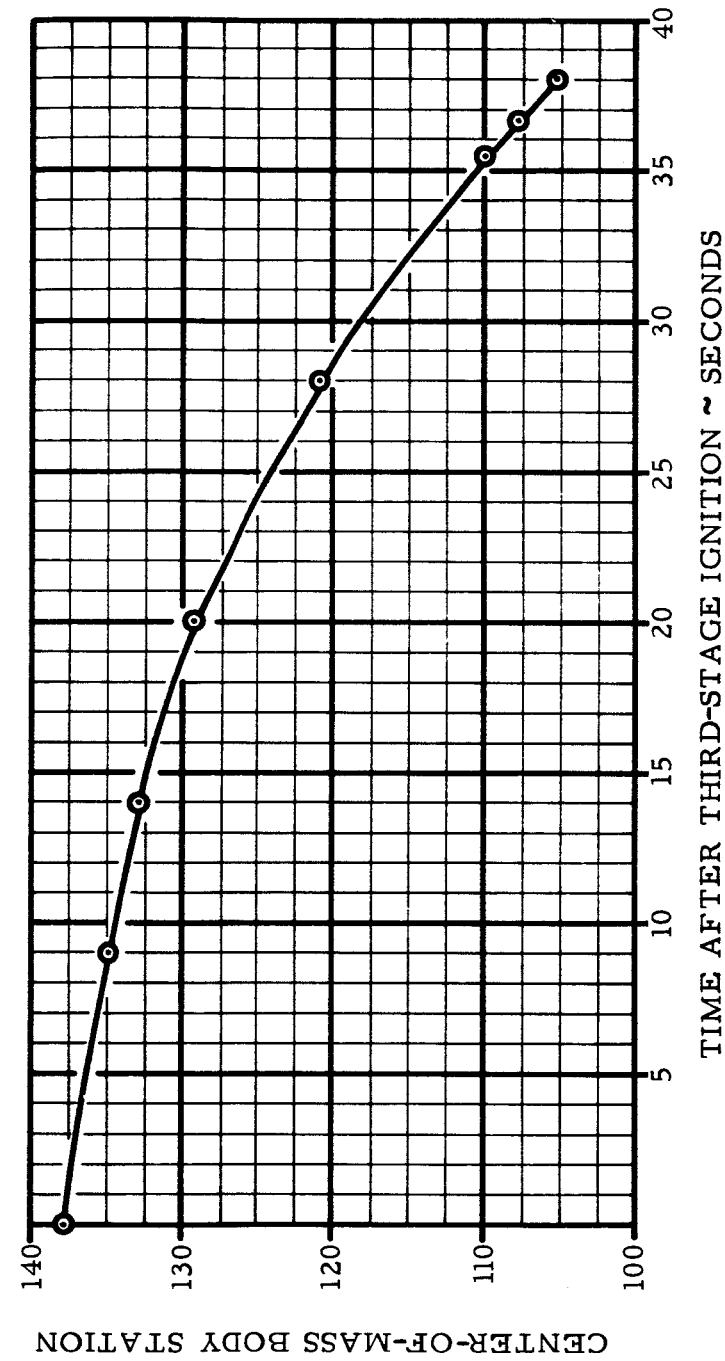


Figure III-14 Third-Step Center of Mass Vs Time

R-ED 11122
III-15

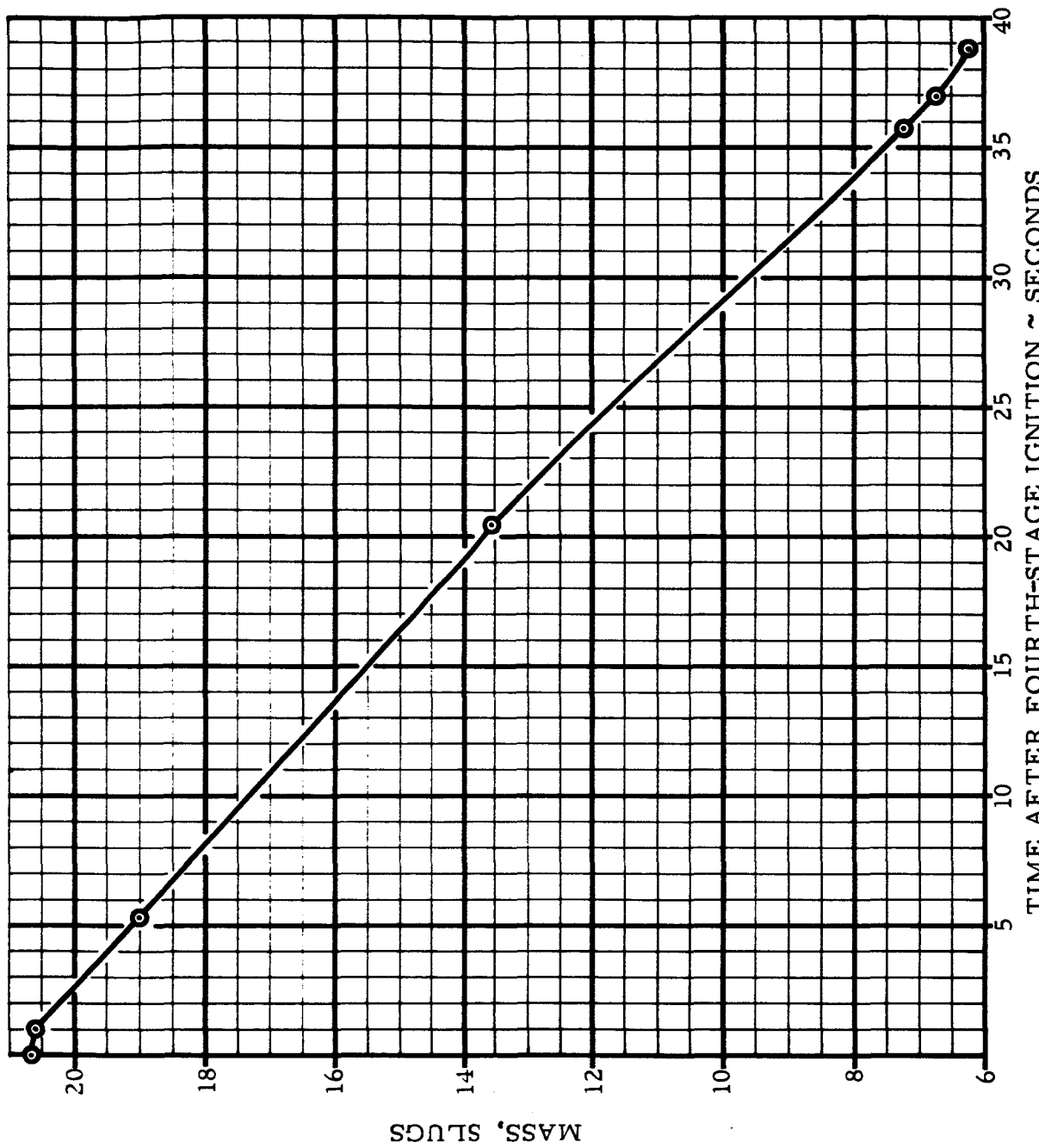
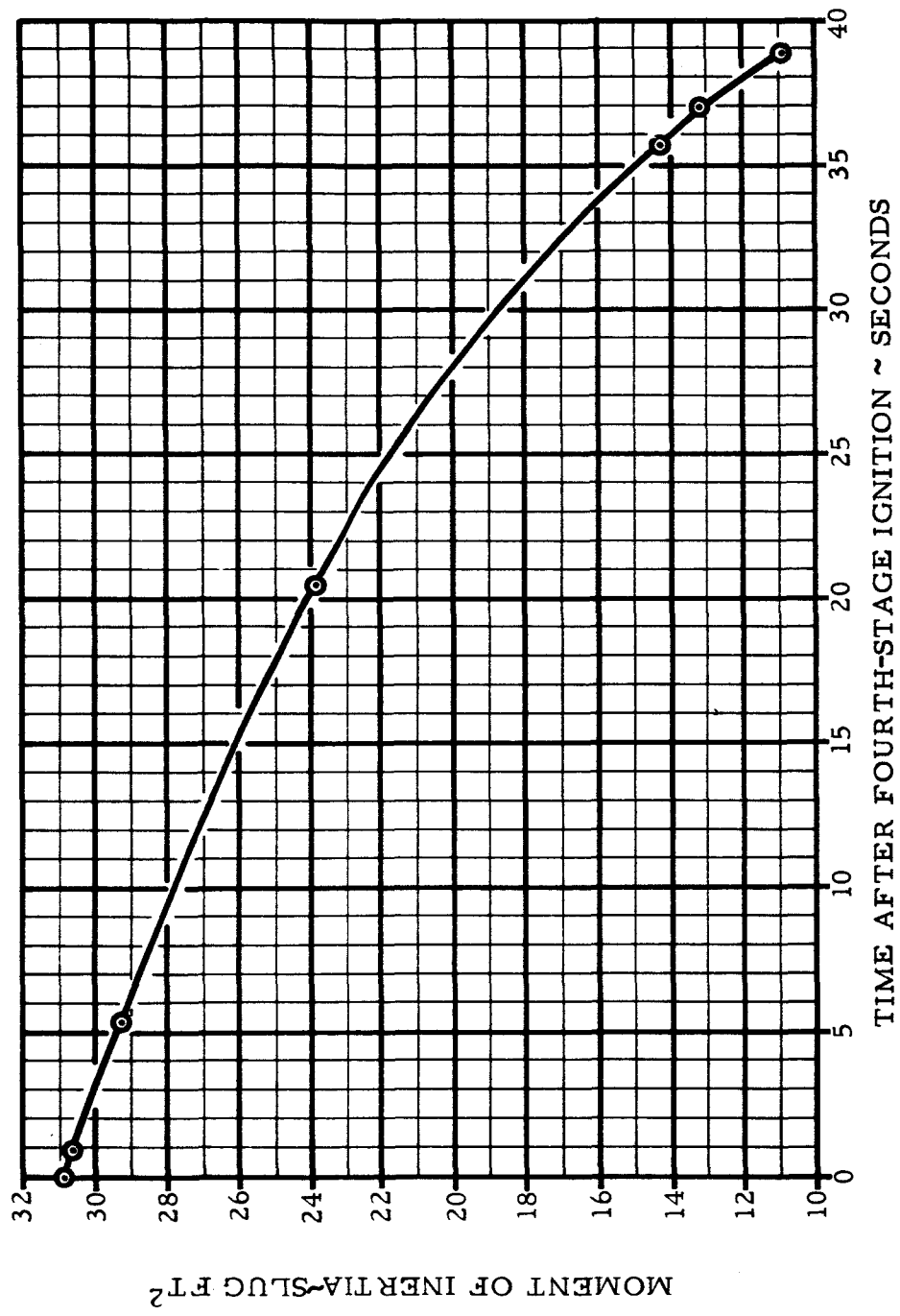


Figure III-15 Fourth-Step Mass Vs Time

R-ED 11122
III-16

Figure III-16 Fourth-Step Pitch or Yaw Moment of Inertia Vs Time



R-ED 11122
III-17

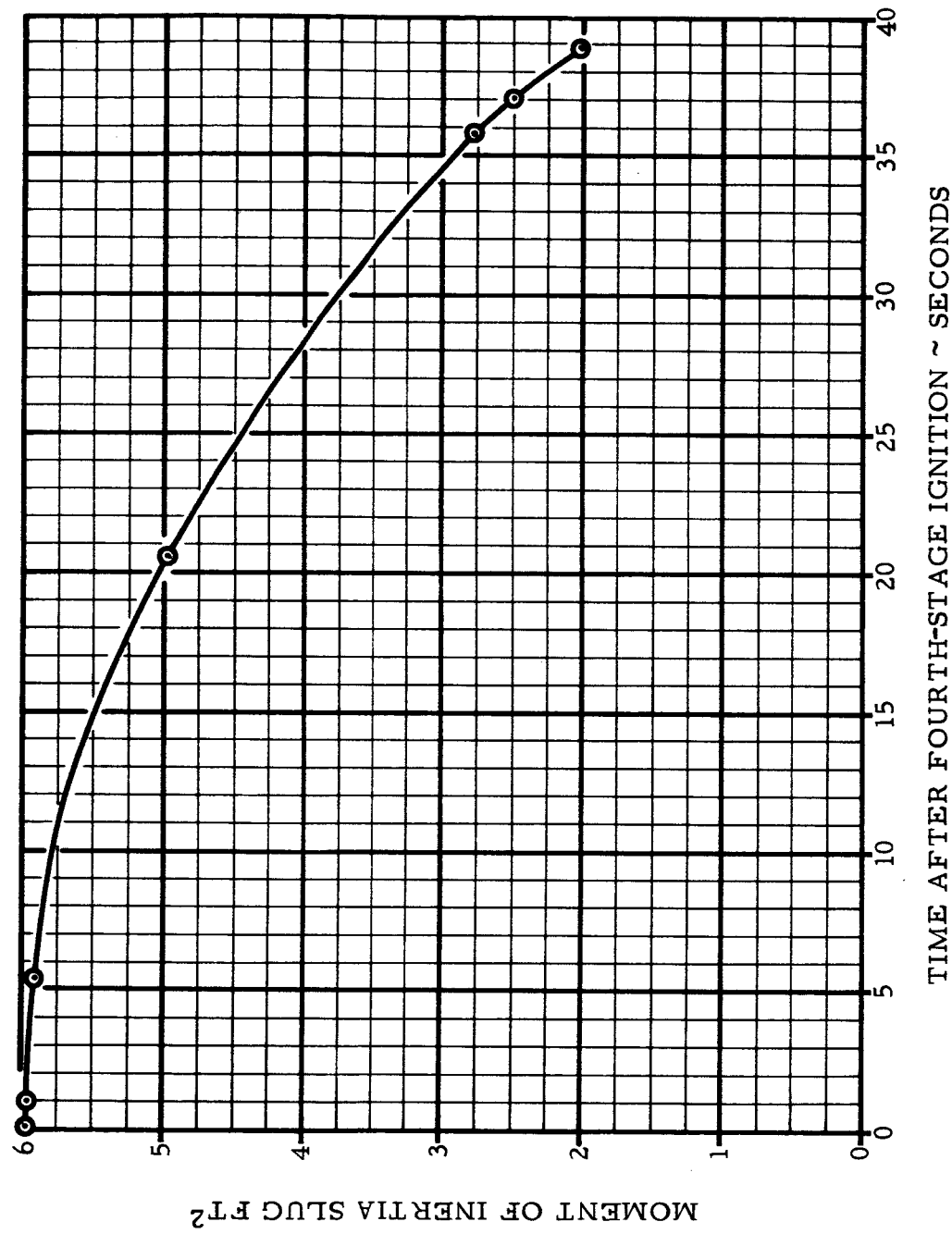


Figure III-17 Fourth-Step Roll Moment of Inertia Vs Time

R-ED 11122
III-18

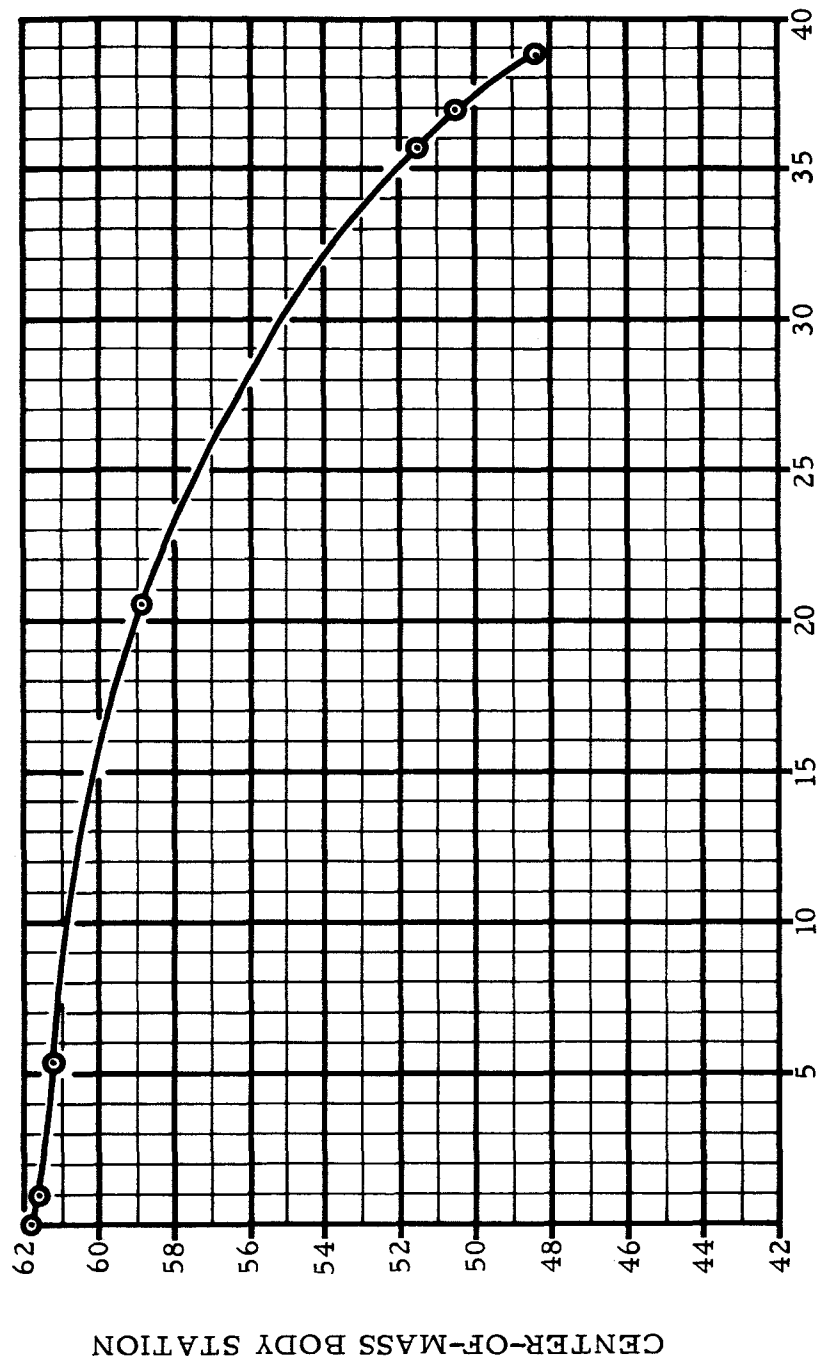


Figure III-18 Fourth-Step Center of Mass Vs Time

R-ED 11122
III-19

SECTION IV

**WEIGHTS AND INERTIA OF FOURTH VEHICLE
(25.7-Inch Diameter Fourth Stage)**

**R-ED 11122
IV-1**

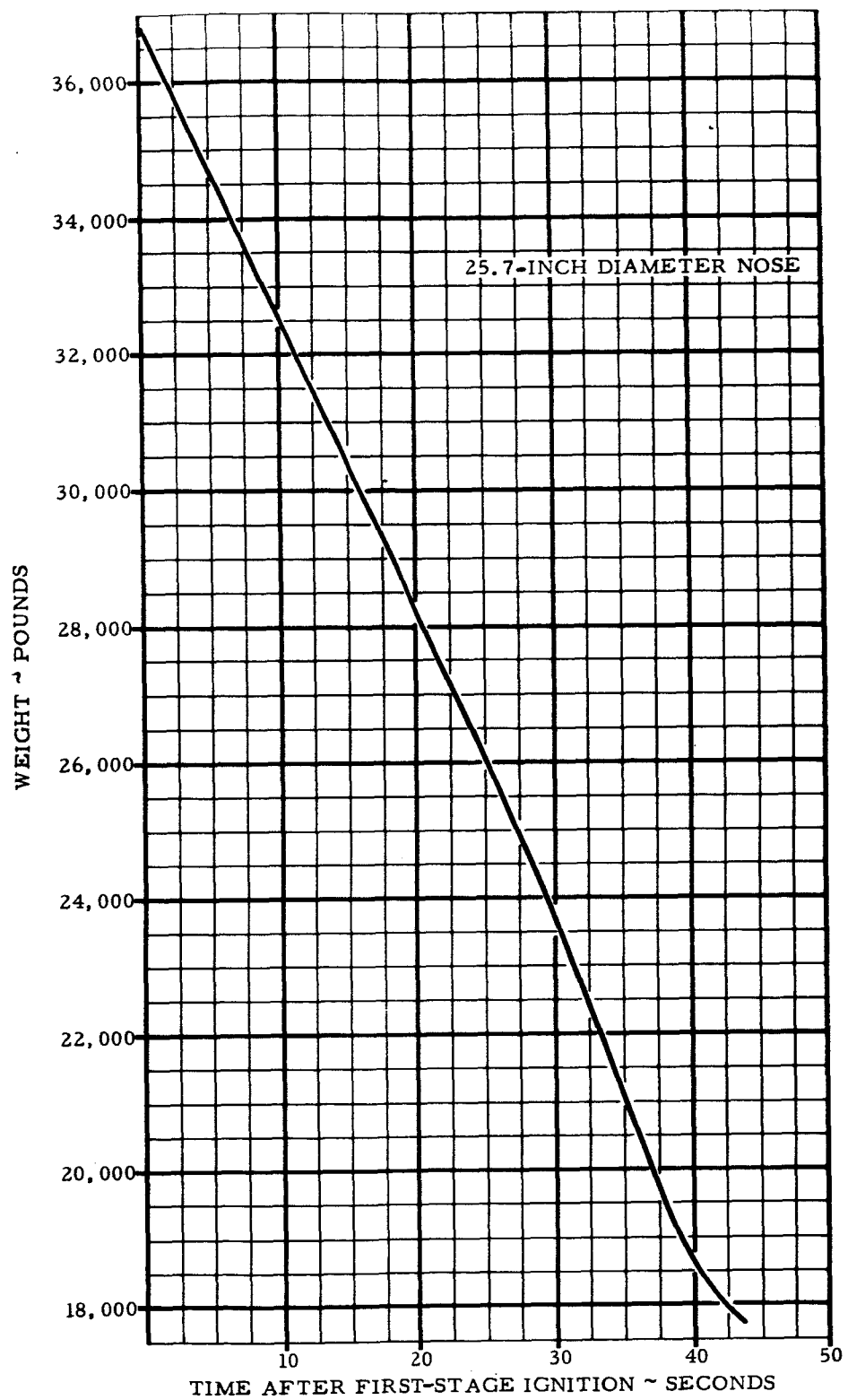


Figure IV-1 First-Step Weight Vs Time

R-ED 11122
IV-2

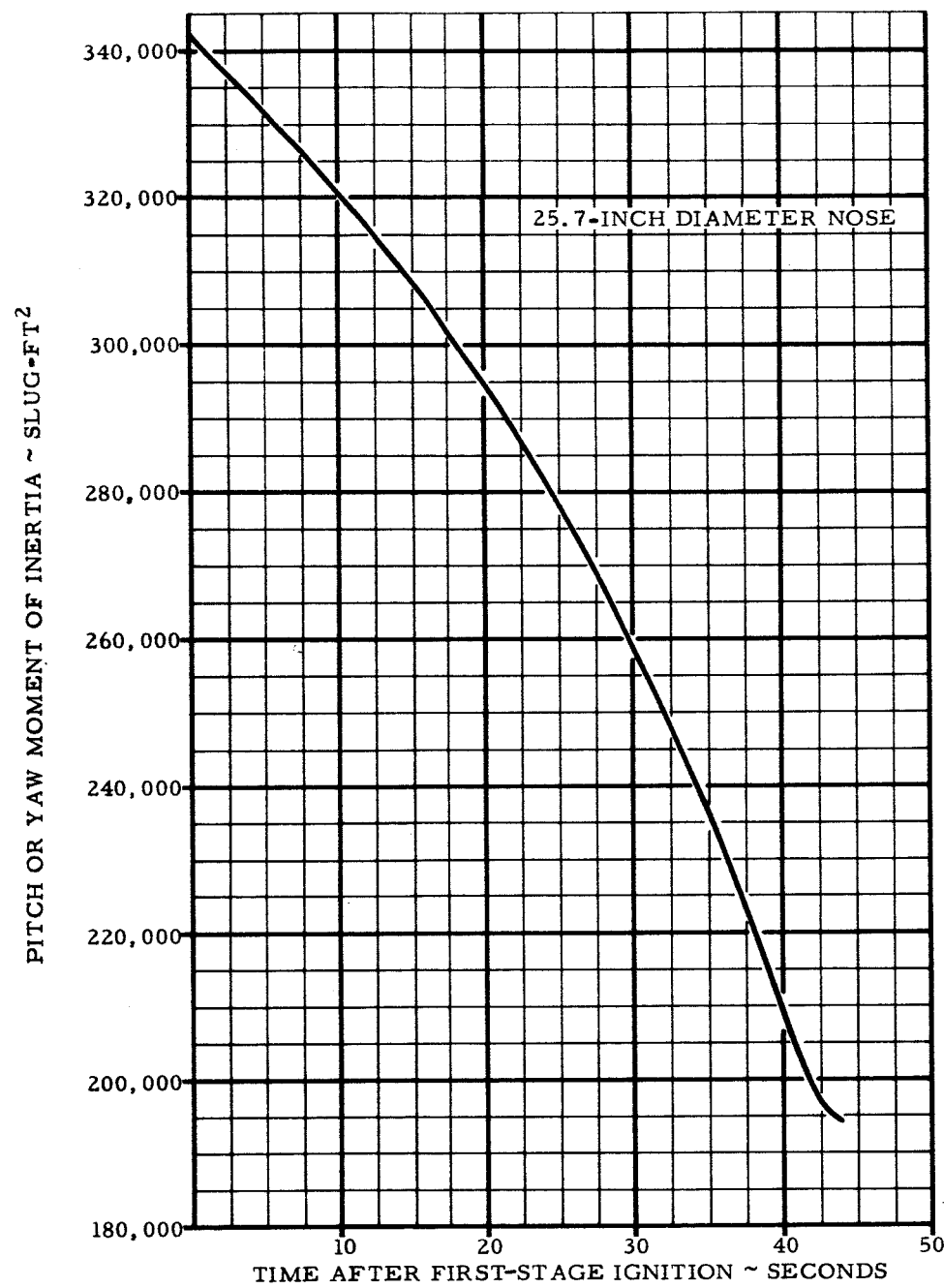


Figure IV-2 First-Step Pitch and Yaw Moment of Inertia Vs Time

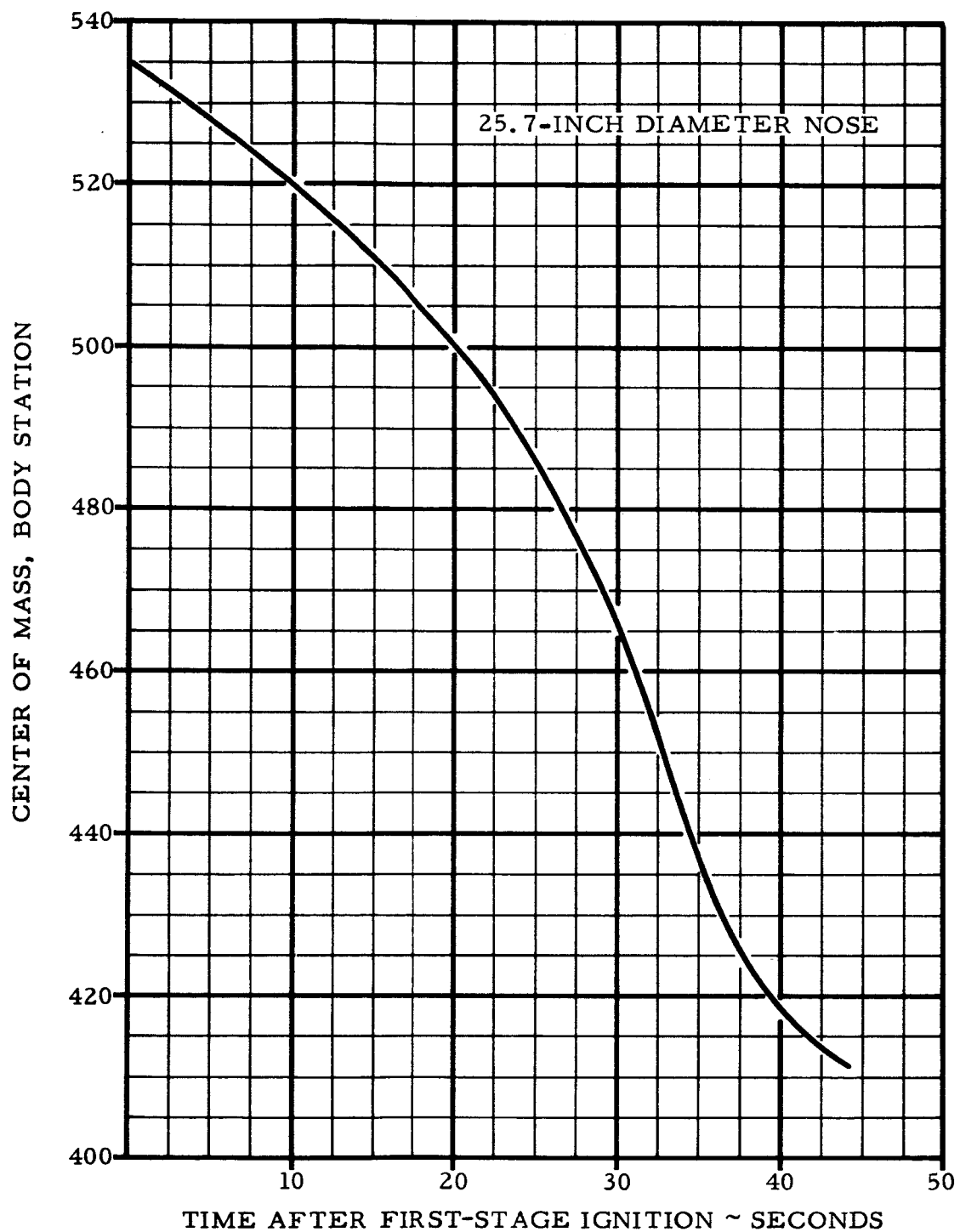


Figure IV-3 First-Step Center-of-Mass Location Vs Time

SECTION V

**STRUCTURE OF FIRST THREE VEHICLES
(20-Inch Diameter Fourth Stage)**

**R-ED 11122
V-1**

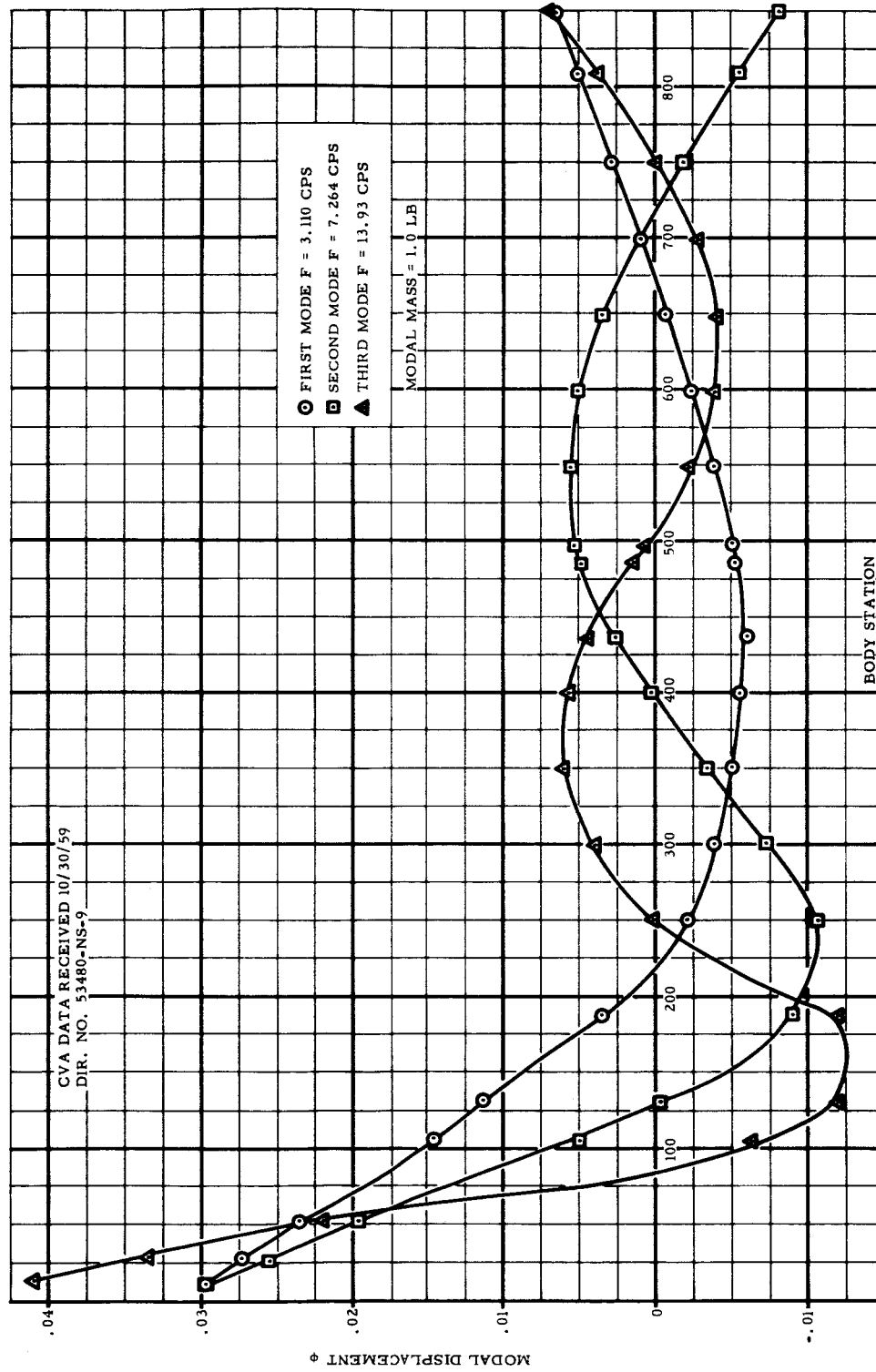


Figure V-1 First-Step Bending-Mode Shapes and Frequencies at Launch

R-ED 11122
V-2

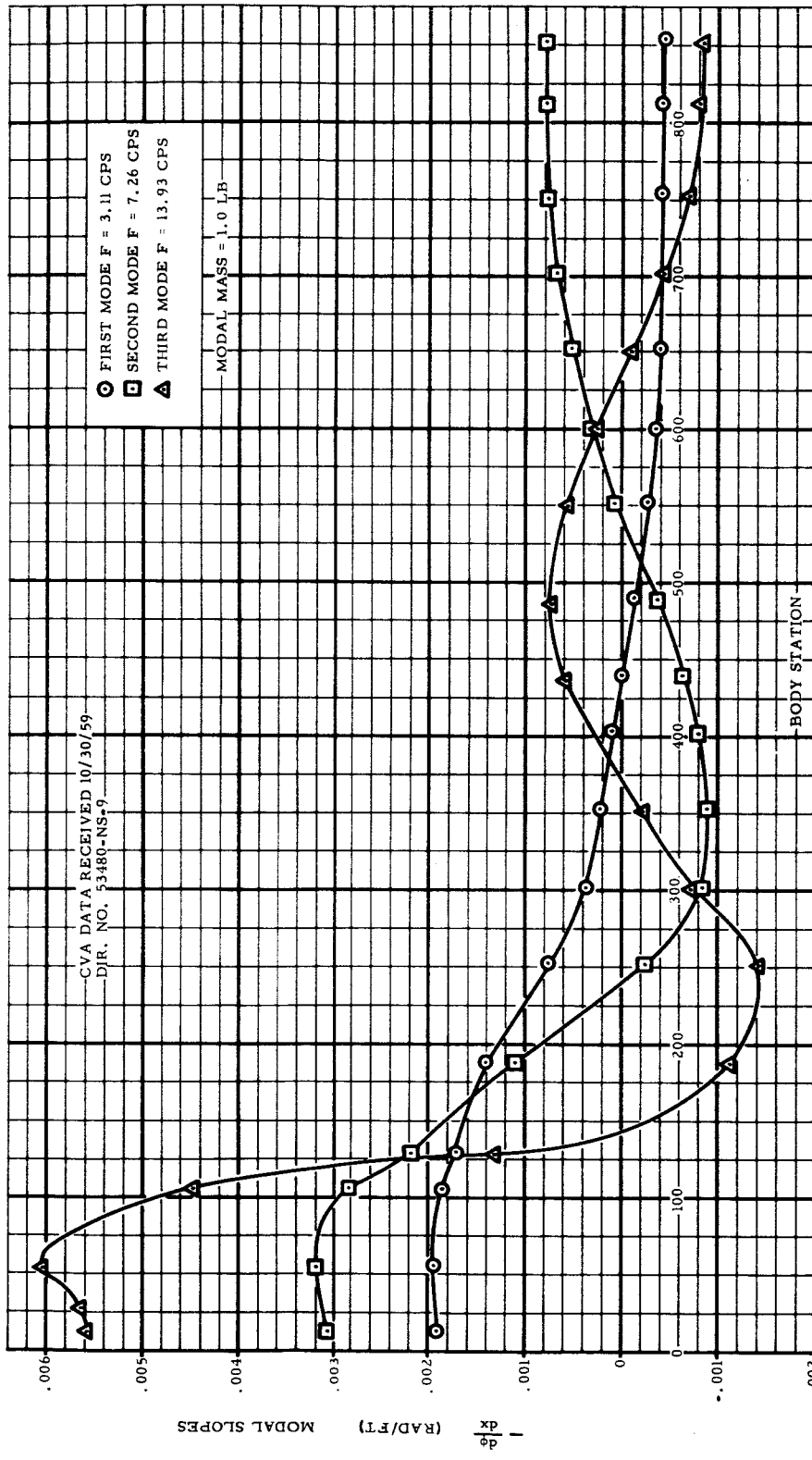


Figure V-2 First-Step Bending-Mode Slopes at Launch

R-ED 11122
V-3

Tabulated Data Taken from CVA DIR No. 53480-NS-9 of 10/30/59

CONFIGURATION		CONDITIONS				
Structural Shell over Fourth Step Modal Mass for Each Mode = 1.0 Lb		Launch 150-Lb Payload Nose at Body-Station 5				
Body Station (x)	1st Mode $f^* = 3.11$ cps	2nd Mode $f^* = 7.26$ cps		3rd Mode $f^* = 13.93$ cps		
	(Inch / Inch)	(Rad/Inch)	(Inch/Inch)	(Rad/Inch)	(Inch/Inch)	(Rad/Inch)
12	.02974	-.1563	.02977	-.2555	.04098	-.4657
28	.02724	-.1567	.02568	-.2570	.03352	-.4708
52	.02347	-.1590	.01948	-.2665	.02210	-.5046
105	.01494	-.1519	.00493	-.2345	-.00616	-.3719
131	.01123	-.1403	-.00013	-.1754	-.01164	-.1088
188	.00338	-.1140	-.00903	-.0913	-.01204	.0960
250	-.00222	-.0610	-.01067	.0210	.00030	.1368
300	-.00380	-.0272	-.00725	.0725	.00403	.0578
350	-.00494	-.0174	-.00342	.0762	.00608	.0184
400	-.00554	-.0069	.00037	.0707	.00586	-.0226
437	-.00561	.0034	.00280	.0551	.00435	-.0488
486	-.00519	.0130	.00498	.0356	.00158	-.0632
498	-.00498	.0202	.00530	.0165	.00074	-.0621
550	-.00379	.0254	.00564	-.0031	-.00209	-.0445
600	-.00239	.0300	.00500	-.0221	-.00382	-.0199
650	-.00079	.0335	.00343	-.0392	-.00407	.0110
700	.00096	.0360	.00108	-.0524	-.00272	.0400
750	.00281	.0373	-.00180	-.0603	-.00008	.0603
810	.00507	.0378	-.00558	-.0632	.00399	.0688
850	.00659	.0378	-.00812	-.0635	.00679	.0700

f^* = Bending-mode frequency

Table V-1 First-Step Bending-Mode Shape and Slope at Launch

R-ED 11122

V-4

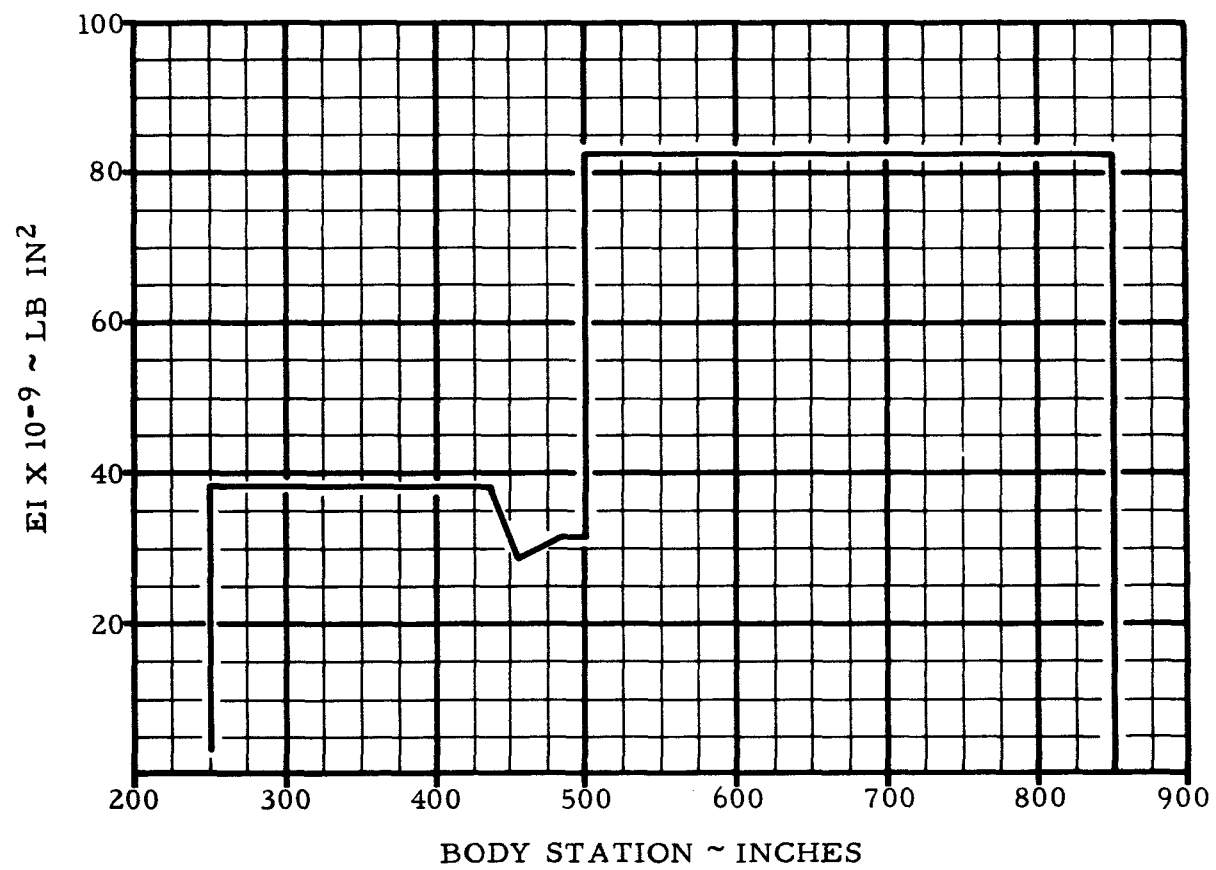


Figure V-3 First-Step Stiffness Distribution of First and Second Stages

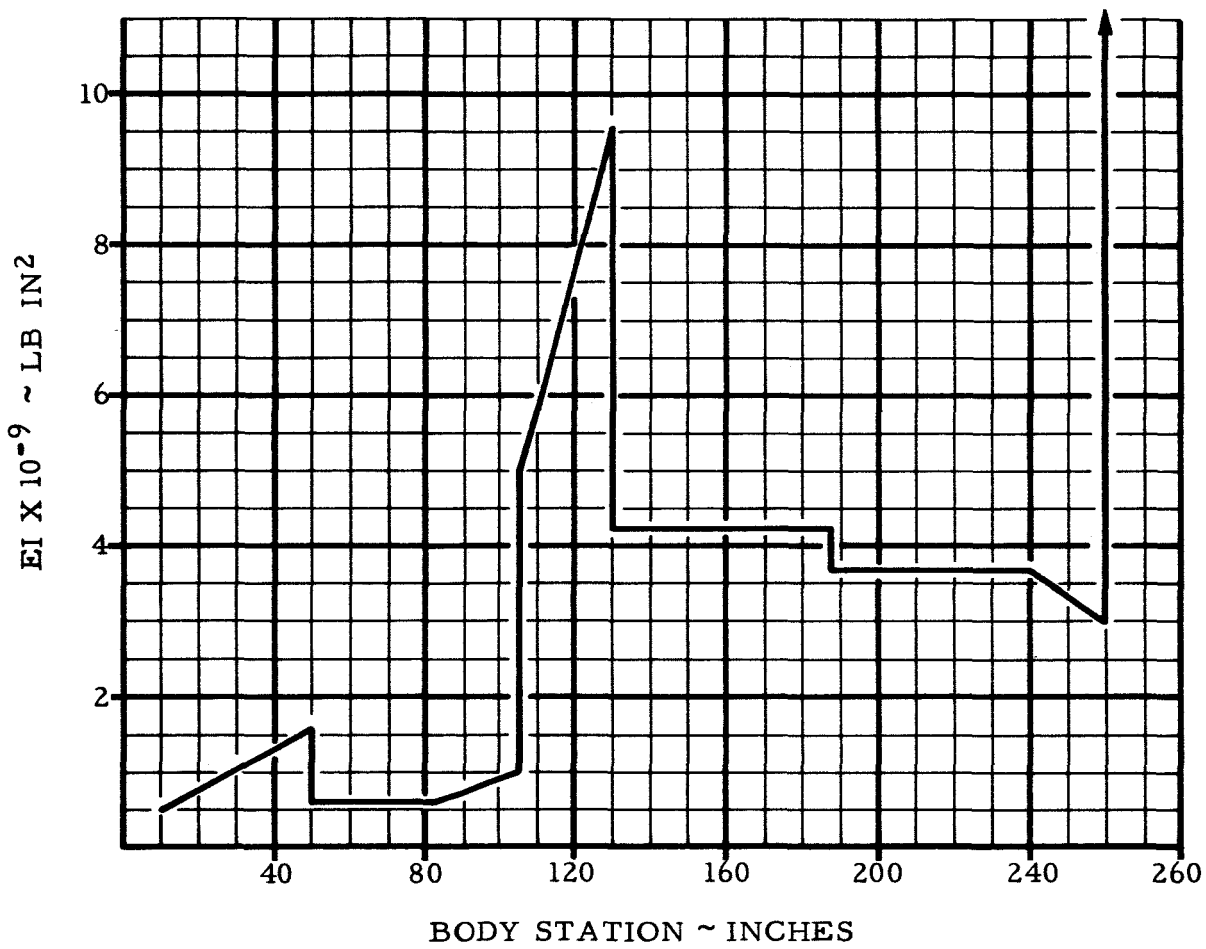
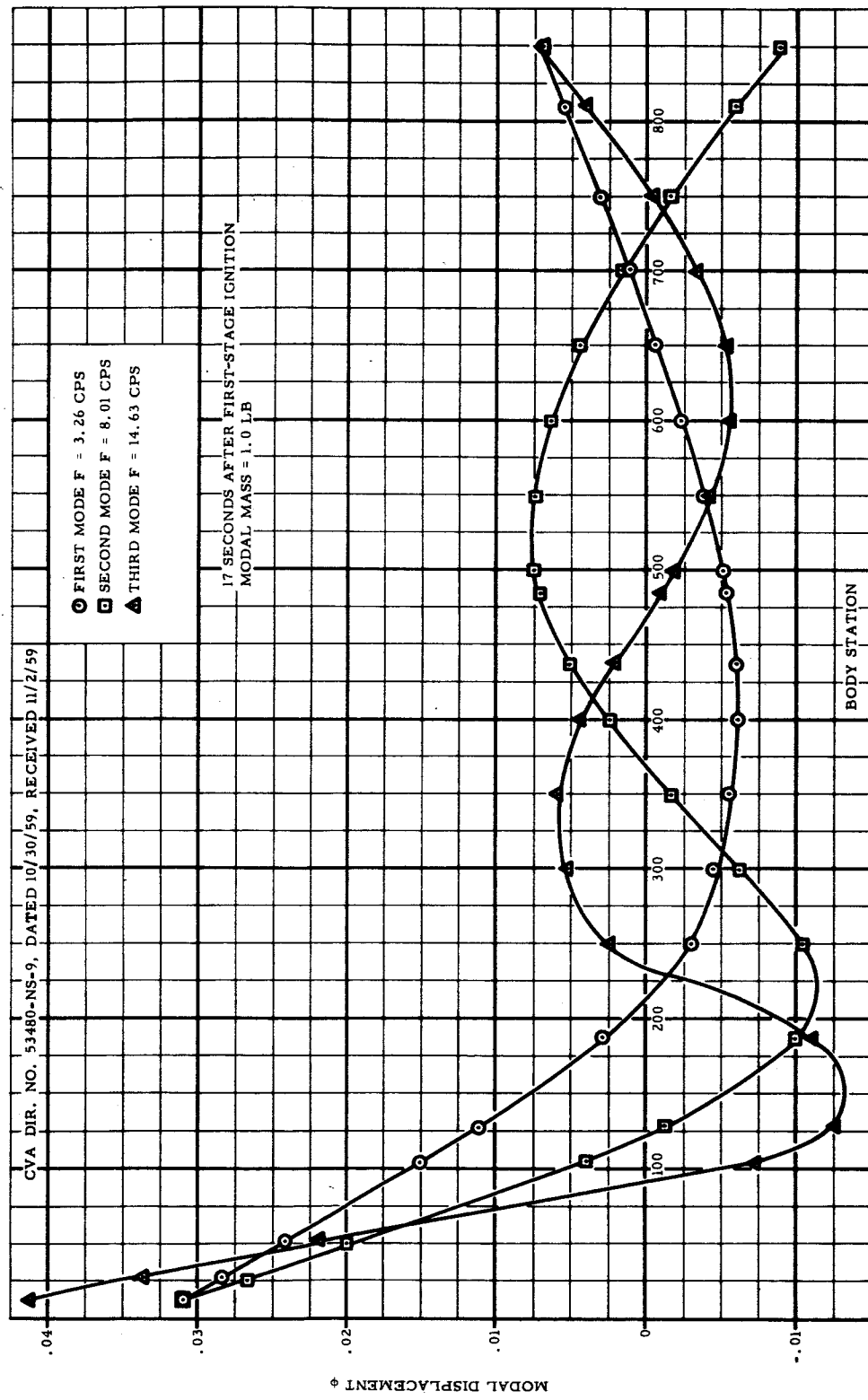


Figure V-4 First-Step Stiffness Distribution of Third and Fourth Stages



R-ED 11122
V-7

Figure V-5 First-Step Bending-Mode Shapes and Frequencies at the Transonic Condition

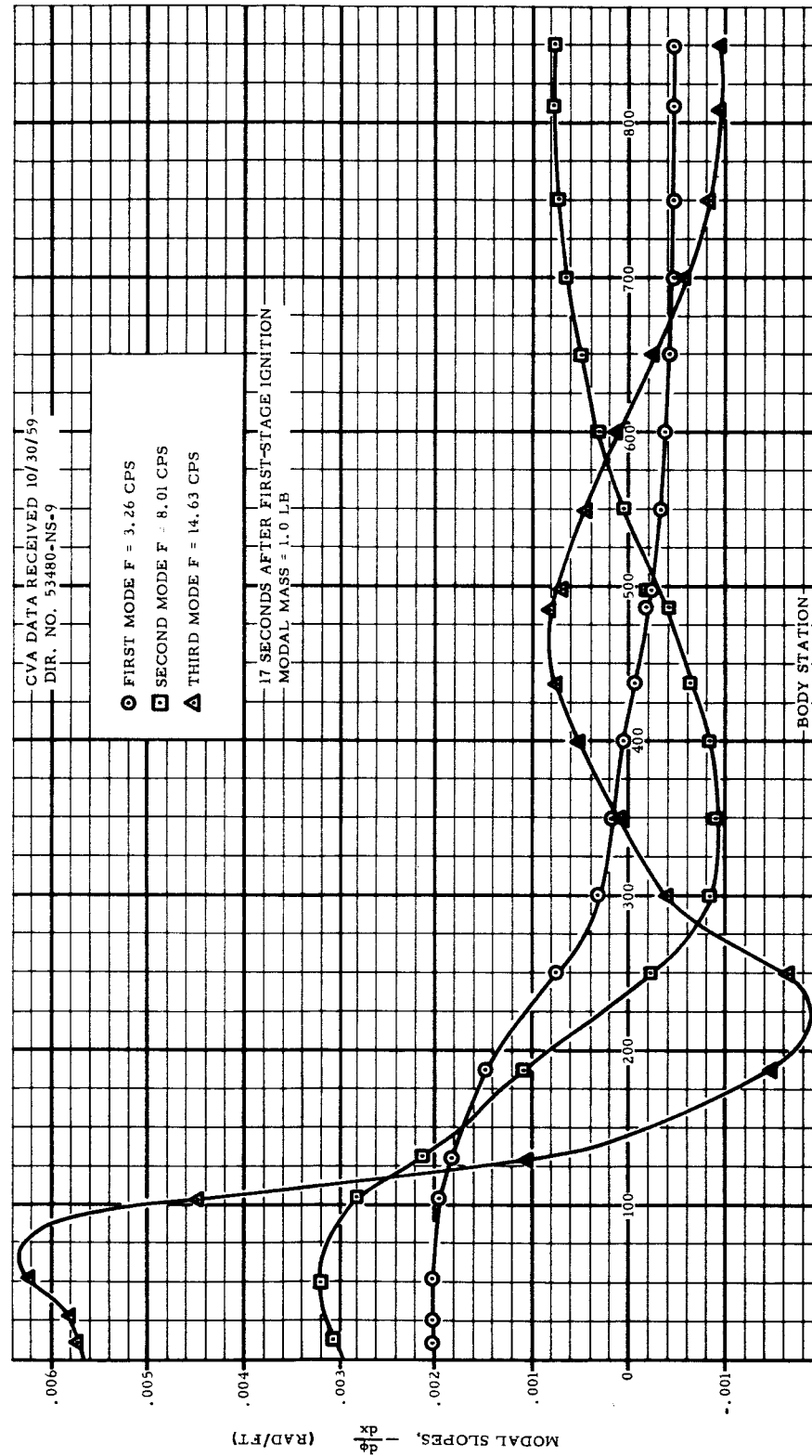


Figure V-6 First-Step Bending-Mode Slopes at the Transonic Condition

Tabulated Data Taken from CVA DIR No. 53480-NS-9 of 10/30/59

CONFIGURATION			CONDITIONS			
Body Station (x)	1st Mode f^* = 3.26 cps		2nd Mode f^* = 8.01 cps		3rd Mode f^* = 14.63 cps	
	ϕ	$+\frac{d\phi}{dx} \times 10^3$	ϕ	$+\frac{d\phi}{dx} \times 10^3$	ϕ	$+\frac{d\phi}{dx} \times 10^3$
12	.03086	-.16739	.03100	-.27831	.04120	-.47771
28	.02818	-.16782	.02654	-.28014	.03356	-.48311
52	.02414	-.17043	.01978	-.29168	.02183	-.51924
105	.01499	-.16246	.00380	-.25213	-.00731	-.37483
131	.01103	-.14926	-.00147	-.17810	-.01251	-.08763
188	.00270	-.12002	-.01021	-.08012	-.01111	.12228
250	-.00312	-.06192	-.01064	.03908	.00253	.13663
300	-.00462	-.02514	-.00639	.08810	.00519	.03417
350	-.00563	-.01457	-.00183	.08828	.00595	-.00694
400	-.00608	-.00360	.00244	.07748	.00450	-.04430
437	-.00602	.00681	.00501	.05649	.00229	-.06248
486	-.00543	.01636	.00714	.03210	-.00091	-.06770
498	-.00518	.02328	.00739	.01029	-.00175	-.05933
550	-.00384	.02808	.00738	-.01022	-.00428	-.03692
600	-.00232	.03220	.00637	-.02968	-.00554	-.00996
650	-.00062	.03540	.00441	-.04700	-.00528	.02062
700	.00122	.03762	.00167	-.06042	-.00348	.04841
750	.00314	.03891	-.00163	-.06894	-.00044	.06840
810	.00550	.03940	-.00594	-.07244	.00412	.07750
850	.00708	.03946	-.00886	-.07297	.00728	.07903

f^* = Bending-mode frequency

Table V-2 First-Step Bending-Mode Shapes and Slope 17 Seconds After Launch

R-ED 11122

V-9

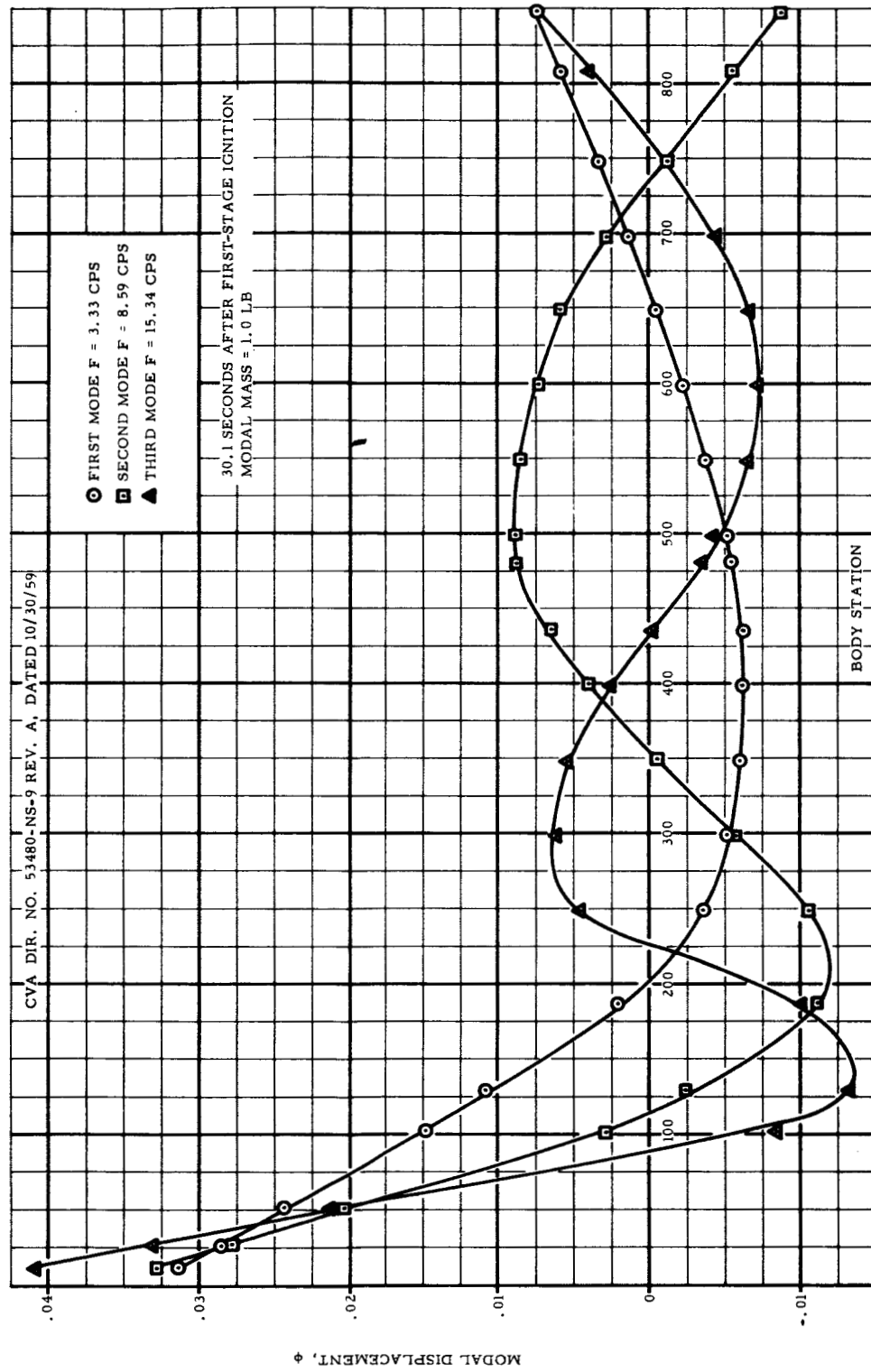
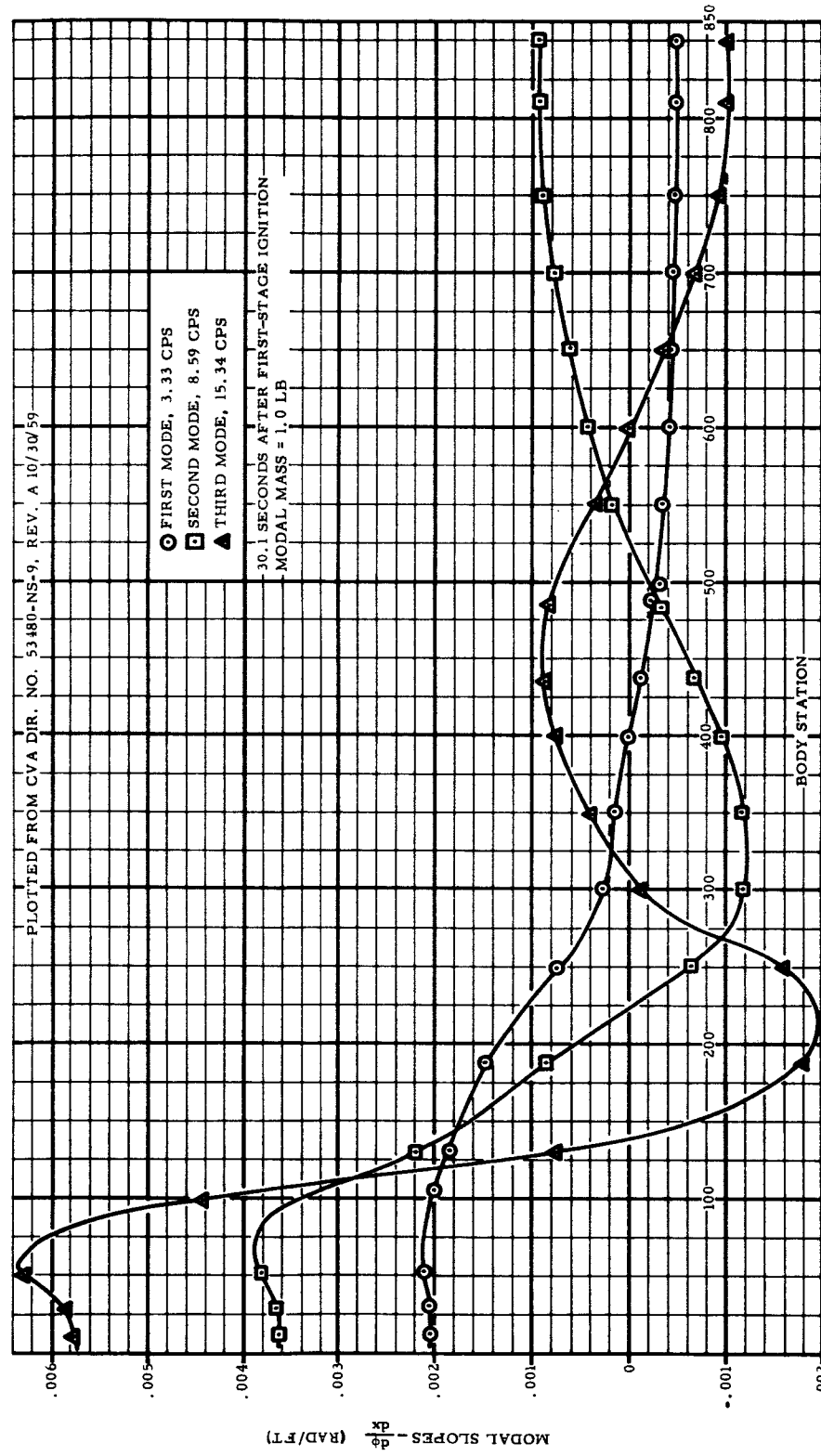


Figure V-7 First-Step Bending-Mode Shapes and Frequencies at the
Maximum q Condition

R-ED 11122
V-10

Figure V-8 First-Step Bending-Mode Slopes at the Maximum q Condition



R-ED 11122
V-11

Tabulated Data Taken from CVA DIR No. 53480-NS-9 Rev A of 11/2/59

CONFIGURATION			CONDITIONS			
Body Station (x)	1st Mode f^* = 3.33 cps		2nd Mode f^* = 8.59 cps		3rd Mode f^* = 15.34 cps	
	ϕ	$+\frac{d\phi}{dx} \times 10^3$	ϕ	$+\frac{d\phi}{dx} \times 10^3$	ϕ	$+\frac{d\phi}{dx} \times 10^3$
(Inch / Inch)	(Rad / Inch)	(Inch / Inch)	(Rad / Inch)	(Inch / Inch)	(Rad / Inch)	(Inch / Inch)
12	.03142	-.17322	.03277	-.30363	.04094	-.48393
28	.02865	-.17368	.02791	-.30577	.03320	-.48957
52	.02447	-.17644	.02052	-.31936	.02132	-.52760
105	.01499	-.16797	.00299	-.27217	-.00836	-.37281
131	.01091	-.15390	-.00256	-.18307	-.01319	-.06425
188	.00232	-.12304	-.01126	-.07127	-.00993	.14710
250	-.00360	-.06211	-.01063	.05428	.00477	.13263
300	-.00504	-.02368	-.00571	.10046	.00618	.00753
350	-.00597	-.01277	-.00059	.09736	.00552	-.03369
400	-.00631	-.00156	.00403	.08191	.00281	-.06518
437	-.00617	.00891	.00667	.05650	-.00001	-.07385
486	-.00549	.01839	.00871	.02844	-.00352	-.06918
498	-.00521	.02513	.00889	.00499	-.00432	-.05444
550	-.00378	.02964	.00861	-.01528	-.00651	-.02920
600	-.00219	.03351	.00735	-.03417	-.00732	-.00112
650	-.00043	.03650	.00519	-.05074	-.00662	.02892
700	.00146	.03861	.00228	-.06367	-.00443	.05581
750	.00343	.03988	-.00118	-.07219	-.00104	.07562
810	.00585	.04039	-.00569	-.07594	.00397	.08524
850	.00747	.04047	-.00876	-.07659	.00745	.08706

f^* = Ending-mode frequency

Table V-3 First-Step Bending-Mode Shape and Slope 30.1 Seconds After Launch

Tabulated Data Taken from CVA DIR No. 53480-NS-9 Rev A of 11/2/59

CONFIGURATION		CONDITIONS				
		Structural Shell over Fourth Step Modal Mass for Each Mode = 1.0 Lb				
		11.5% Fuel Remaining 35.4 Sec after Launch 150-Lb Payload Nose at Body-Station 5				
Body Station (x)	1st Mode f^* = 3.38 cps	2nd Mode f^* = 9.04 cps			3rd Mode f^* = 16.06 cps	
	ϕ $+ \frac{d\phi}{dx} \times 10^3$	ϕ $+ \frac{d\phi}{dx} \times 10^3$	ϕ $+ \frac{d\phi}{dx} \times 10^3$		ϕ $+ \frac{d\phi}{dx} \times 10^3$	
12	.03172	-.17659	.03458	-.32753	.04066	-.48969
28	.02890	-.17706	.02933	-.32997	.03282	-.49555
52	.02464	-.17993	.02136	-.34545	.02079	-.53543
105	.01498	-.17114	.00236	-.29115	-.00939	-.37000
131	.01082	-.15653	-.00346	-.18799	-.01382	-.03965
188	.00209	-.12468	-.01214	-.06367	-.00862	.17172
250	-.00388	-.06203	-.01060	.06692	.00701	.12642
300	-.00527	-.02261	-.00515	.10996	.00705	-.02134
350	-.00614	-.01149	.00040	.10388	.00488	-.06128
400	-.00642	-.00014	.00524	.08442	.00092	-.08477
437	-.00622	.01034	.00790	.05551	-.00242	-.08238
486	-.00547	.01978	.00982	.02475	-.00607	-.06700
498	-.00518	.02641	.00994	.00042	-.00679	-.04643
550	-.00369	.03075	.00944	-.01899	-.00852	-.02012
600	-.00205	.03446	.00802	-.03675	-.00886	.00748
650	-.00024	.03733	.00577	-.05203	-.00777	.03552
700	.00169	.03939	.00282	-.06398	-.00531	.06029
750	.00370	.04066	-.00063	-.07204	-.00174	.07898
810	.00617	.04120	-.00513	-.07577	.00345	.08852
850	.00782	.04129	-.00819	-.07647	.00707	.09047

f^* = Bending-mode frequency

Table V-4 First-Step Bending-Mode Shape and Slope 35.4 Seconds after Launch

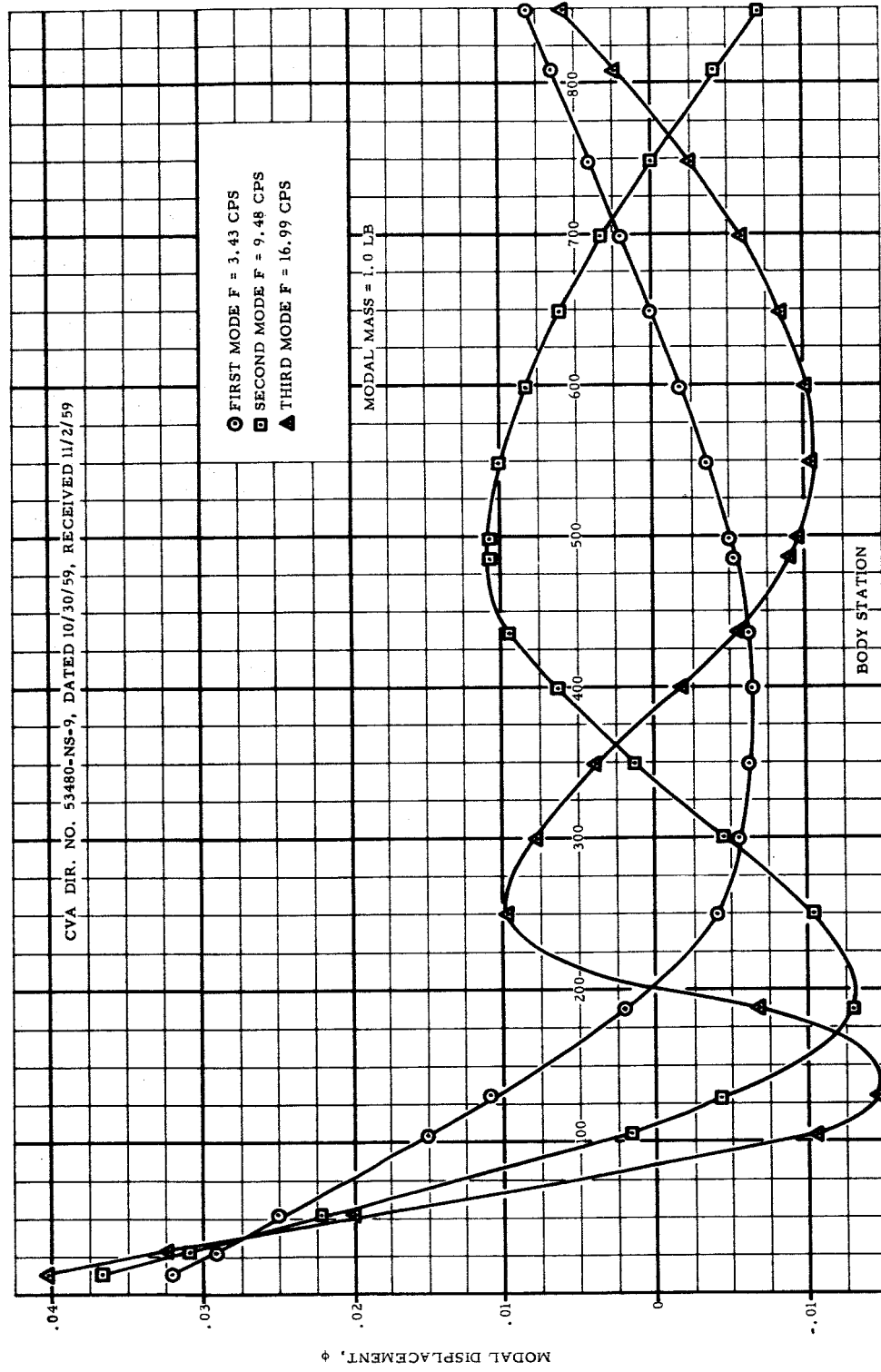


Figure V-9 First-Step Bending—Mode Shapes and Frequencies at
Burnout

R-ED 11122
V-14

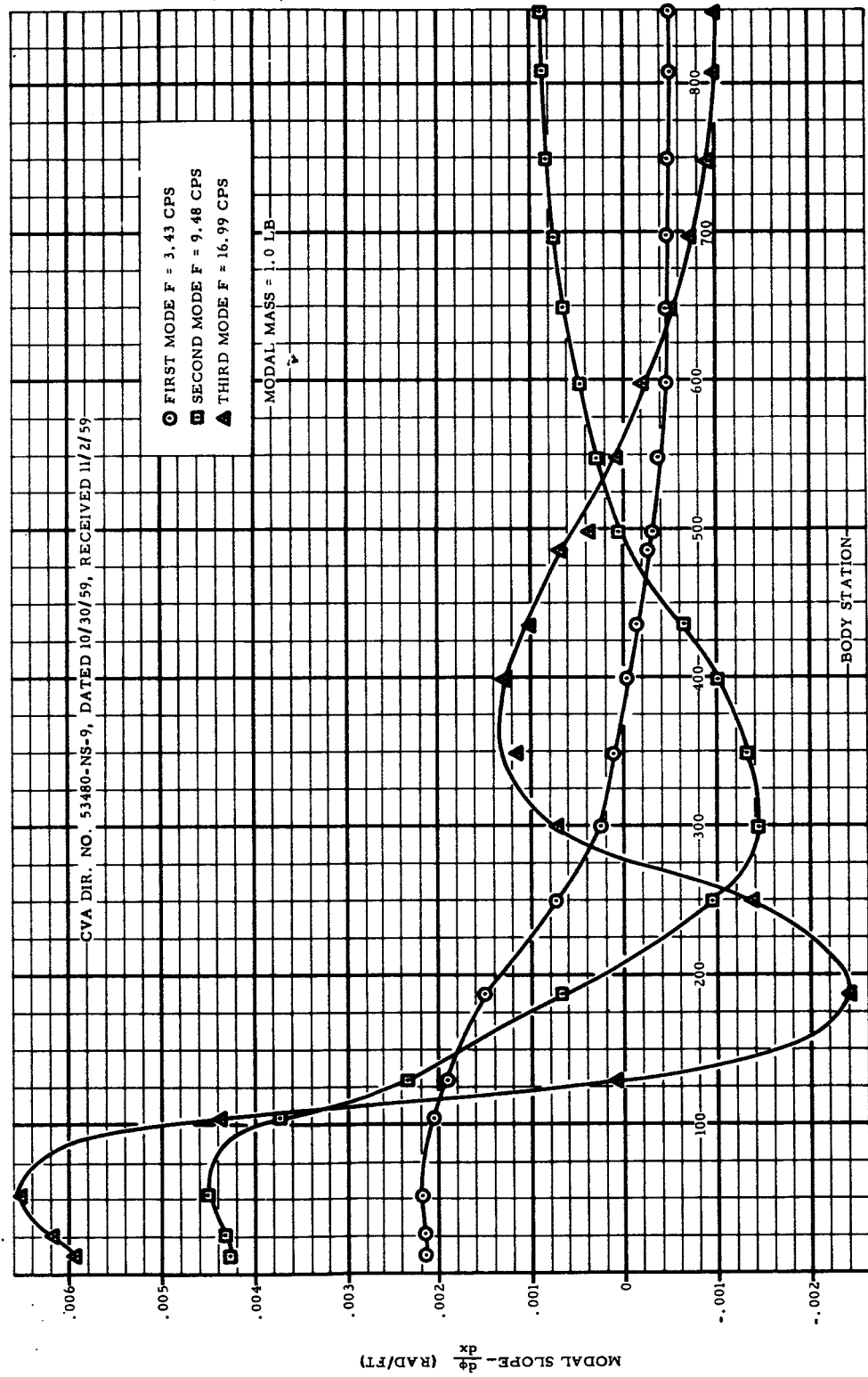


Figure V-10 First-Step Bending-Mode Slopes at Burnout

R-ED 11122
V-15

Tabulated Data Taken from CVA DIR No. 53480-NS-9 of 10/30/59

CONFIGURATION			CONDITIONS			
Body Station (x)	Structural Shell over Fourth Step Modal Mass for Each Mode = 1.0Lb		Burnout 150-Lb Payload Nose at Body Station 5			
	1st Mode f^* = 3.43 cps	$\frac{d\phi}{dx} \times 10^3$	2nd Mode f^* = 9.48 cps	$\frac{d\phi}{dx} \times 10^3$	3rd Mode f^* = 16.99 cps	$\frac{d\phi}{dx} \times 10^3$
12	.03194	-.1792	.03667	-.3547	.04020	-.4954
28	.02907	-.1797	.03099	-.3575	.03228	-.5015
52	.02475	-.1826	.02235	-.3752	.02009	-.5435
105	.01494	-.1736	.00167	-.3126	-.01061	-.3649
131	.01072	-.1585	-.00444	-.1931	-.01452	-.0077
188	.00189	-.1258	-.01305	-.0548	-.00683	.2012
250	-.00410	-.0618	-.01048	.0804	.00975	.1156
300	-.00544	-.0215	-.00452	.1190	.00794	-.0593
350	-.00626	-.0102	.00142	.1095	.00383	-.0954
400	-.00647	.0012	.00643	.0857	-.00160	-.1058
437	-.00622	.0017	.00906	.0533	-.00541	-.0876
486	-.00540	.0211	.01080	.0200	-.00894	-.0580
498	-.00509	.0277	.01086	-.0047	-.00947	-.0311
550	-.00354	.0319	.01013	-.0225	-.01042	-.0061
600	-.00184	.0355	.00857	-.0384	-.01012	.0181
650	.00001	.0383	.00629	-.0517	-.00861	.0409
700	.00199	.0403	.00341	-.0619	-.00602	.0605
750	.00404	.0416	.00009	-.0690	-.00256	.0758
810	.00657	.0422	-.00421	-.0724	.00238	.0840
850	.00826	.0423	-.00714	-.0732	.00581	.0859

f^* = Bending-mode frequency

Table V-5 First-Step Bending-Mode Shape and Slope at Burnout

 R-ED 11122
 V-16

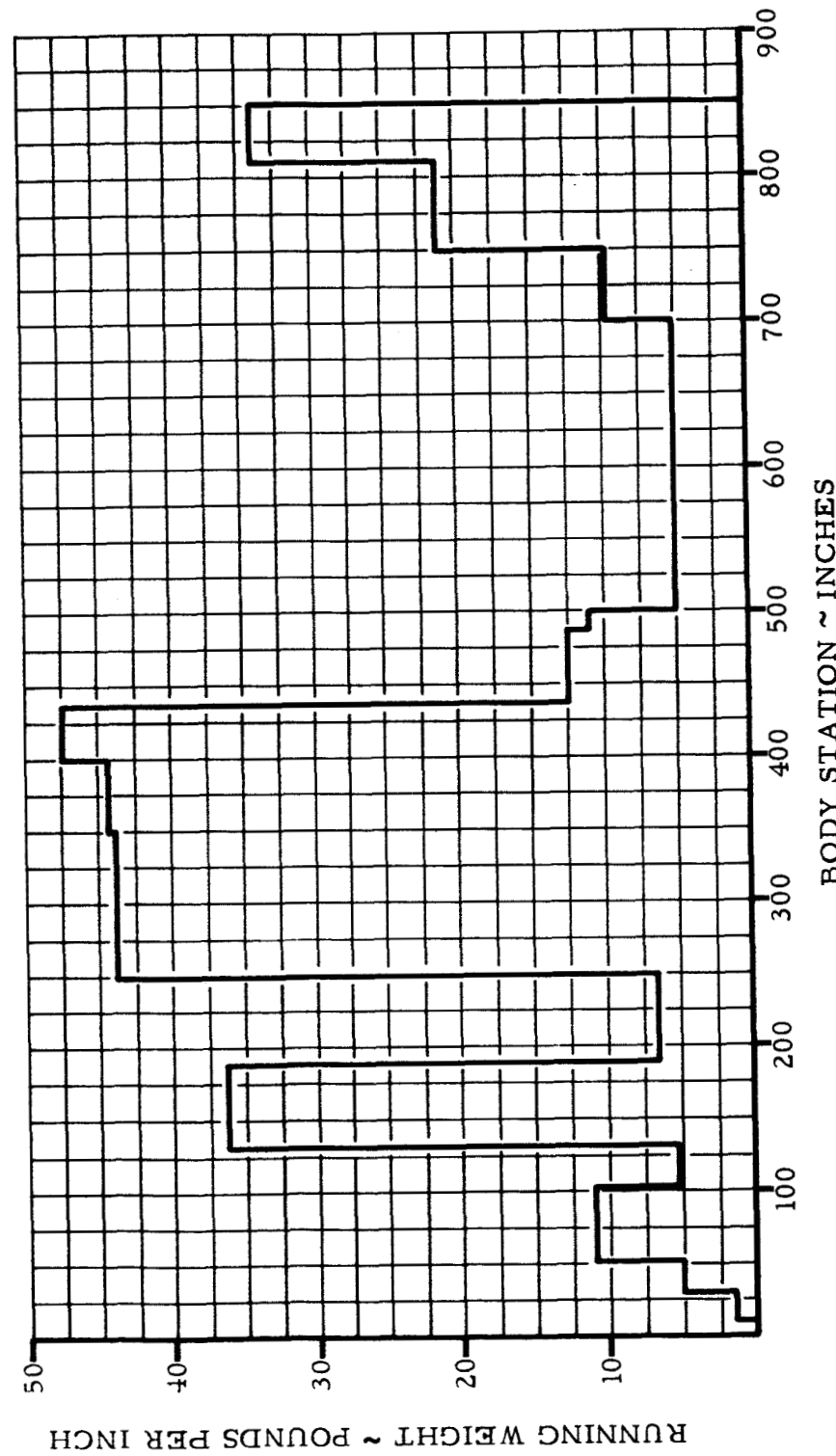


Figure V-11 First-Step Mass Distribution at First-Stage Burnout

R-ED 11122
V-17

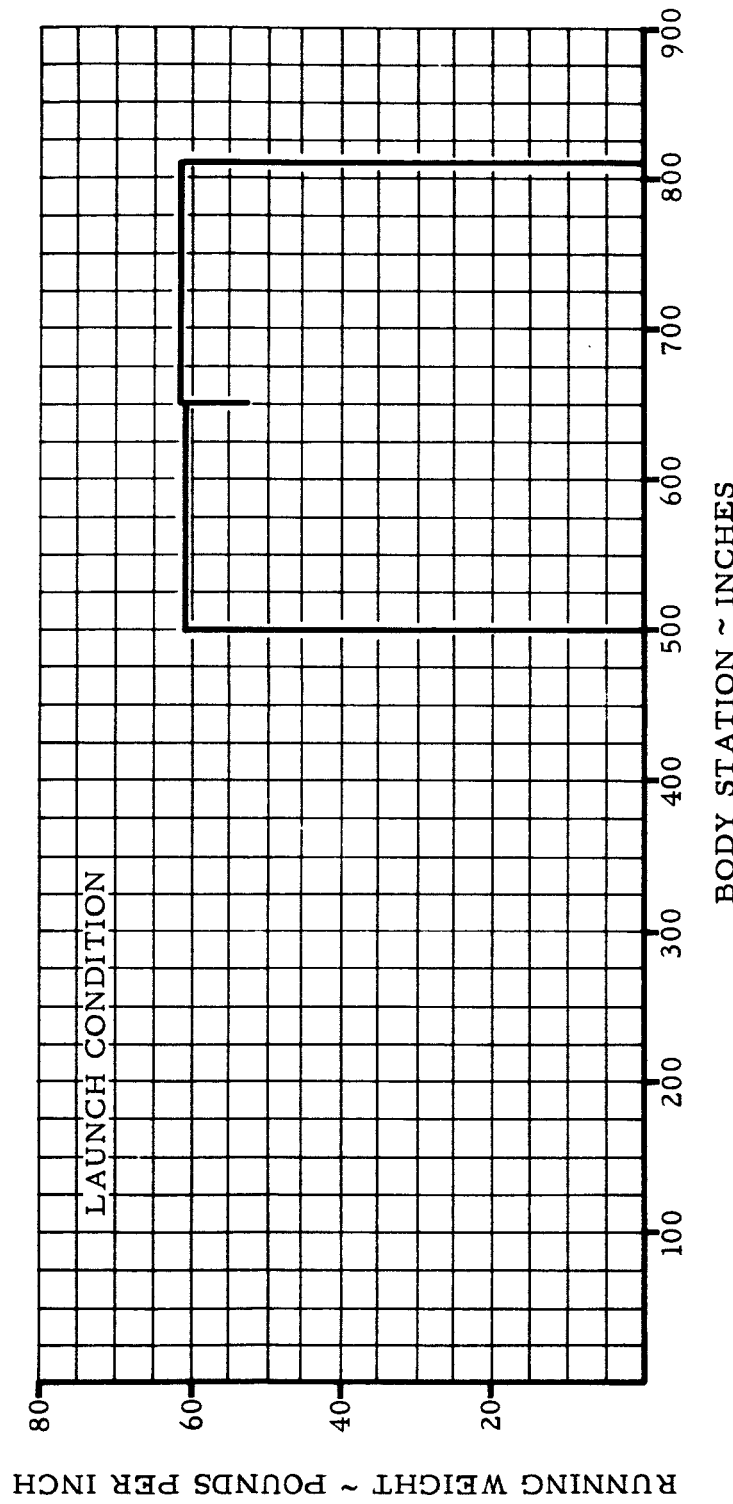


Figure V-12 First-Step Propellant Mass Distribution at First-Stage Ignition

R-ED 11122
V-18

MODAL INERTIA = 1.0 LB IN²

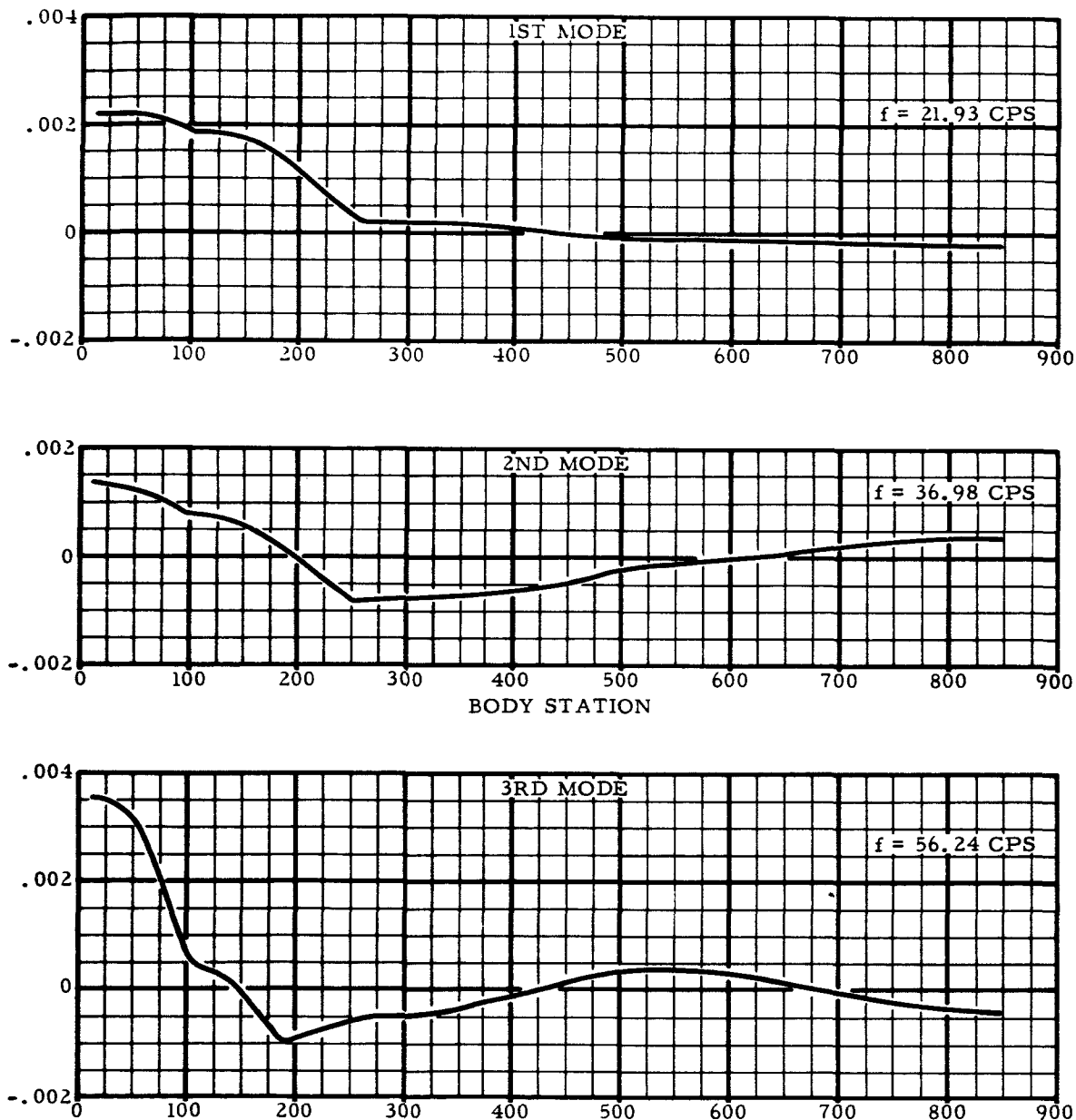
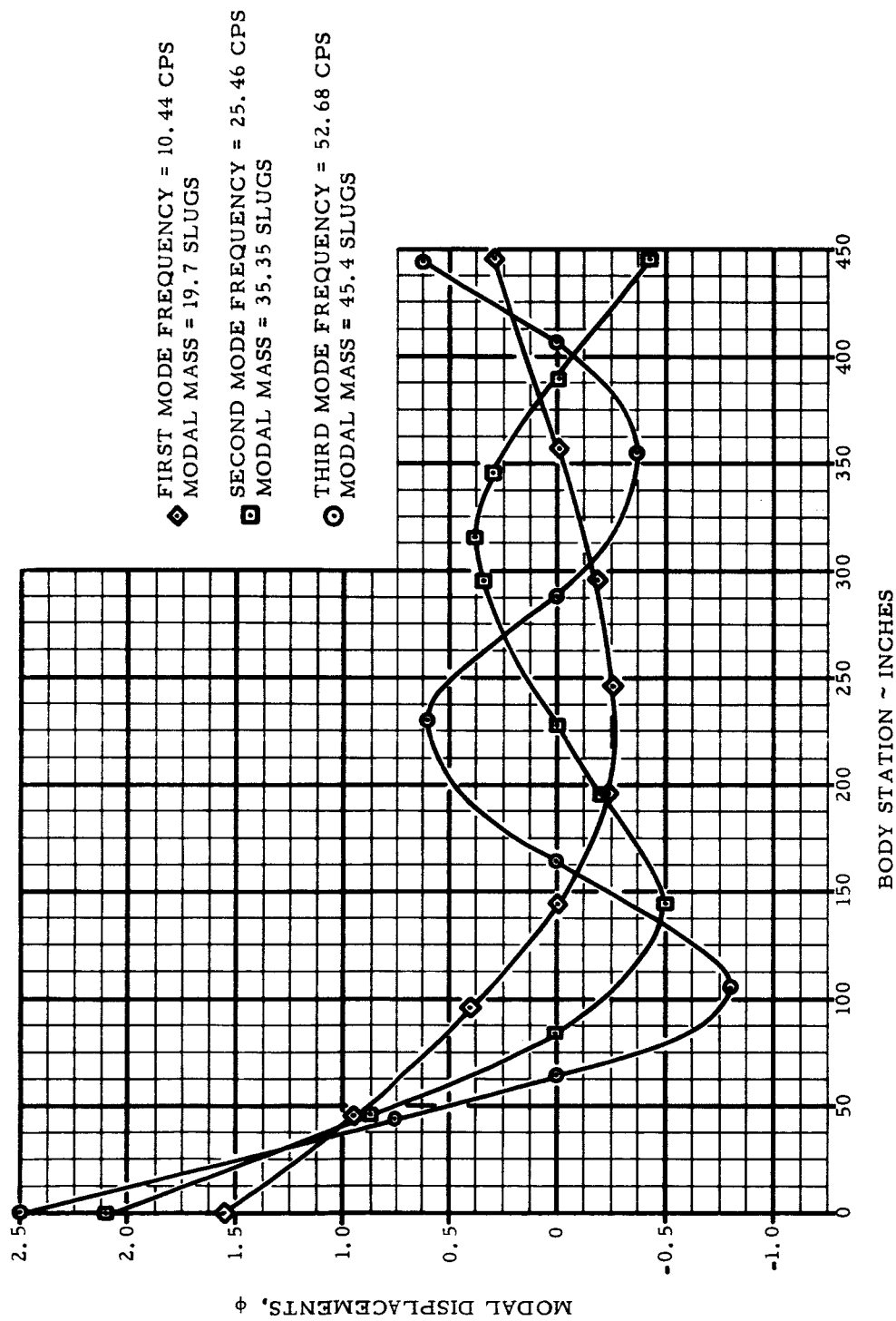


Figure V-13 First-Step Torsion Mode Shapes at Launch



R - ED 11122
V - 20

Figure V-14 Second-Step Bending-Mode Shapes and Frequencies at
Second-Stage Ignition

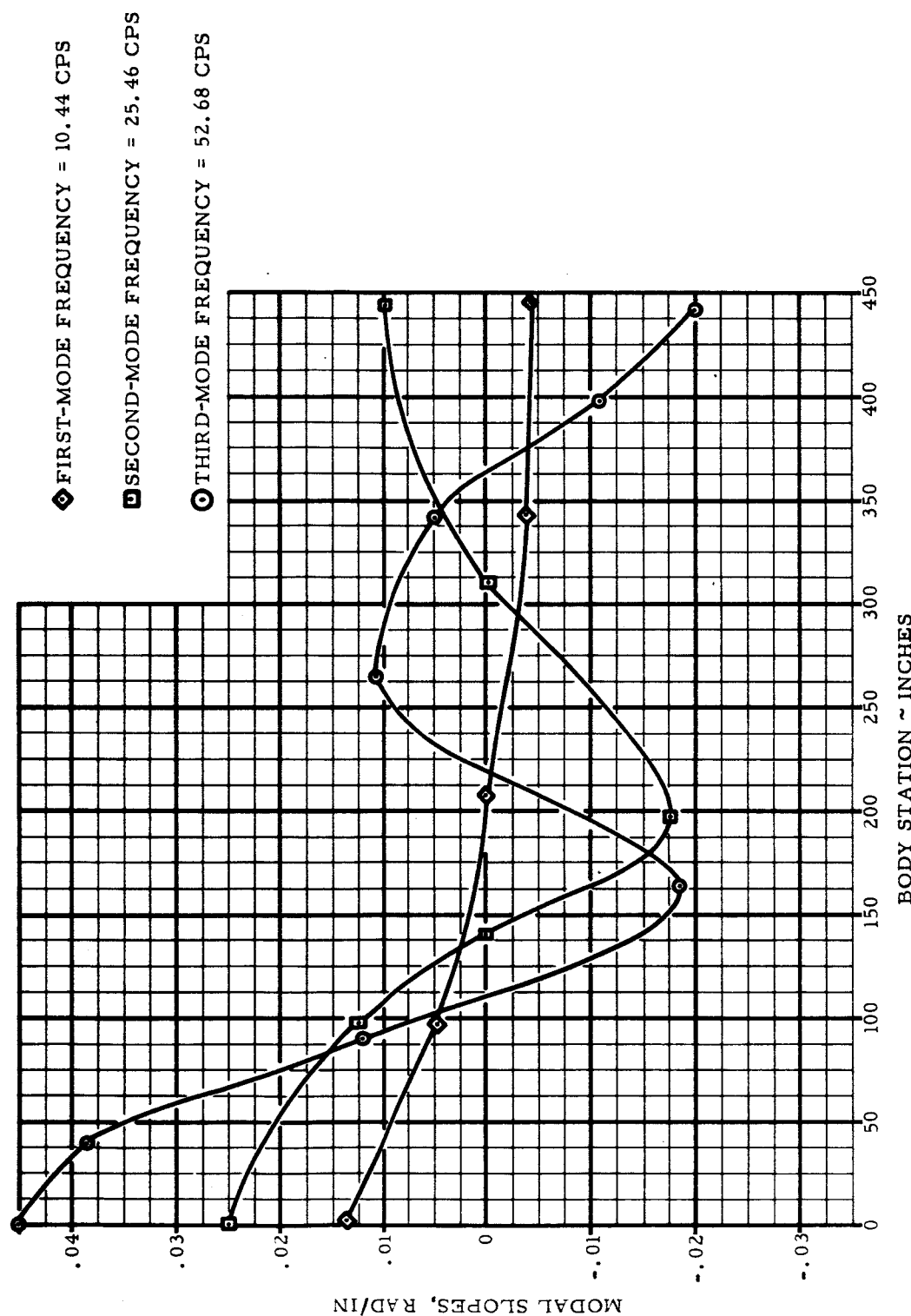


Figure V-15 Second-Step Bending-Mode Slopes at Second-Stage Ignition

SECTION VI

**STRUCTURE OF FOURTH VEHICLE
(25.7-Inch Diameter Fourth Stage)**

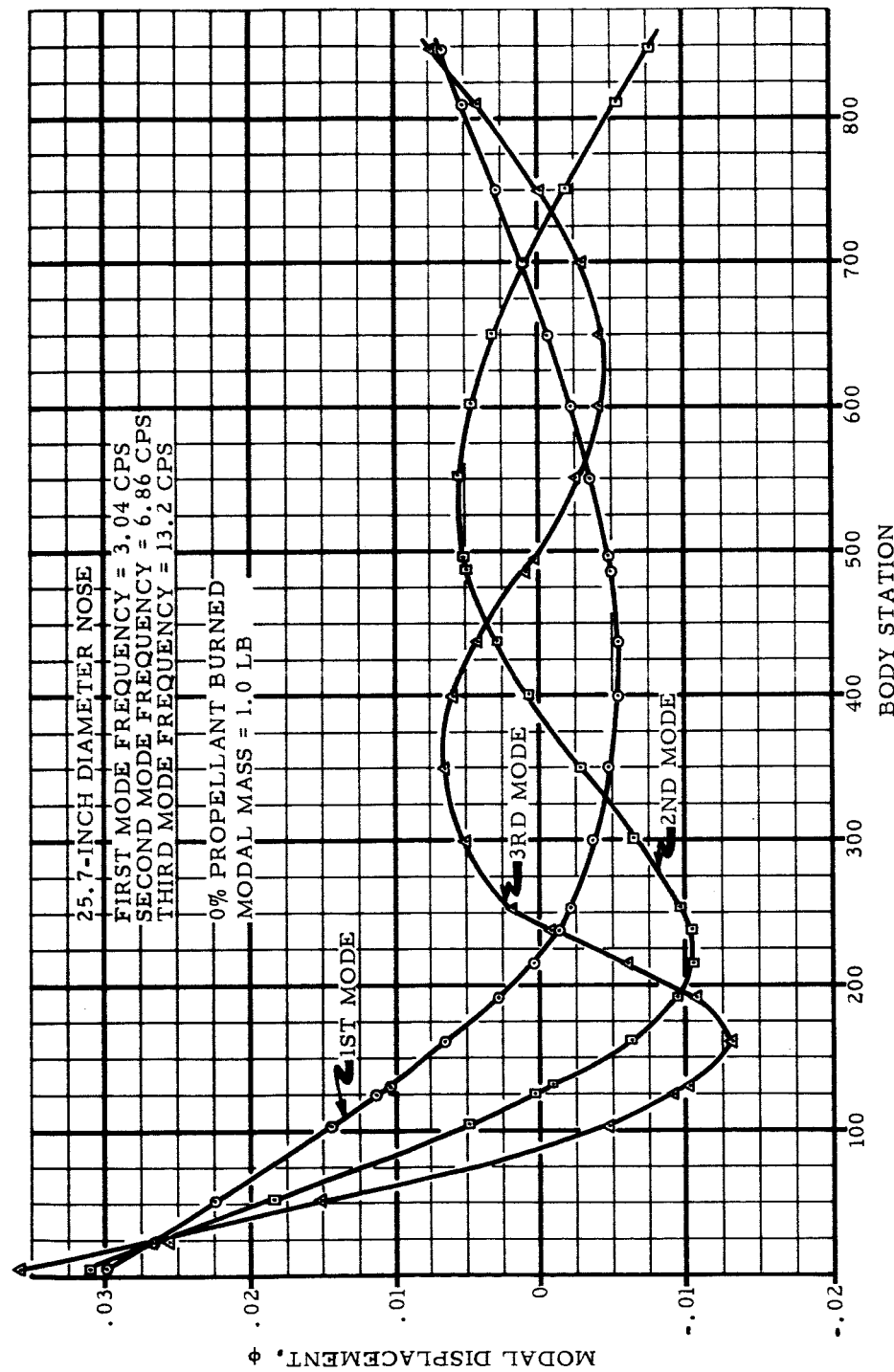
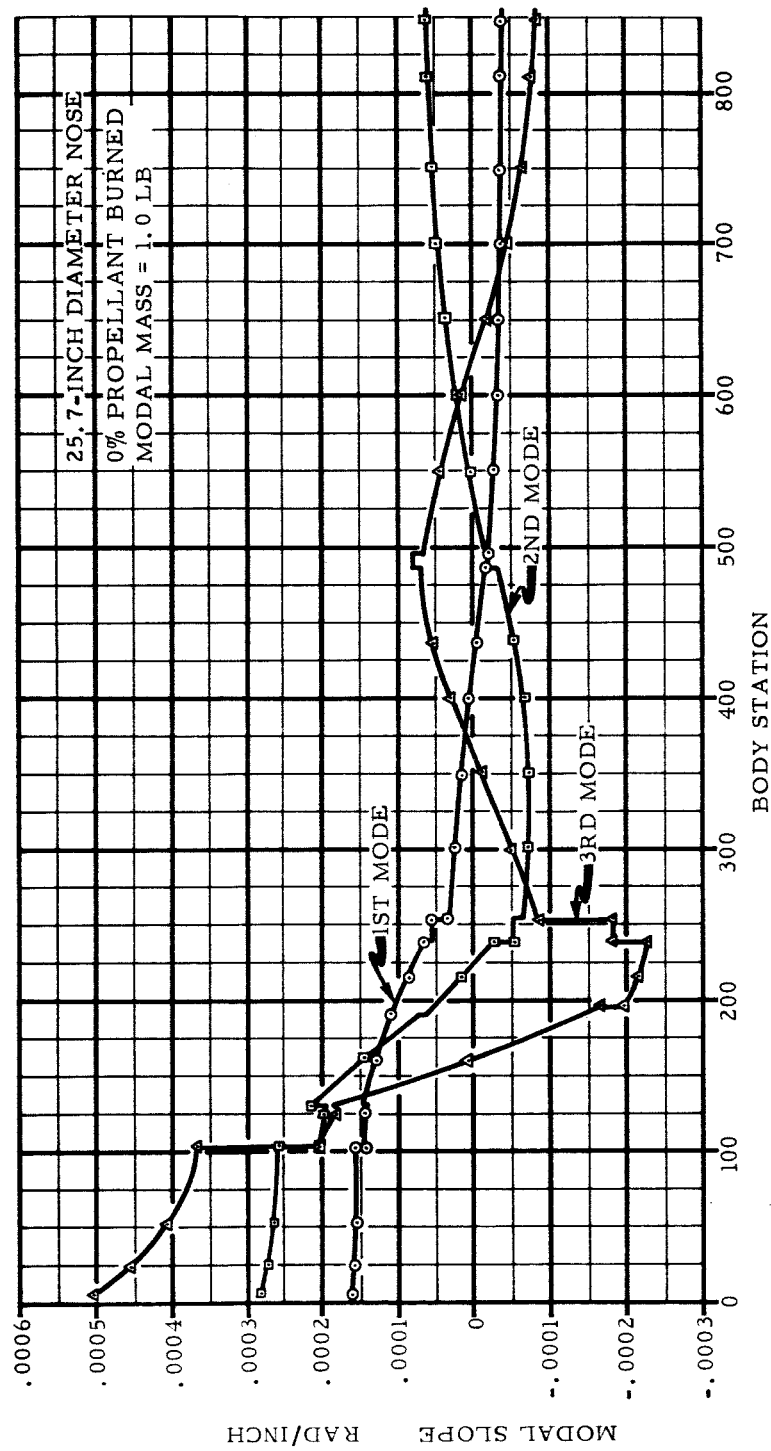


Figure VI-1 First-Step Bending-Mode Shapes and Frequencies at Launch

Figure VI-2 First-Step Bending-Mode Slopes at Launch
VI-3



Tabulated Data Taken from CVA DIR No. 86240LD-61NS-1 of 11/17/60

CONFIGURATION		CONDITIONS			
Structural Shell over Fourth Step		Launch			
Modal Mass for each Mode 1.0 Lb		150-Lb Payload			
Nose Diameter 25.7 In		100 Percent Fuel Remaining			
Nose at Body Station 5		CM (Center of Mass) at Body Sta 535.5			
Weight 36,861 Lbs		Moment of Inertia about CM=			
		$1.5887 \times 10^9 \text{ Lb-In}^2$			
Body Station (x)	1st-Mode $\phi \times 10^{-5}$ where $f^* = 3.04 \text{ cps}$	2nd-Mode $\phi \times 10^{-5}$ where $f^* = 6.86 \text{ cps}$	3rd-Mode $\phi \times 10^{-5}$ where $f^* = 13.2 \text{ cps}$	4th-Mode $\phi \times 10^{-5}$ where $f^* = 19.8 \text{ cps}$	Panel Point
5	2994.18	3100.47	3591.11	2561.96	001
24	2690.36	2566.01	2681.66	1717.10	002
52	2250.25	1818.09	1508.47	735.908	003
103	1452.15	483.168	-478.226	-777.145	004
125	1138.68	37.9695	-910.315	-912.246	005
131	1053.85	-80.5520	-1018.44	-937.085	006
161	639.072	-615.872	-1314.00	-718.089	007
191	279.621	-944.485	-1078.17	-51.7654	008
215	41.3924	-1046.23	-566.752	579.260	009
238	-137.977	-1036.08	-83.4360	1018.19	010
253	-215.842	-959.542	186.649	1091.85	011
300	-362.778	-645.500	497.213	624.885	012
350	-476.002	-280.588	653.961	-8.62991	013
400	-537.026	72.5812	592.186	-558.572	014
437	-545.439	294.807	422.457	-770.673	015

f^* = Bending-mode frequency

Table VI-1a First-Step Bending Mode Shapes at Launch

R-ED 11122
VI-4

Body Station (x)	1st-Mode ϕ $\times 10^{-5}$ where $f^* = 3.04$ cps	2nd-Mode ϕ $\times 10^{-5}$ where $f^* = 6.86$ cps	3rd-Mode ϕ $\times 10^{-5}$ where $f^* = 13.2$ cps	4th-Mode ϕ $\times 10^{-5}$ where $f^* = 19.8$ cps	Panel Point
486	-502.490	491.415	101.299	-694.711	016
496	-484.810	511.798	30.8223	-624.109	017
550	-362.845	531.984	-262.647	-149.734	018
600	-224.364	460.955	-424.623	290.904	019
650	-65.6557	306.652	-432.566	550.512	020
700	107.897	83.7021	-278.757	511.496	021
750	290.584	-185.603	4.23811	172.870	022
810	514.647	-535.794	431.356	-473.381	023
848	657.848	-765.365	729.771	-967.223	024

f^* = Bending-mode frequency

Table VI-1b First-Step Bending-Mode Shapes at Launch R-ED 11122
VI-5

Modal Slopes, Rad/In

Tabulated Data Taken from CVA DIR No. 86240LD-61NS-1 of 11/17/60

CONFIGURATION		CONDITIONS			
Structural Shell over Fourth Step		Launch			
Modal Mass for each Mode = 1.0 Lb		150-Lb Payload			
Nose at Body Station 5		100 Percent Fuel Remaining			
Weight = 36,861 Lbs		CM (Center of Mass) at Body Sta 535.5			
Nose Diameter = 25.7 In		Moment of Inertia about CM =			
		$1.5887 \times 10^9 \text{ Lb-In}^2$			
Body Station (x)	1st-Mode -dφ/dx $\times 10^{-6}$ where f* = 3.04 cps	2nd-Mode -dφ/dx $\times 10^{-6}$ where f* = 6.86 cps	3rd-Mode -dφ/dx $\times 10^{-6}$ where f* = 13.2 cps	4th-Mode -dφ/dx $\times 10^{-6}$ where f* = 19.8 cps	Panel Point
5	161.007	287.024	502.778	482.757	1F
5	161.007	287.024	502.778	482.757	1A
24	158.805	275.561	454.540	406.567	2F
24	158.805	275.561	454.540	406.567	2A
52	156.937	265.213	408.559	331.376	3F
52	156.937	265.213	408.559	331.376	3A
103	156.043	258.286	370.539	261.978	4F
103	143.354	206.156	209.123	77.1323	4A
125	141.623	198.570	183.685	45.6868	5F
125	141.623	198.570	183.685	45.6868	5A
131	141.151	196.501	176.747	37.1106	6F
131	147.478	212.891	187.085	1.55654	6A
161	129.038	143.989	9.95456	-147.554	7F
161	129.038	143.989	9.95456	-147.554	7A
191	110.597	75.0863	-167.176	-296.663	8F
191	110.126	66.2988	-197.571	-299.739	8A

f* = Bending-mode frequency

Table No. VI-2a First-Step Bending-Mode Slope at Launch

R-ED 11122

VI-6

Modal Slopes, Rad/In

Body Station (x)	1st-Mode $-d\phi/dx$ $\times 10^{-6}$ where $f^* = 3.04$ cps	2nd-Mode $-d\phi/dx$ $\times 10^{-6}$ where $f^* = 6.86$ cps	3rd-Mode $-d\phi/dx$ $\times 10^{-6}$ where $f^* = 13.2$ cps	4th-Mode $-d\phi/dx$ $\times 10^{-6}$ where $f^* = 19.8$ cps	Panel Point
215	88.3980	18.4926	-211.946	-226.116	9F
215	88.3980	18.4926	-211.946	-226.116	9A
238	67.5753	-27.3218	-225.720	-155.560	10F
238	51.9100	-51.0263	-180.057	-49.1074	10A
253	51.9100	-51.0263	-180.057	-49.1074	11F
253	35.4390	-63.8303	-82.9045	86.1021	11A
300	27.0872	-69.8044	-49.2504	112.605	12F
300	27.0872	-69.8044	-49.2504	112.605	12A
350	17.4248	-71.8081	-9.49725	118.346	13F
350	17.4248	-71.8081	-9.49725	118.346	13A
400	6.49731	-64.5572	31.6179	79.7215	14F
400	6.49731	-64.5572	31.6179	79.7215	14A
437	-2.47546	-51.4837	54.3355	25.9922	15F
437	-2.47546	-51.4837	54.3355	25.9922	15A
486	-15.0543	-28.7648	76.7490	-56.9964	16F
486	-17.6806	-20.3834	70.4771	-70.6017	16A
496	-17.6806	-20.3834	70.4771	-70.6017	17F
496	-19.9326	-13.0552	65.7439	-87.7020	17A
550	-25.2393	5.57888	42.9484	-87.9926	18F
550	-25.2393	5.57888	42.9484	-87.9926	18A
600	-29.7189	22.5331	16.9919	-70.0246	19F
600	-29.7189	22.5331	16.9919	-70.0246	19A
650	-33.2261	37.7253	-14.5865	-22.0593	20F
650	-33.2261	37.7253	-14.5865	-22.0593	20A
700	-35.6240	49.2256	-43.6804	37.7642	21F

f^* = Bending-mode frequency

Table No. VI-2b First-Step Bending-Mode Slope at Launch

R-ED 11122

VI-7

Modal Slopes, Rad/In

Body Station (x)	1st-Mode $-d\phi/dx$ $x \cdot 10^{-6}$ where $f^* = 3.04$ cps	2nd-Mode $-d\phi/dx$ $x \cdot 10^{-6}$ where $f^* = 6.86$ cps	3rd-Mode $-d\phi/dx$ $x \cdot 10^{-6}$ where $f^* = 13.2$ cps	4th-Mode $-d\phi/dx$ $x \cdot 10^{-6}$ where $f^* = 19.8$ cps	Panel Point
700	-35.6240	49.2256	-43.6804	37.7642	21A
750	-36.9041	55.9085	-63.2298	85.8998	22F
750	-36.9041	55.9085	-63.2298	85.8998	22A
810	-37.5524	59.6193	-75.6827	121.331	23F
810	-37.5524	59.6193	-75.6827	121.331	23A
848	-37.8166	61.2077	-81.3780	138.586	24F
848	-37.8166	61.2077	-81.3780	138.586	24A

f^* = Bending-mode frequency

Table No. VI-2c First-Step Bending-Mode Slope at Launch

R-ED 11122
VI-8

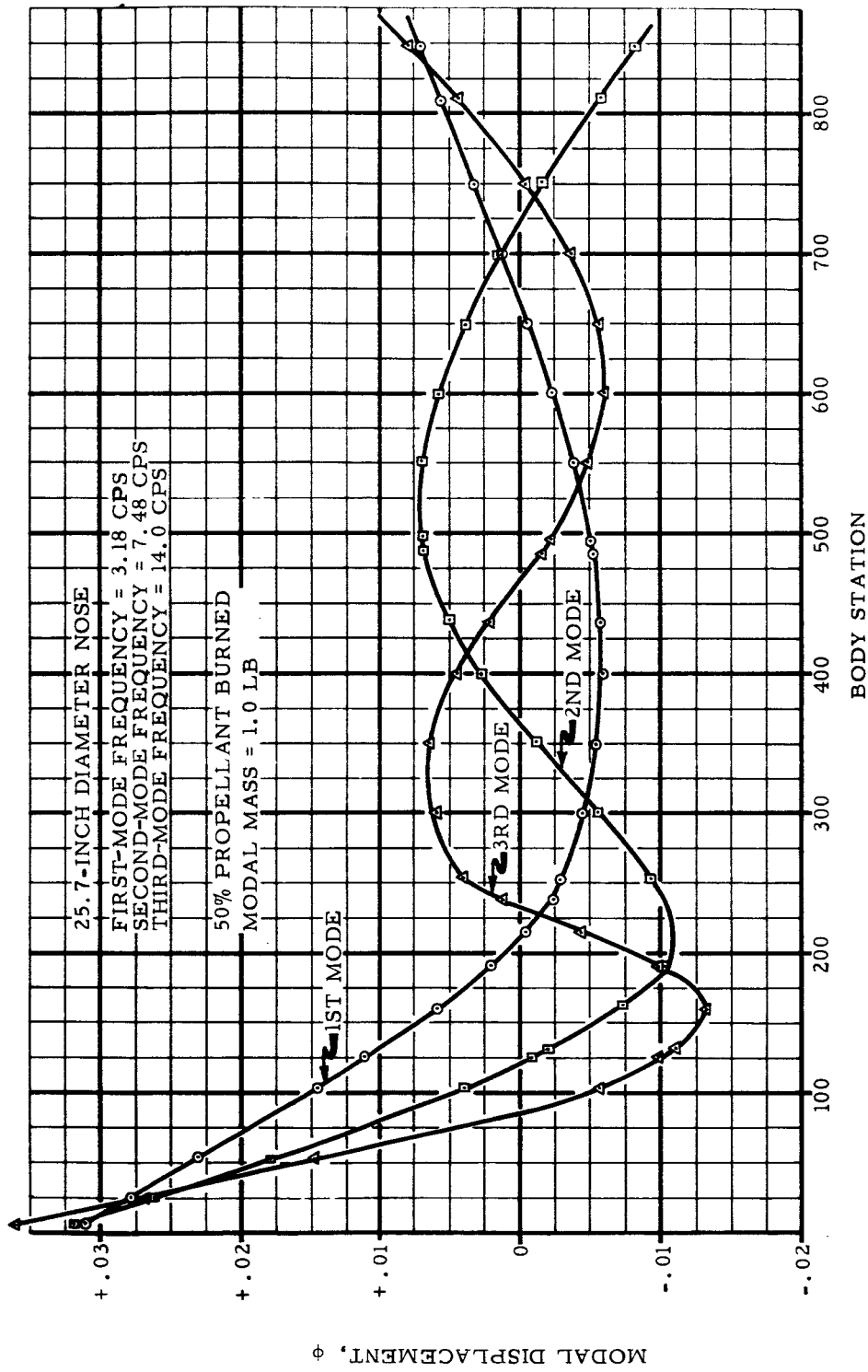


Figure VI-3 First-Step Bending-Mode Shapes and Frequencies with
50 Percent Propellant Remaining

R-ED 11122
VI-9

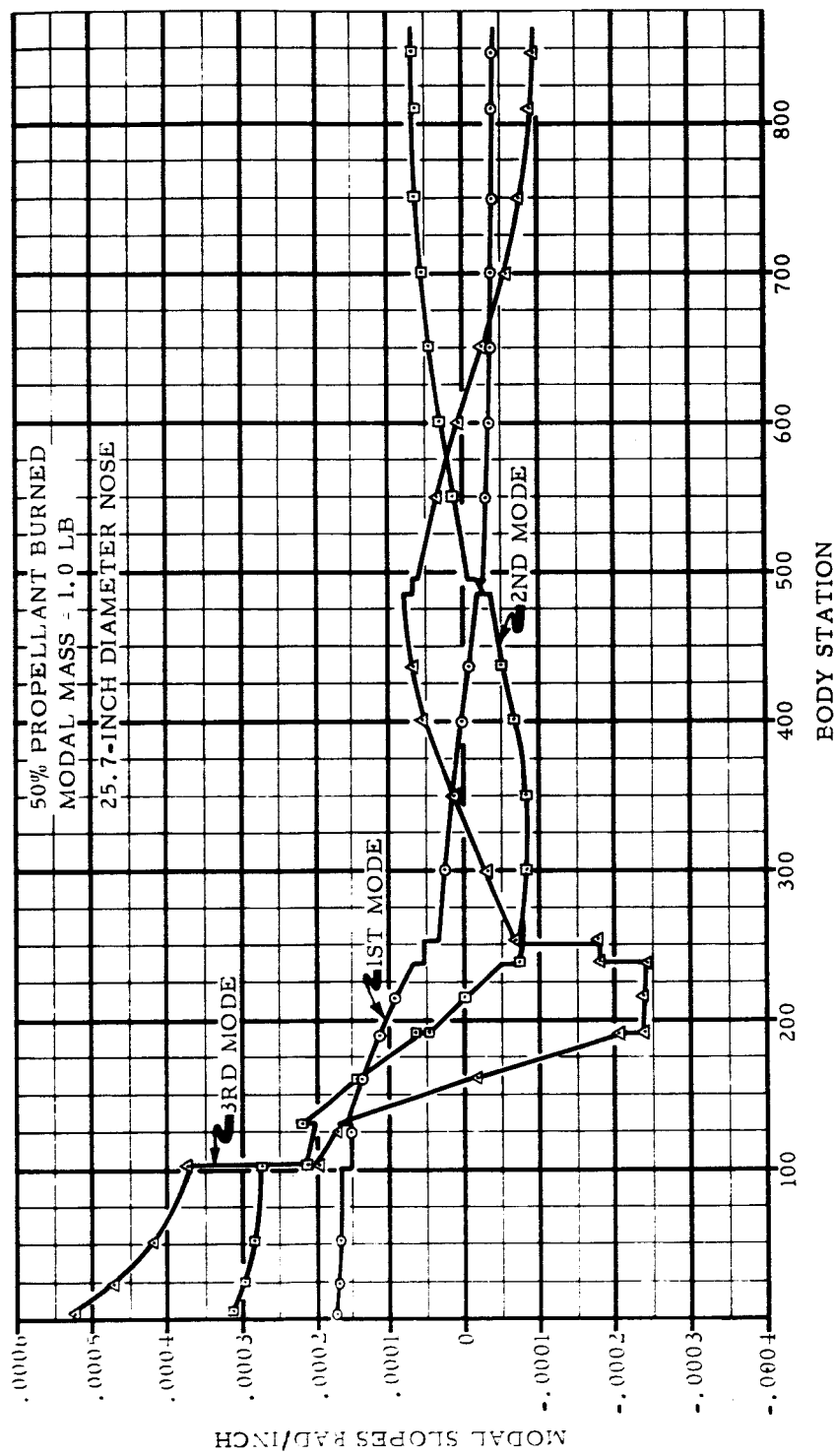


Figure VI-4 First-Step Bending-Mode Slopes with 50 Percent Propellant Remaining

R-ED 11122
VI-10

Tabulated Data Taken from CVA DIR No. 86240LD-61NS-of 11/17/60

CONFIGURATION		CONDITIONS			
Structural Shell over Fourth Step		150-Lb Payload			
Modal Mass for each Mode = 1.0 Lb		50 Percent Fuel Remaining			
Nose at Body Station 5		CM (Center of Mass) at Body Sta 495.2			
Weight = 27,321 Lbs		Moment of Inertia about CM =			
Nose Diameter = 25.7 In		$1.3377 \times 10^9 \text{ Lb-In}^2$			
Body Station (x)	1st-Mode ϕ $\times 10^{-5}$ where $f^* = 3.18 \text{ cps}$	2nd-Mode ϕ $\times 10^{-5}$ where $f^* = 7.48 \text{ cps}$	3rd-Mode ϕ $\times 10^{-5}$ where $f^* = 14.0 \text{ cps}$	4th-Mode ϕ $\times 10^{-5}$ where $f^* = 21.5 \text{ cps}$	Panel Point
5	3111.16	3182.33	3617.76	2460.97	001
24	2784.85	2605.62	2668.39	1601.97	002
52	2312.64	1804.08	1457.80	632.305	003
103	1456.65	378.712	-574.040	-817.980	004
125	1122.04	-81.3264	-985.384	-901.145	005
131	1031.53	-203.346	-1086.91	-911.222	006
161	589.742	-742.969	-1320.32	-593.523	007
191	209.883	-1042.55	-991.982	134.677	008
215	-39.0426	-1099.42	-426.947	748.980	009
238	-223.770	-1040.79	120.165	1132.65	010
253	-301.429	-933.278	389.189	1148.98	011
300	-439.983	-551.704	604.829	549.861	012
350	-540.990	-126.834	637.678	-181.780	013
400	-586.899	264.106	453.705	-726.264	014
437	-582.957	496.029	214.417	-858.356	015
486	-523.463	680.156	-149.212	-618.233	016

f^* = Bending-mode frequency

Table No. VI-3a First-Step Bending-Mode Shape with 50 Percent Propellant Remaining

R-ED 11122

VI-11

Body Station (x)	1st-Mode $\phi \times 10^5$ where $f^* = 3.18$ cps	2nd-Mode $\phi \times 10^5$ where $f^* = 7.48$ cps	3rd-Mode $\phi \times 10^5$ where $f^* = 14.0$ cps	4th-Mode $\phi \times 10^5$ where $f^* = 21.5$ cps	Panel Point
496	-502.555	694.403	-219.306	-513.613	017
550	-365.449	678.882	-483.221	56.4987	018
600	-215.123	573.134	-599.401	514.707	019
650	-46.5336	384.934	-558.367	745.822	020
700	135.552	128.846	-360.580	661.132	021
750	326.225	-174.447	-37.6161	270.788	022
810	560.028	-568.668	441.613	459.173	023
848	709.721	-828.851	779.765	-1029.72	024

f^* = Bending-mode frequency

Table No. VI-3b First-Step Bending-Mode Shape with 50 Percent Propellant Remaining
 R-ED 11122
 VI-12

Modal Slopes, Rad/In

Tabulated Data Taken from CVA DIR No. 86240LD-61NS-1 of 11/17/60

CONFIGURATION		CONDITIONS			
Structural Shell over Fourth Step Modal Mass for each Mode = 1.0 Lb Nose at Body Station 5 Weight = 27, 321 Lbs Nose Diameter = 25.7 In		150-Lb Payload 50 Percent Fuel Remaining CM (Center of Mass) at Body Sta 495.2 Moment of Inertia about CM = $1.3377 \times 10^9 \text{ Lb-In}^2$			
Body Station (x)	1st-Mode $-d\phi/dx$ $\times 10^{-6}$ where $f^* = 3.18 \text{ cps}$	2nd-Mode $-d\phi/dx$ $\times 10^{-6}$ where $f^* = 7.48 \text{ cps}$	3rd-Mode $-d\phi/dx$ $\times 10^{-6}$ where $f^* = 14.0 \text{ cps}$	4th-Mode $-d\phi/dx$ $\times 10^{-6}$ where $f^* = 21.5 \text{ cps}$	Panel Point
5	172.990	310.507	526.880	494.872	1F
5	172.990	310.507	526.880	494.872	1A
24	170.490	296.549	472.455	409.336	2F
24	170.490	296.549	472.455	409.336	2A
52	168.362	283.861	420.319	324.356	3F
52	168.362	283.861	420.319	324.356	3A
103	167.322	275.109	376.482	244.384	4F
103	153.068	213.620	200.932	54.3079	4A
125	151.119	204.596	173.018	21.2968	5F
125	151.119	204.596	173.018	21.2968	5A
131	150.587	202.135	165.404	12.2937	6F
131	157.583	219.881	171.427	-37.4829	6A
161	136.941	139.868	-15.8215	-174.317	7F
161	136.941	139.868	-15.8215	-174.317	7A
191	116.298	59.8536	-203.070	-311.150	8F
191	115.669	48.8101	-234.184	-301.481	8A
215	91.7688	-1.42169	-236.679	-210.438	9F
215	91.7688	-1.42169	-236.679	-210.438	9A

f^* = Bending-mode frequency

Table No. VI-4a First-Step Bending-Mode Slope with 50 Percent Propellant Remaining
 R-ED 11122
 VI-13

Modal Slopes, Rad/In

Body Station (x)	1st-Mode $-\frac{d\phi}{dx}$ $\times 10^{-6}$ where $f^* = 3.18$ cps	2nd-Mode $-\frac{d\phi}{dx}$ $\times 10^{-6}$ where $f^* = 7.48$ cps	3rd-Mode $-\frac{d\phi}{dx}$ $\times 10^{-6}$ where $f^* = 14.0$ cps	4th-Mode $-\frac{d\phi}{dx}$ $\times 10^{-6}$ where $f^* = 21.5$ cps	Panel Point
238	68.8641	-49.5605	-239.070	-123.188	10F
238	51.7724	-71.6733	-179.349	-10.8856	10A
253	51.7724	-71.6733	-179.349	-10.8856	11F
253	33.9754	-79.3507	-64.9285	118.335	11A
300	24.9839	-83.0212	-26.8332	136.608	12F
300	24.9839	-83.0212	-26.8332	136.608	12A
350	14.6916	-81.5810	15.1124	127.613	13F
350	14.6916	-81.5810	15.1124	127.613	13A
400	3.29263	-69.2762	52.8161	66.8296	14F
400	3.29263	-69.2762	52.8161	66.8296	14A
437	-5.83076	-51.8812	68.7762	-.742541	15F
437	-5.83076	-51.8812	68.7762	-.742541	15A
486	-18.4519	-23.2729	79.6438	-97.2662	16F
486	-20.9080	-14.2470	70.0935	-104.620	16A
496	-20.9080	-14.2470	70.0935	-104.620	17F
496	-22.9625	-6.61506	62.1849	-112.811	17A
550	-27.8174	12.3633	35.5615	-98.3407	18F
550	-27.8174	12.3633	35.5615	-98.3407	18A
600	-31.8916	29.3948	7.51459	-68.9323	19F
600	-31.8916	29.3948	7.51459	-68.9323	19A
650	-35.0675	44.4288	-23.8822	-14.6424	20F
650	-35.0675	44.4288	-23.8822	-14.6424	20A
700	-37.2759	55.9381	-52.0751	47.5034	21F
700	-37.2759	55.9381	-52.0751	47.5034	21A

f^* = Bending-mode frequency

Table No. VI-4b First-Step Bending-Mode Slope with 50 Percent Propellant Remaining

R-ED 11122

Modal Slopes, Rad/In

Body Station (x)	1st-Mode $-d\phi/dx$ $\times 10^{-6}$ where $f^* = 3.18$ cps	2nd-Mode $-d\phi/dx$ $\times 10^{-6}$ where $f^* = 7.48$ cps	3rd-Mode $-d\phi/dx$ $\times 10^{-6}$ where $f^* = 14.0$ cps	4th-Mode $-d\phi/dx$ $\times 10^{-6}$ where $f^* = 21.5$ cps	Panel Point
750	-38.5132	62.9519	-71.5379	97.8834	22F
750	-38.5132	62.9519	-71.5379	97.8834	22A
810	-39.2279	67.3969	-85.4527	139.100	23F
810	-39.2279	67.3969	-85.4527	139.100	23A
848	-39.5582	69.5417	-92.5222	161.190	24F
848	-39.5582	69.5417	-92.5222	161.190	24A ..

f^* = Bending-mode frequency

Table No. VI-4c First-Step Bending-Mode Slope with 50 Percent Propellant Remaining

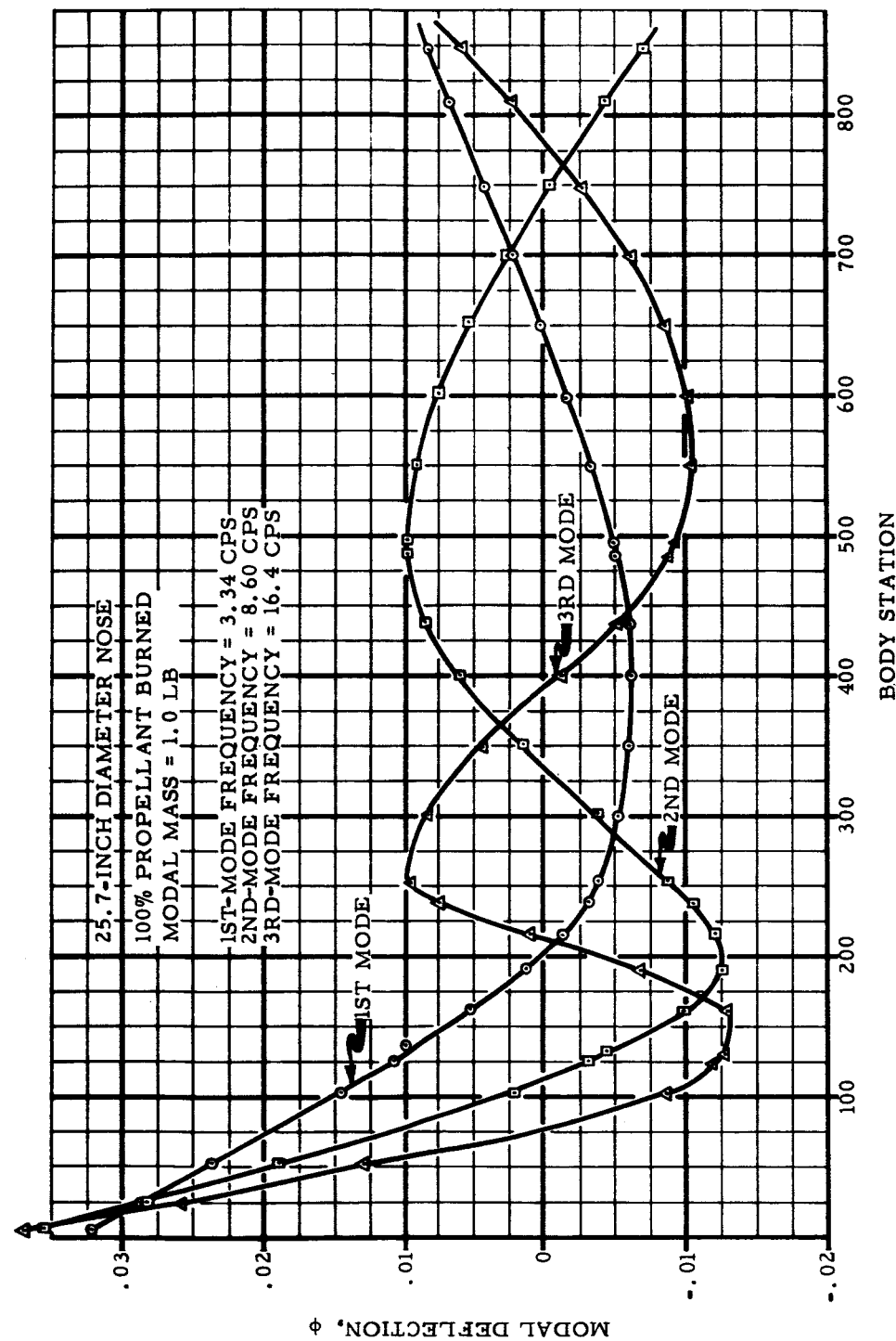


Figure VI-5 First-Step Bending-Mode Shapes and Frequencies at Burnout

R-ED 11122
VI-16

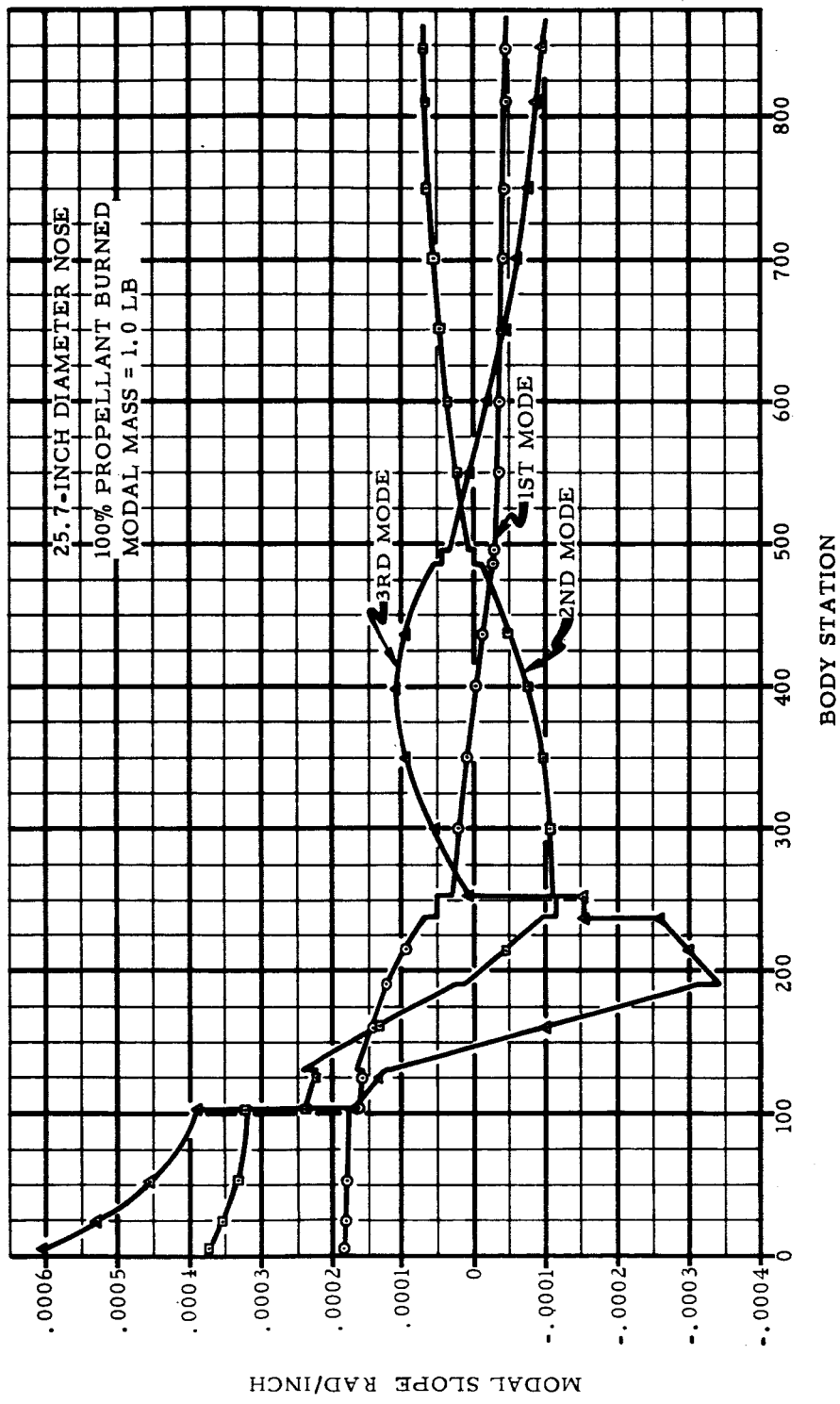


Figure VI-6 First-Step Bending-Mode Slopes at Burnout

R-ED 11122
VI-17

Tabulated Data Taken from CVA DIR No. 86240LD-61NS-1 of 11/17/60

CONFIGURATION		CONDITIONS			
Structural Shell over Fourth Step Modal Mass for each Mode = 1.0 Lb Nose at Body Station 5 Weight = 17,781 Lbs Nose Diameter = 25.7 In		150-Lb Payload Burnout Zero Percent Fuel Remaining CM (Center of Mass) at Body Sta 411.6 Moment of Inertia about CM = 0.9025×10^9			
Body Station (x)	1st-Mode ϕ $\times 10^{-5}$ where $f^* = 3.34$ cps	2nd-Mode ϕ $\times 10^{-5}$ where $f^* = 8.60$ cps	3rd-Mode ϕ $\times 10^{-5}$ where $f^* = 16.4$ cps	4th-Mode ϕ $\times 10^{-5}$ where $f^* = 29.0$ cps	Panel Point
5	3225.66	3542.11	3710.81	2482.90	001
24	2875.10	2846.30	2632.95	1393.59	002
52	2368.40	1891.78	1308.95	322.548	003
103	1450.33	206.935	-845.151	-1009.06	004
125	1093.61	-303.314	-1180.34	-891.723	005
131	997.173	-437.622	-1258.05	-843.715	006
161	527.465	-1004.52	-1275.71	-102.727	007
191	127.645	-1248.12	-657.404	778.148	008
215	-130.522	-1207.62	109.209	1123.62	009
238	-318.391	-1044.34	751.670	1125.65	010
253	-393.823	-872.299	984.034	893.828	011
300	-516.784	-366.147	835.204	99.8801	012
350	-597.540	161.605	436.230	-582.798	013
400	-620.191	605.319	-111.174	-711.598	014
437	-598.008	838.713	-506.115	-380.350	015
486	-514.692	980.220	-881.616	434.035	016

f^* = Bending-mode frequency

Table No. VI-5a First-Step Bending-Mode Shape at Burnout

R-ED 11122

VI-18

Body Station (x)	1st-Mode ϕ $\times 10^{-5}$ where $f^* = 3.34$ cps	2nd-Mode ϕ $\times 10^{-5}$ where $f^* = 8.60$ cps	3rd-Mode ϕ $\times 10^{-5}$ where $f^* = 16.4$ cps	4th-Mode ϕ $\times 10^{-5}$ where $f^* = 29.0$ cps	Panel Point
496	-489.187	980.607	-925.470	622.499	017
550	-330.162	901.684	-1031.57	1424.58	018
600	-162.221	750.286	-1002.52	1919.84	019
650	21.7551	534.358	-852.830	2052.87	020
700	217.901	266.674	-594.849	1765.65	021
750	422.351	-38.4439	-249.756	1066.72	022
810	673.282	-432.540	240.547	-222.857	023
848	834.434	-694.229	587.673	-1286.10	024

f^* = Bending-mode frequency

Table No. VI-5b First-Step Bending-Mode Shape at Burnout

R-ED 11122

VI-19

Modal Slopes, Rad/In

Tabulated Data Taken from CVA DIR No. 86240LD-61NS-1 of 11/17/69

CONFIGURATION		CONDITIONS			
Structural Shell over Fourth Step Modal Mass for each Mode = 1.0 Lb Nose at Body Station .5 Weight = 17,781 Lbs Nose Diameter = 25.7 In		150-Lb Payload Burnout Zero Percent Fuel Remaining CM (Center of Mass) at Body Sta 411.6 Moment of Inertia about CM = $0.9025 \times 10^9 \text{ Lb-In}^2$			
Body Station (x)	1st-Mode $-d\phi/dx \times 10^{-6}$ where $f^* = 3.34 \text{ cps}$	2nd-Mode $-d\phi/dx \times 10^{-6}$ where $f^* = 8.60 \text{ cps}$	3rd-Mode $-d\phi/dx \times 10^{-6}$ where $f^* = 16.4 \text{ cps}$	4th-Mode $-d\phi/dx \times 10^{-6}$ where $f^* = 29.0 \text{ cps}$	Panel Point
5	185.942	376.453	605.469	650.456	1F
5	185.942	376.453	605.469	650.456	1A
24	183.075	355.983	529.117	496.187	2F
24	183.075	355.983	529.117	496.187	2A
52	180.627	337.165	454.965	339.482	3F
52	180.627	337.165	454.965	339.482	3A
103	179.403	323.558	389.782	182.719	4F
103	163.251	238.284	170.303	-32.3764	4A
125	161.035	225.579	134.415	-74.2963	5F
125	161.035	225.579	134.415	-74.2963	5A
131	160.430	222.113	124.627	-85.7289	6F
131	168.217	242.850	111.881	-223.681	6A
161	144.922	135.083	-100.108	-270.311	7F
161	144.922	135.083	-100.108	-270.311	7A
191	121.625	27.3145	-312.097	-316.939	8F
191	120.788	10.7639	-339.895	-217.001	8A

f^* = Bending-mode frequency

Table No. VI-6a First-Step Bending-Mode Slope at Burnout

Modal Slopes, Rad/In

Body Station (x)	1st-Mode $-d\phi/dx$ $\times 10^{-6}$ where $f^* = 3.34$ cps	2nd-Mode $-d\phi/dx$ $\times 10^{-6}$ where $f^* = 8.60$ cps	3rd-Mode $-d\phi/dx$ $\times 10^{-6}$ where $f^* = 16.4$ cps	4th-Mode $-d\phi/dx$ $\times 10^{-6}$ where $f^* = 29.0$ cps	Panel Point
215	94.3505	-44.5078	-298.950	-70.8929	9F
215	94.3505	-44.5078	-298.950	-70.8929	9A
238	69.0143	-97.4764	-259.711	69.1272	10E
238	50.2882	-114.695	-154.910	154.548	10A
253	50.2882	-114.695	-154.910	154.548	11F
253	31.0125	-108.730	8.34621	184.619	11A
300	21.3113	-106.654	54.9860	153.231	12F
300	21.3113	-106.654	54.9860	153.231	12A
350	10.3407	-97.1466	94.6377	81.1478	13F
350	10.3407	-97.1466	94.6377	81.1478	13A
400	-1.51904	-73.9934	107.906	-40.4964	14F
400	-1.51904	-73.9934	107.906	-40.4964	14A
437	-10.7314	-48.3656	93.7879	-122.515	15F
437	-10.7314	-48.3656	93.7879	-122.515	15A
486	-23.2743	-9.39344	59.4785	-209.887	16F
486	-25.5051	-.386382	43.8535	-188.464	16A
496	-25.5051	-.386382	43.8535	-188.464	17F
496	-27.3002	6.48190	32.8655	-174.226	17A
550	-31.5981	22.7487	6.42987	-122.841	18F
550	-31.5981	22.7487	6.42987	-122.841	18A
600	-35.1917	36.7329	-17.8737	-62.8291	19F
600	-35.1917	36.7329	-17.8737	-62.8291	19A
650	-38.0122	48.3612	-40.7674	15.4196	20F

f^* = Bending-mode frequency

Table No. VI-6b First-Step Bending-Mode Slope at Burnout
R-ED 11122
VI-21

Modal Slopes, Rad/In

Body Station (x)	1st-Mode -dφ/dx $\times 10^{-6}$ where $f^* = 3.34$ cps	2nd-Mode -dφ/dx $\times 10^{-6}$ where $f^* = 8.60$ cps	3rd-Mode -dφ/dx $\times 10^{-6}$ where $f^* = 16.4$ cps	4th-Mode -dφ/dx $\times 10^{-6}$ where $f^* = 29.0$ cps	Panel Point
650	-38.0122	48.3612	-40.7674	15.4196	20A
700	-40.0596	57.2800	-60.3075	98.6149	21F
700	-40.0596	57.2800	-60.3075	98.6149	21A
750	-41.3137	63.1415	-74.7909	173.942	22F
750	-41.3137	63.1415	-74.7909	173.942	22A
810	-42.1810	67.6313	-87.6142	254.647	23F
810	-42.1810	67.6313	-87.6142	254.647	23A
848	-42.6361	70.0996	-95.0838	304.955	24F
848	-42.6361	70.0996	-95.0838	304.955	24A

f^* = Bending-mode frequency

Table No. VI-6c First-Step Bending-Mode Slope at Burnout
 R-ED 11122
 VI-22

SECTION VII

ENGINE THRUST

**R-ED 11122
VII-1**

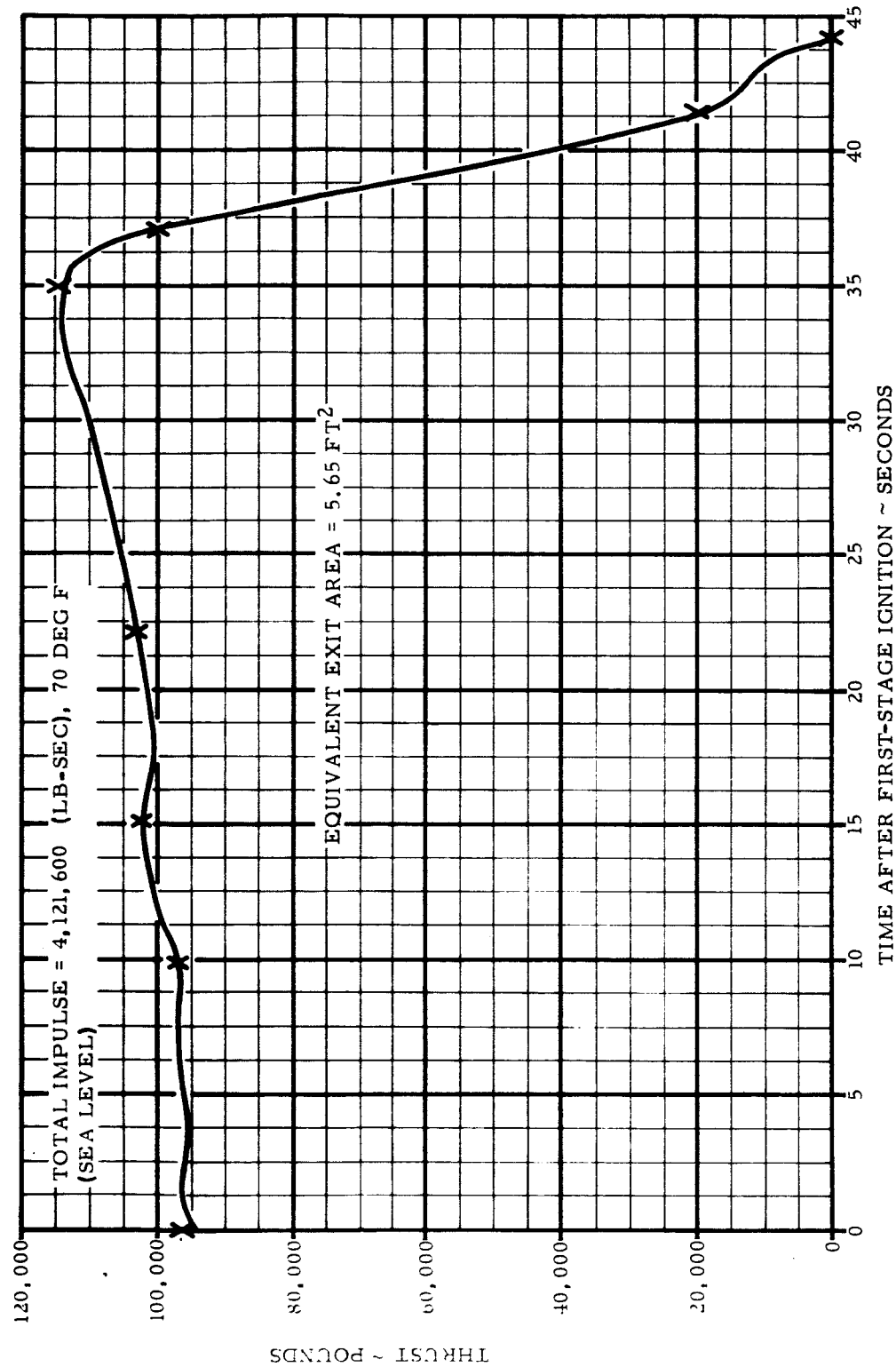


Figure VII-1 First-Stage Motor (Algol) Thrust Vs Time

R-ED 11122
VII-2

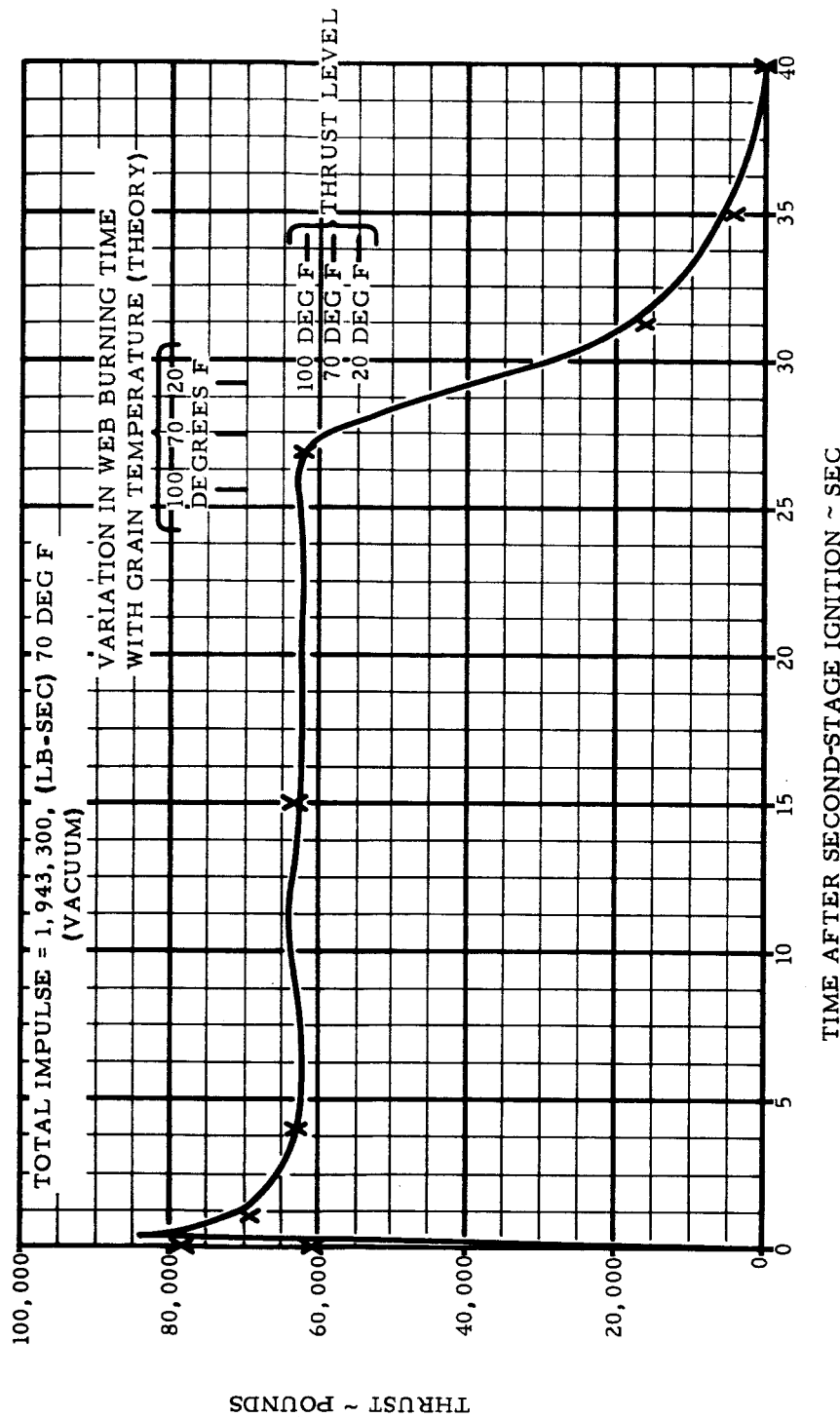


Figure VII-2 Second-Stage Motor (Castor) Thrust Vs Time
VII-3

R-ED 11122
VII-3

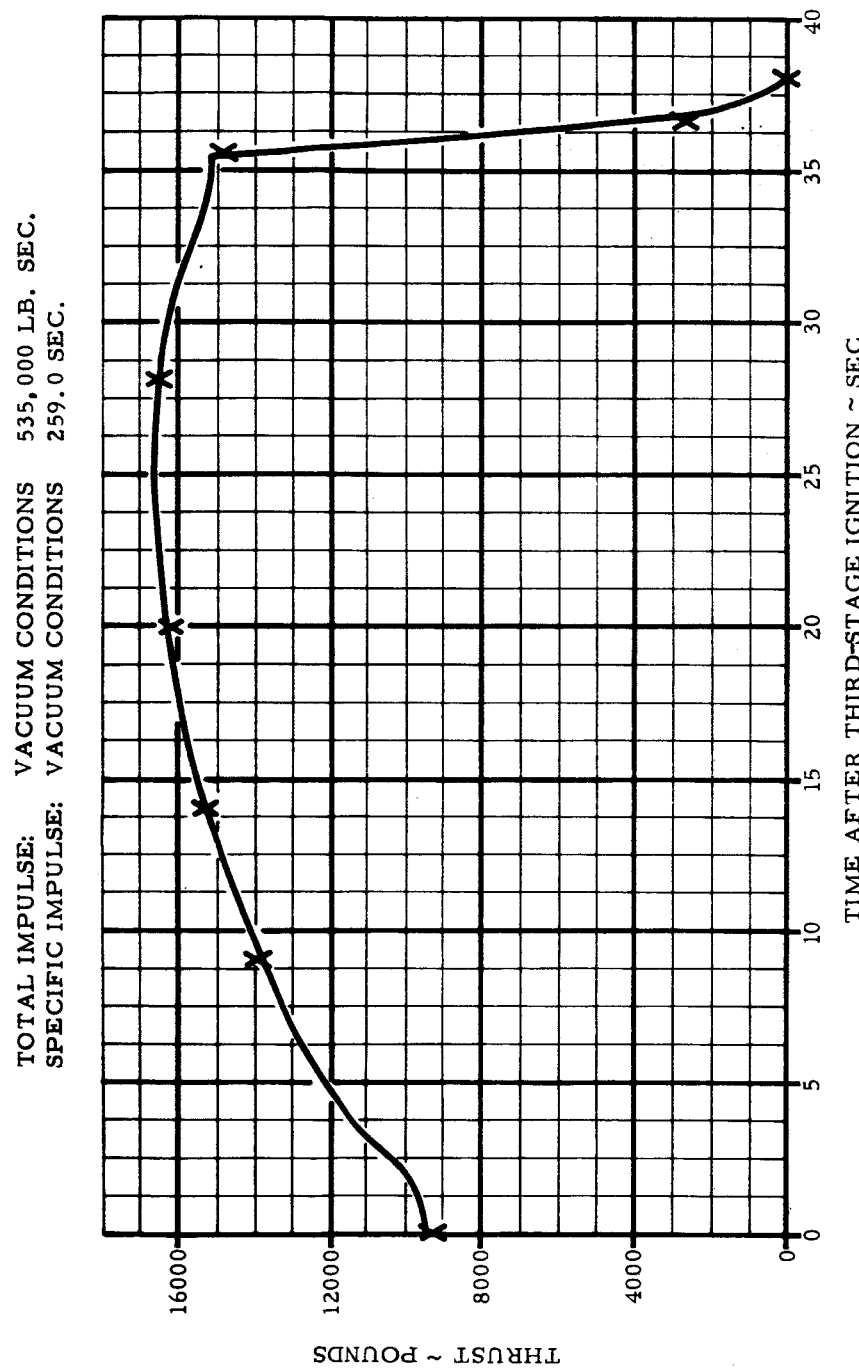


Figure VII-3 Third-Stage Motor (Antares) Thrust Vs Time
VII-4

R-ED 11122
VII-4

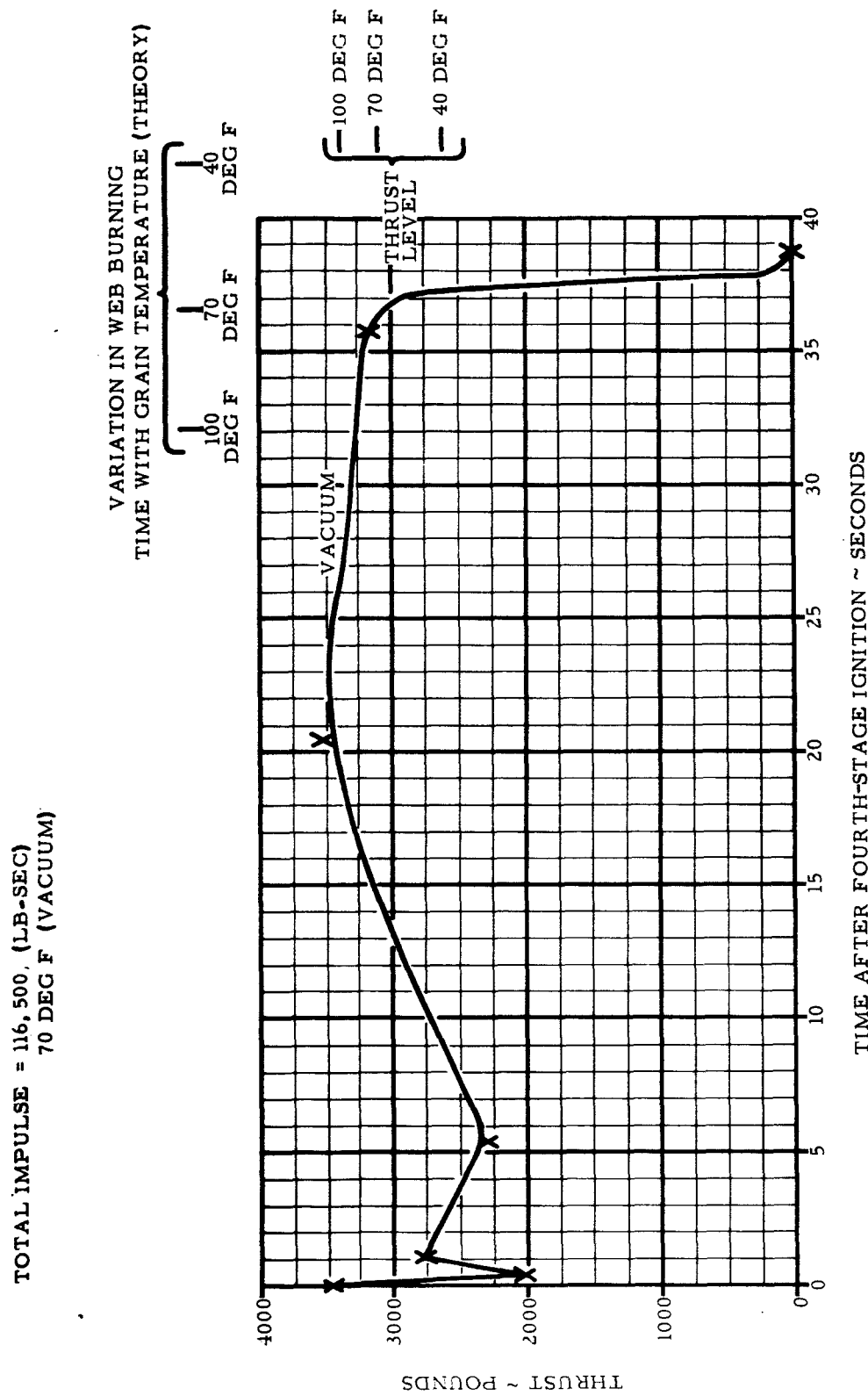


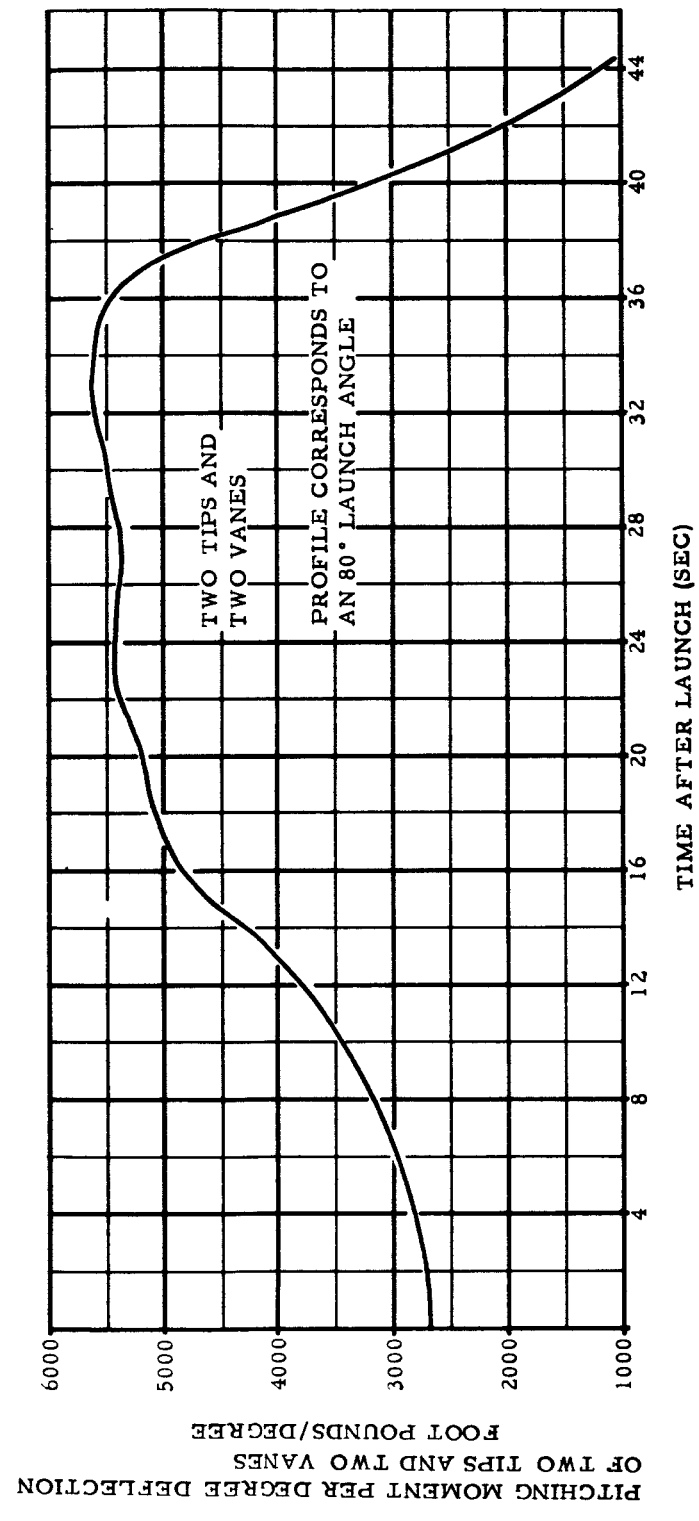
Figure VII-4 Fourth-Stage Motor (Altair) Thrust Vs Time

R-ED 11122
VII-5

SECTION VIII

CONTROL MEMBERS

**R-ED 11122
VIII-1**



R-ED 11122
VIII-2

Figure VIII-1 First-Step Total Pitch Control Moment Vs T

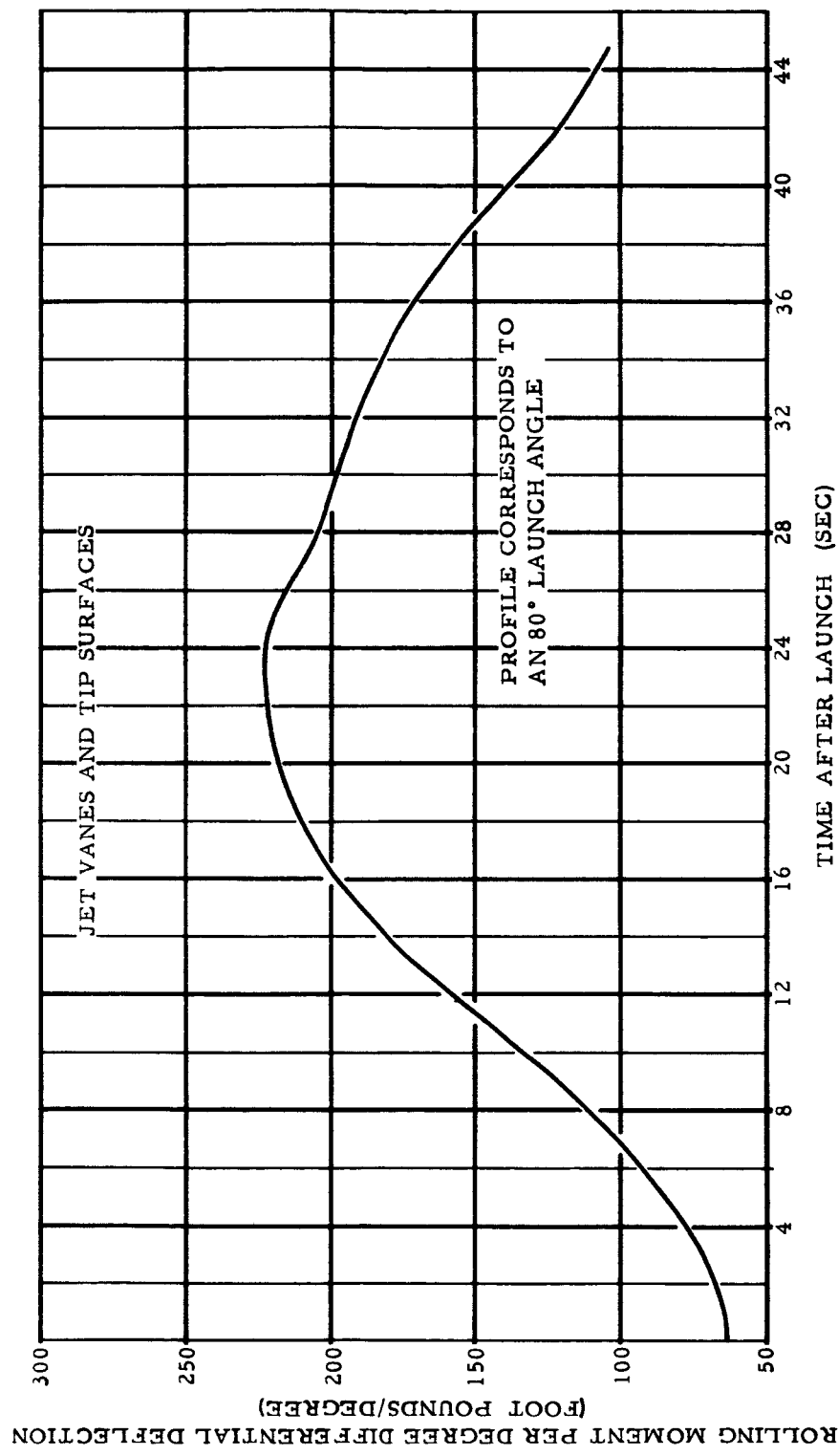


Figure VIII-2 First-Step Total Roll Control Moment Vs Time

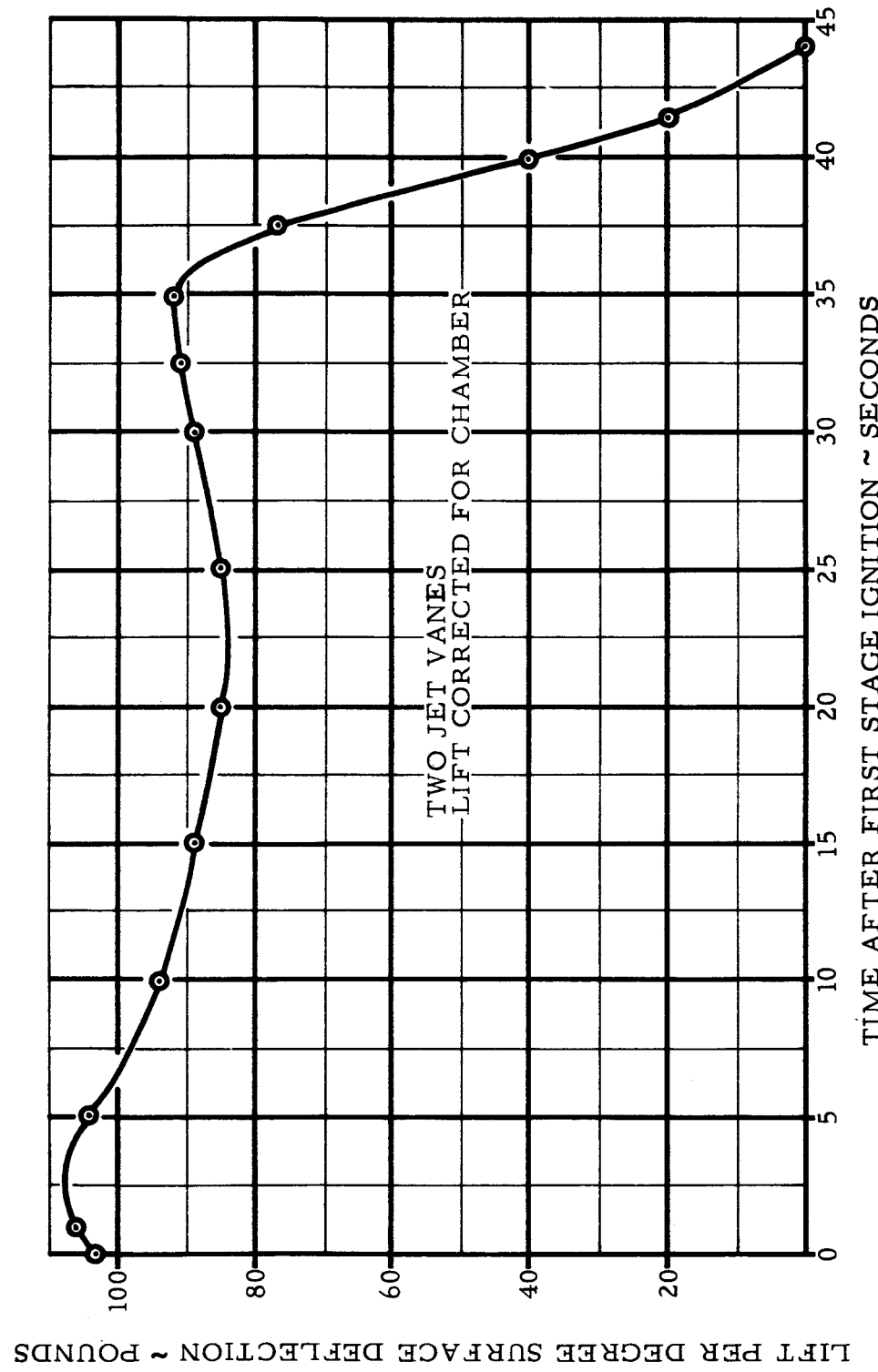


Figure VIII-3 Jet-Vane Lift V's Time

R-ED 11122
VIII-4

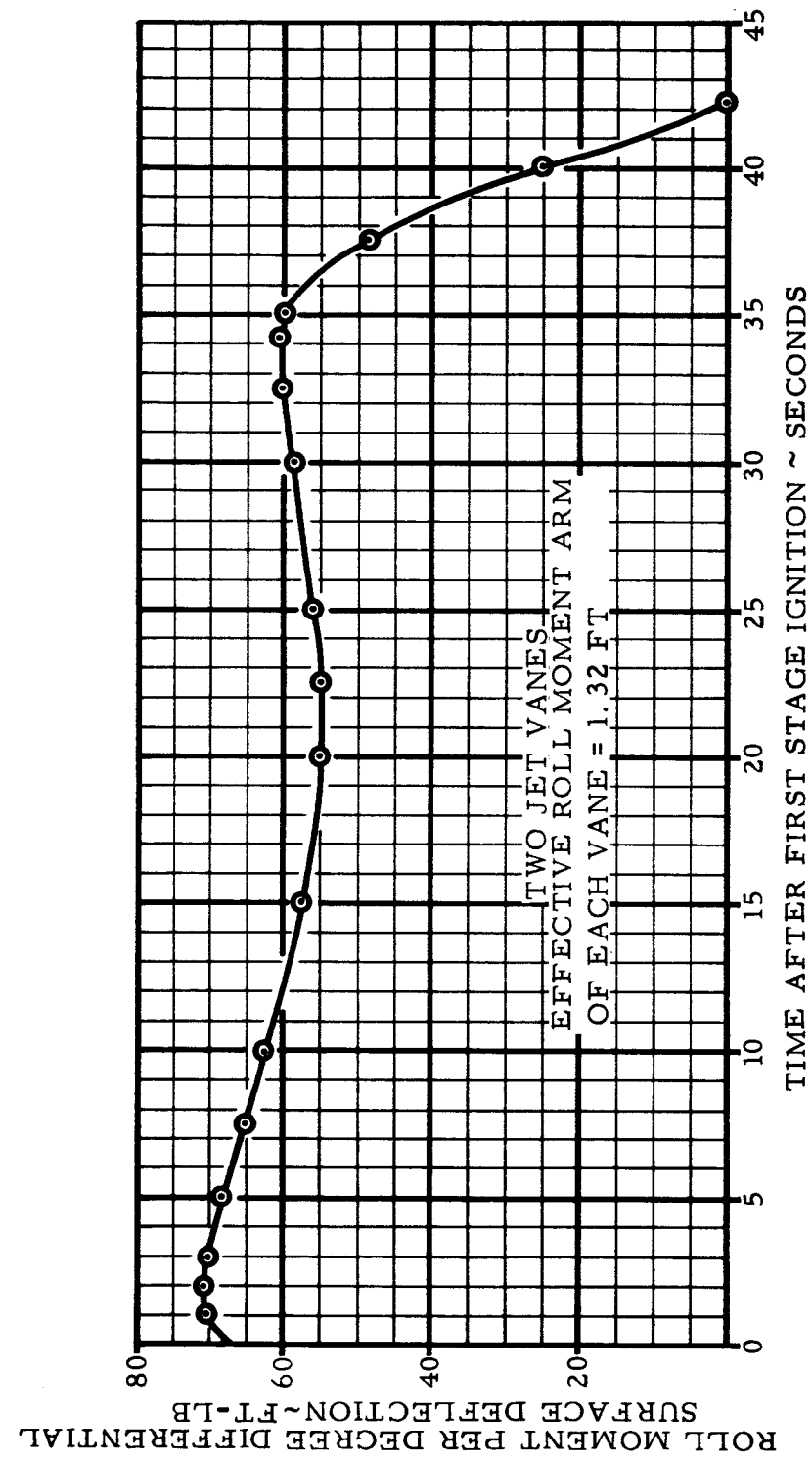


Figure VIII-4 Jet-Vane Roll Moment Vs Time

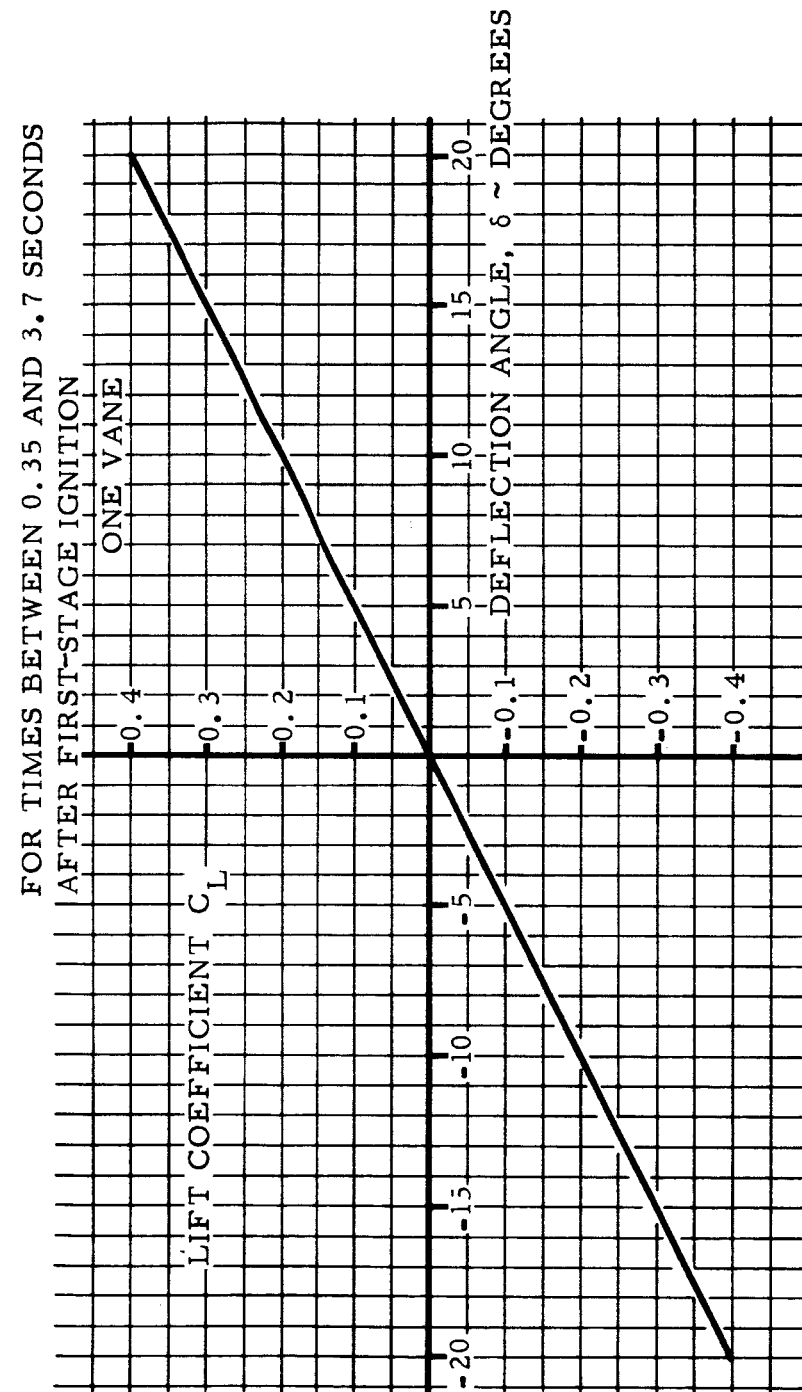


Figure VIII-5 Jet-Vane Lift Coefficient Vs Deflection Two Seconds
After Launch

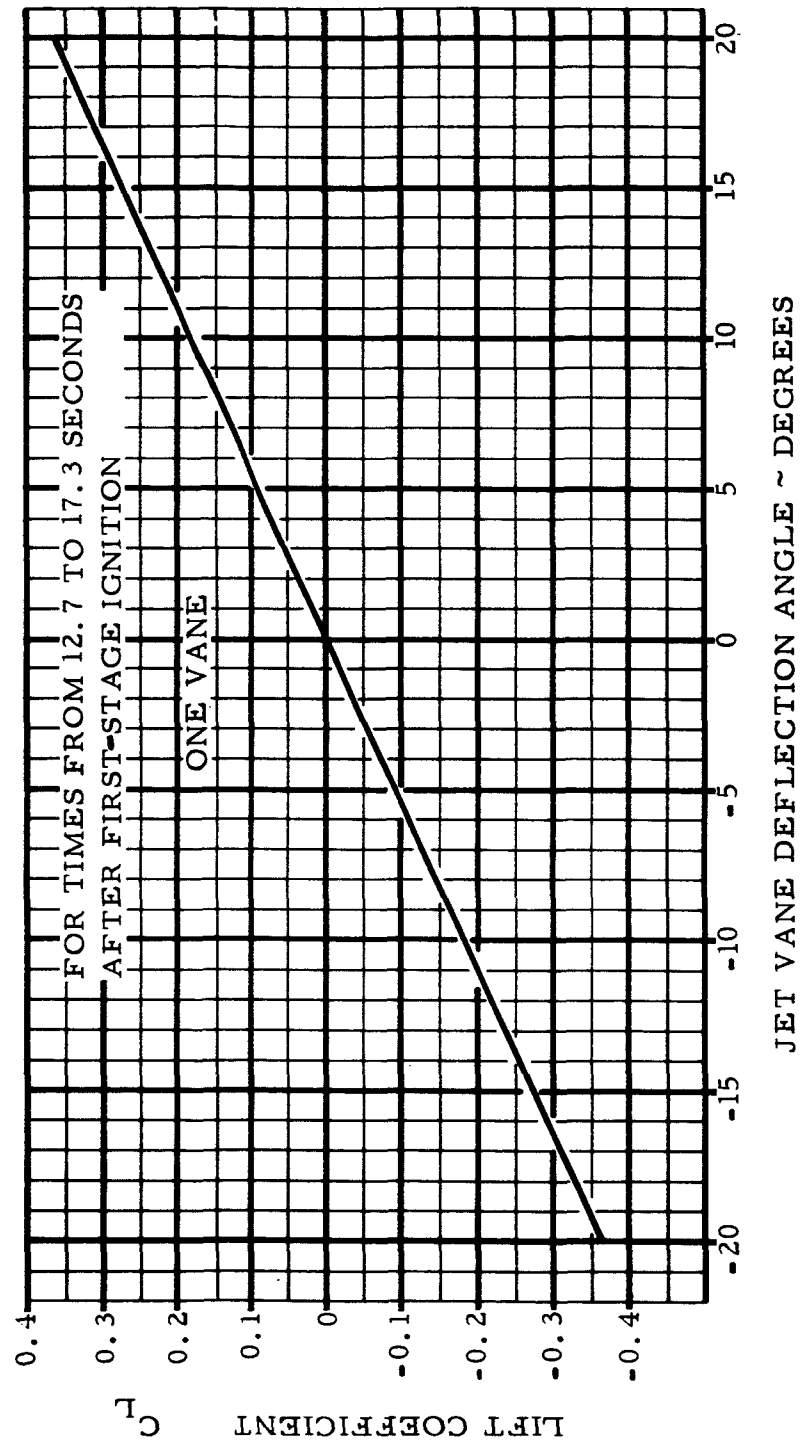


Figure VIII-6 Jet-Vane Lift Coefficient Vs Deflection 15 Seconds
After Launch

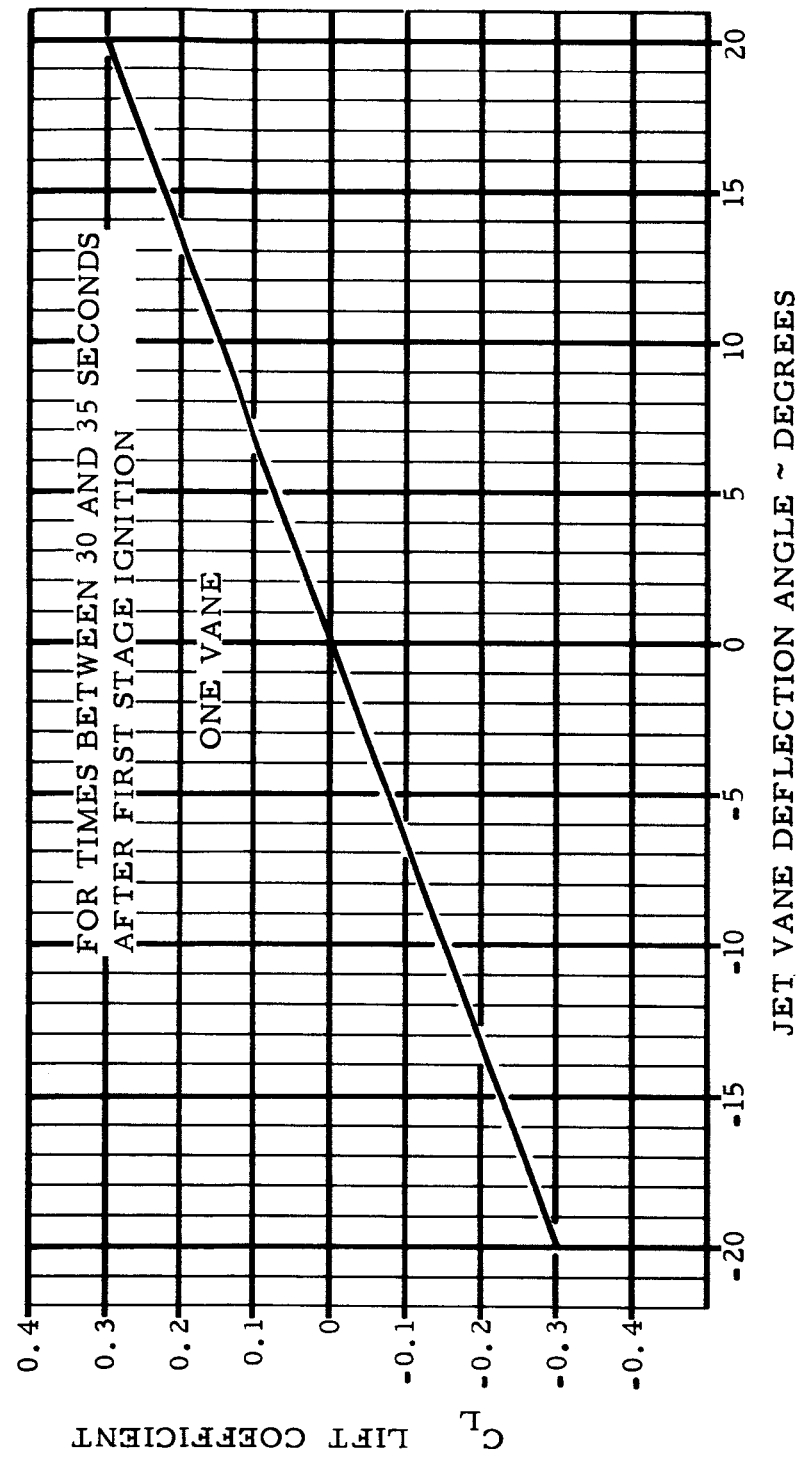


Figure VIII-7 Jet-Vane Lift Coefficient Vs Deflection 32 Seconds
 After Launch

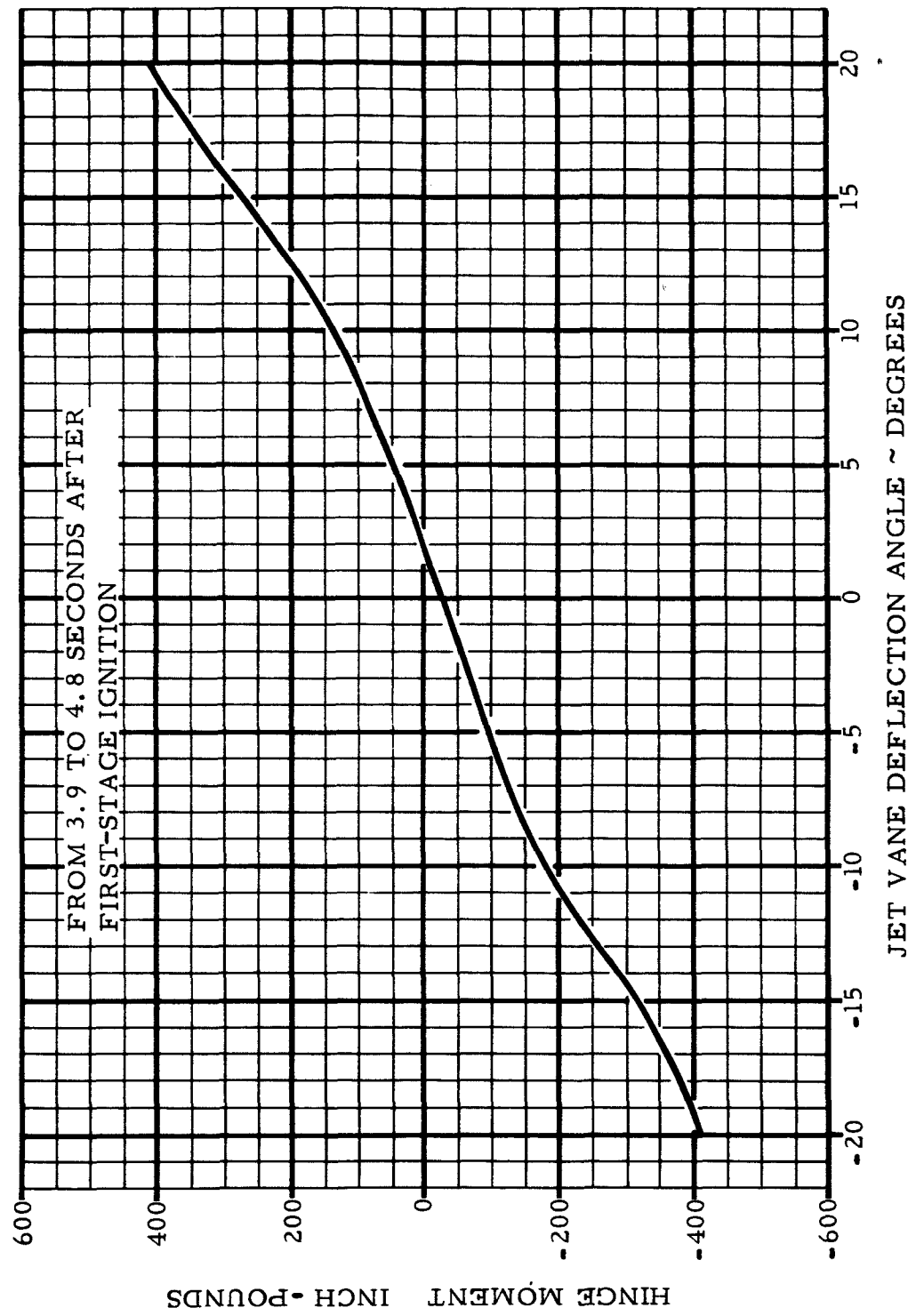


Figure VIII-8 Jet-Vane Hinge Moment Vs Deflection 4 Seconds
After Launch

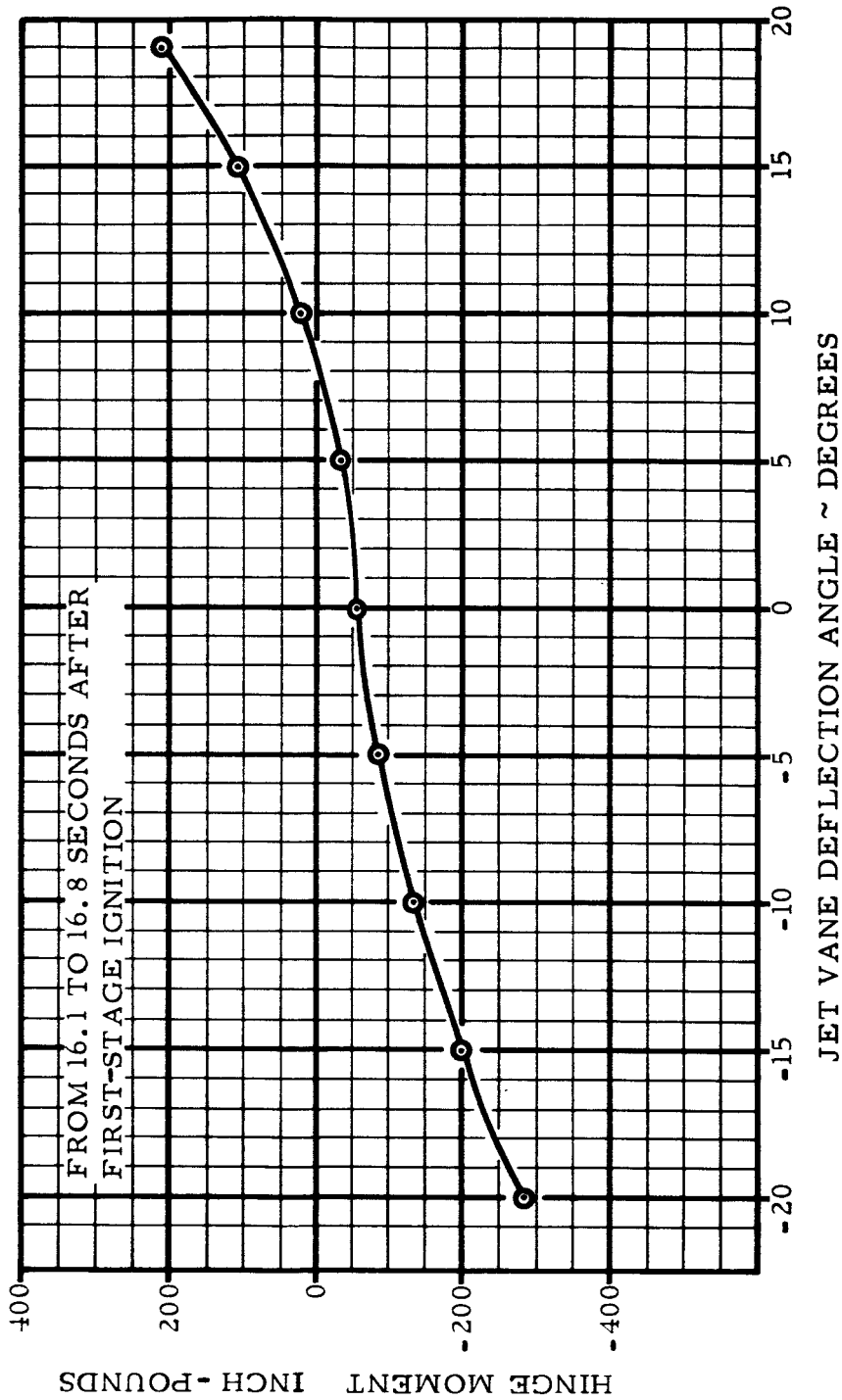


Figure VIII-9 Jet-Vane Hinge Moment Vs Deflection 16 Seconds
After Launch

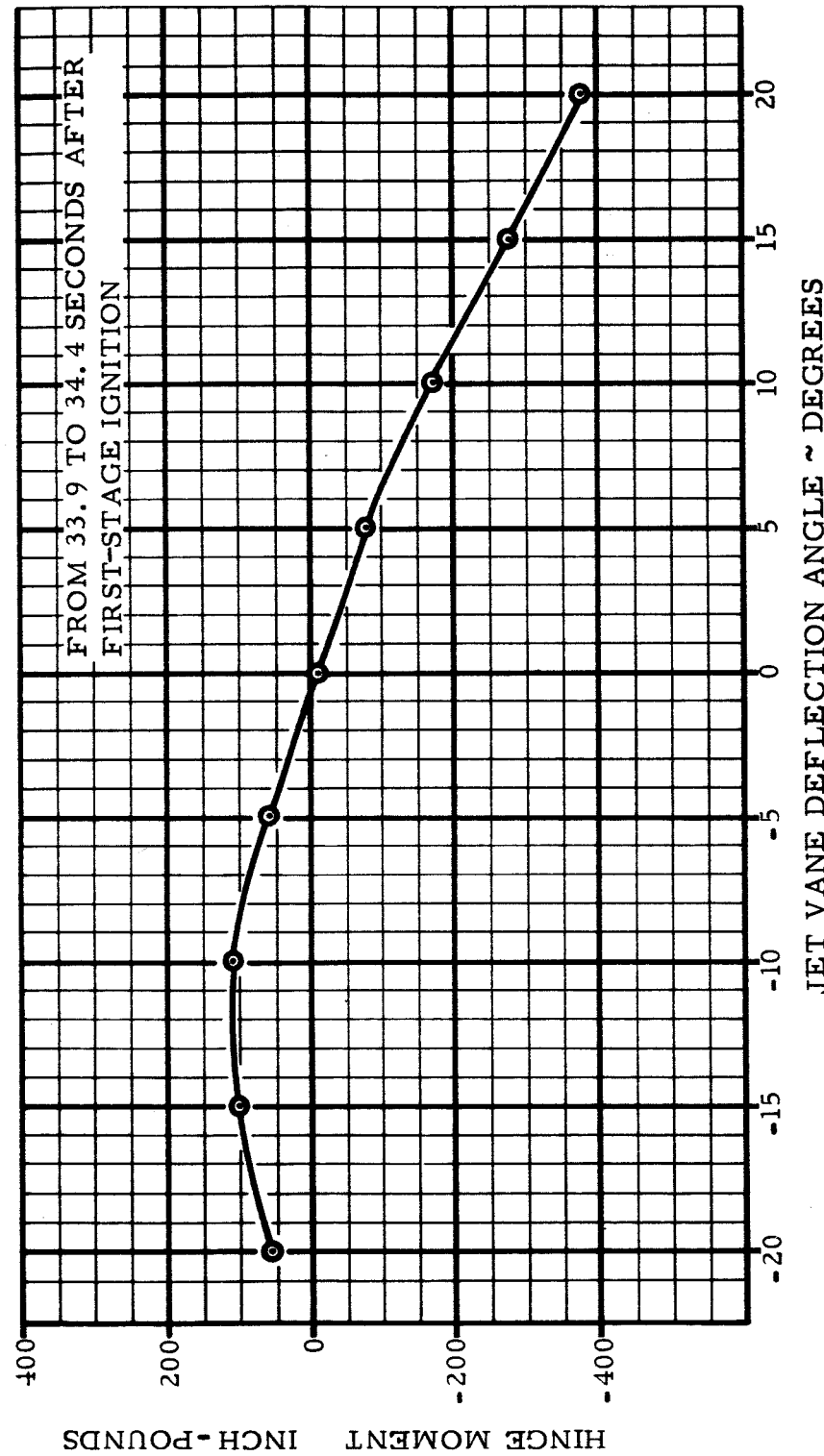


Figure VIII-10 Jet-Vane Hinge Moment Vs Deflection 34 Seconds
After Launch

R-ED 11122
VIII-11

FOR ZERO ANGLE OF ATTACK

REFERENCE AREA = 5.25 FT^2

TWO TIP SURFACES

SCOUT

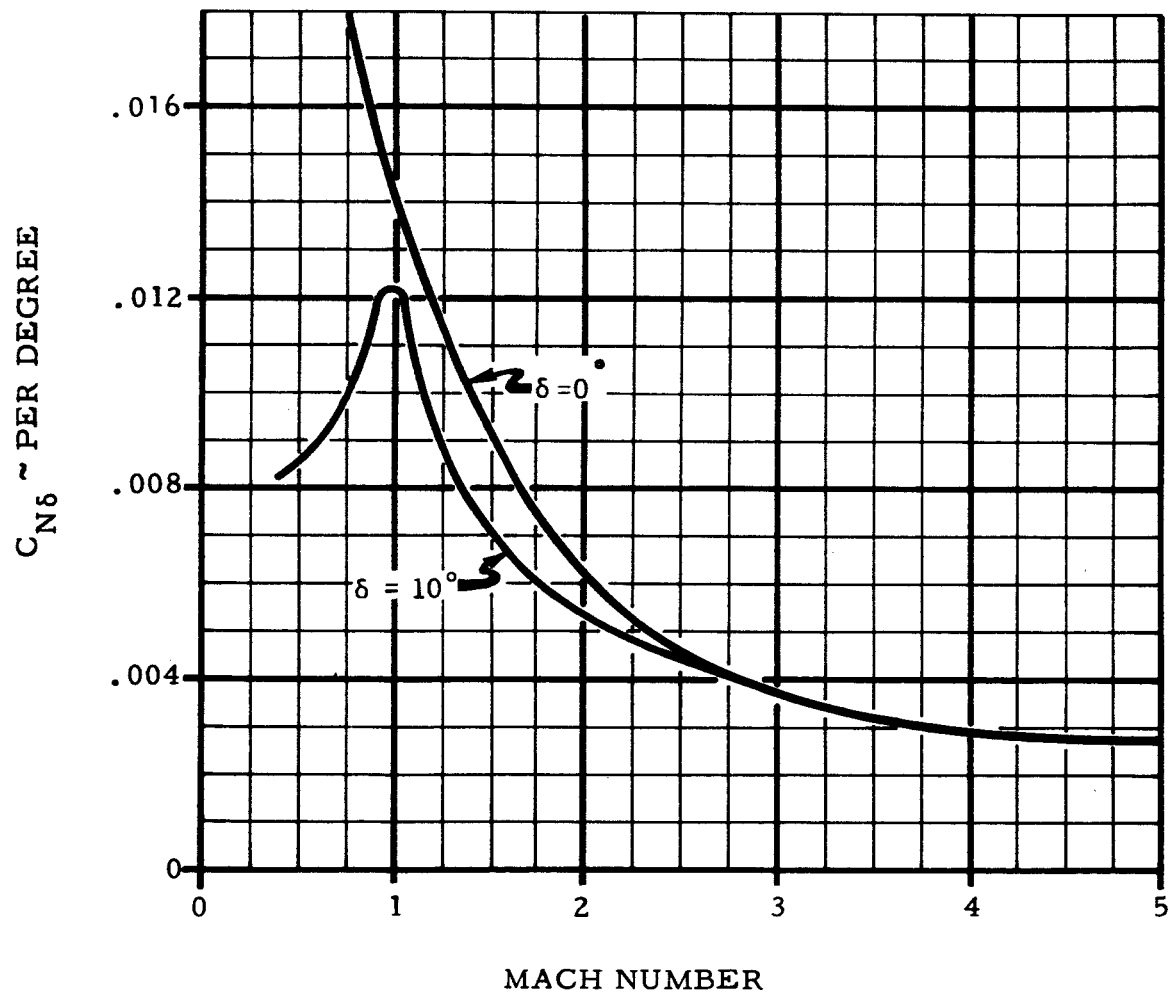
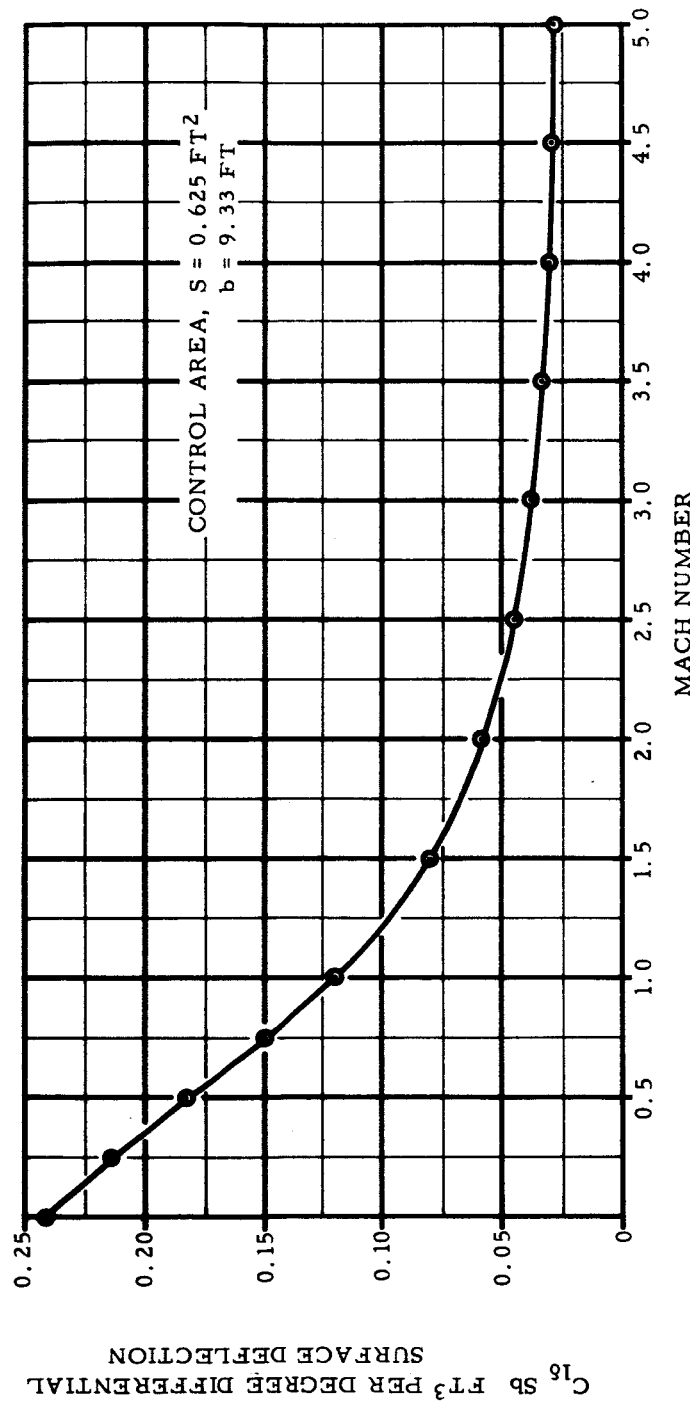


Figure VIII-11 Aerodynamic Tip-Surface Normal-Force Coefficient Vs Mach Number

Figure VIII-12 Aerodynamic Tip-Surface Roll Moment Coefficient
Vs Mach Number



R-ED 11122
VIII-13

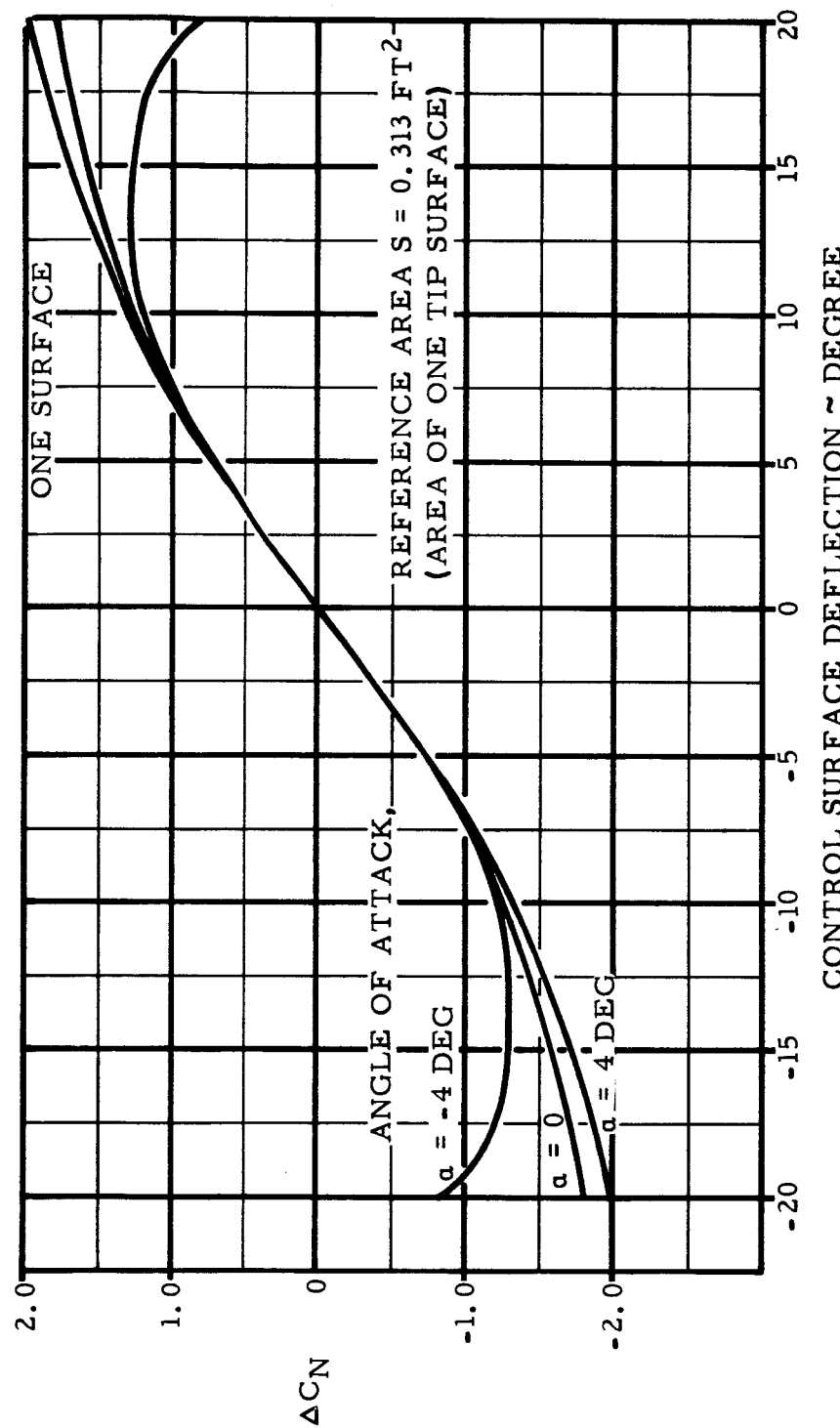


Figure VIII-13 Aerodynamic Tip-Surface Normal-Force Coefficient
 V_s Deflection at Mach 0.8

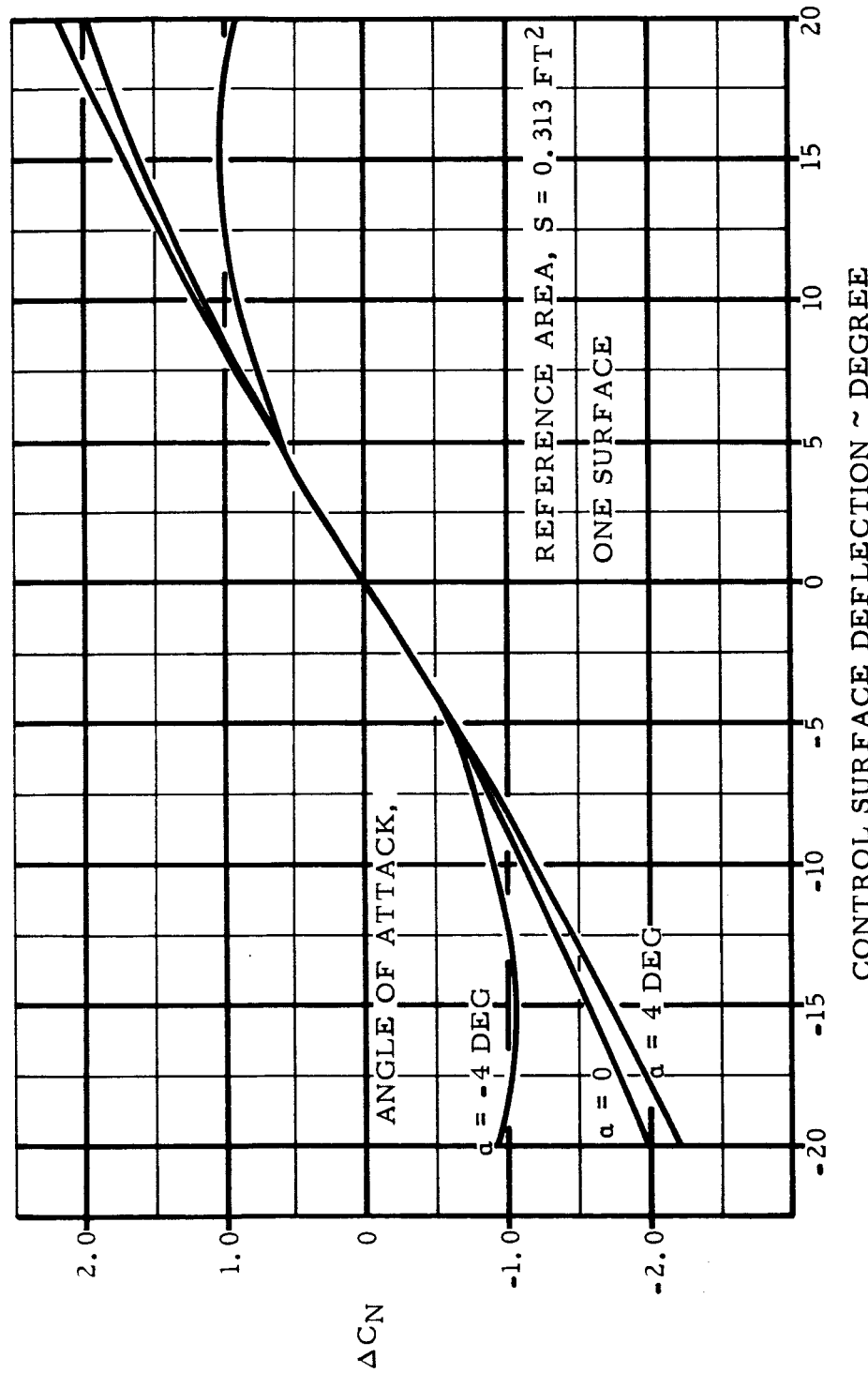


Figure VIII-14 Aerodynamic Tip-Surface Normal-Force Coefficient
 Vs Deflection at Mach 1.0

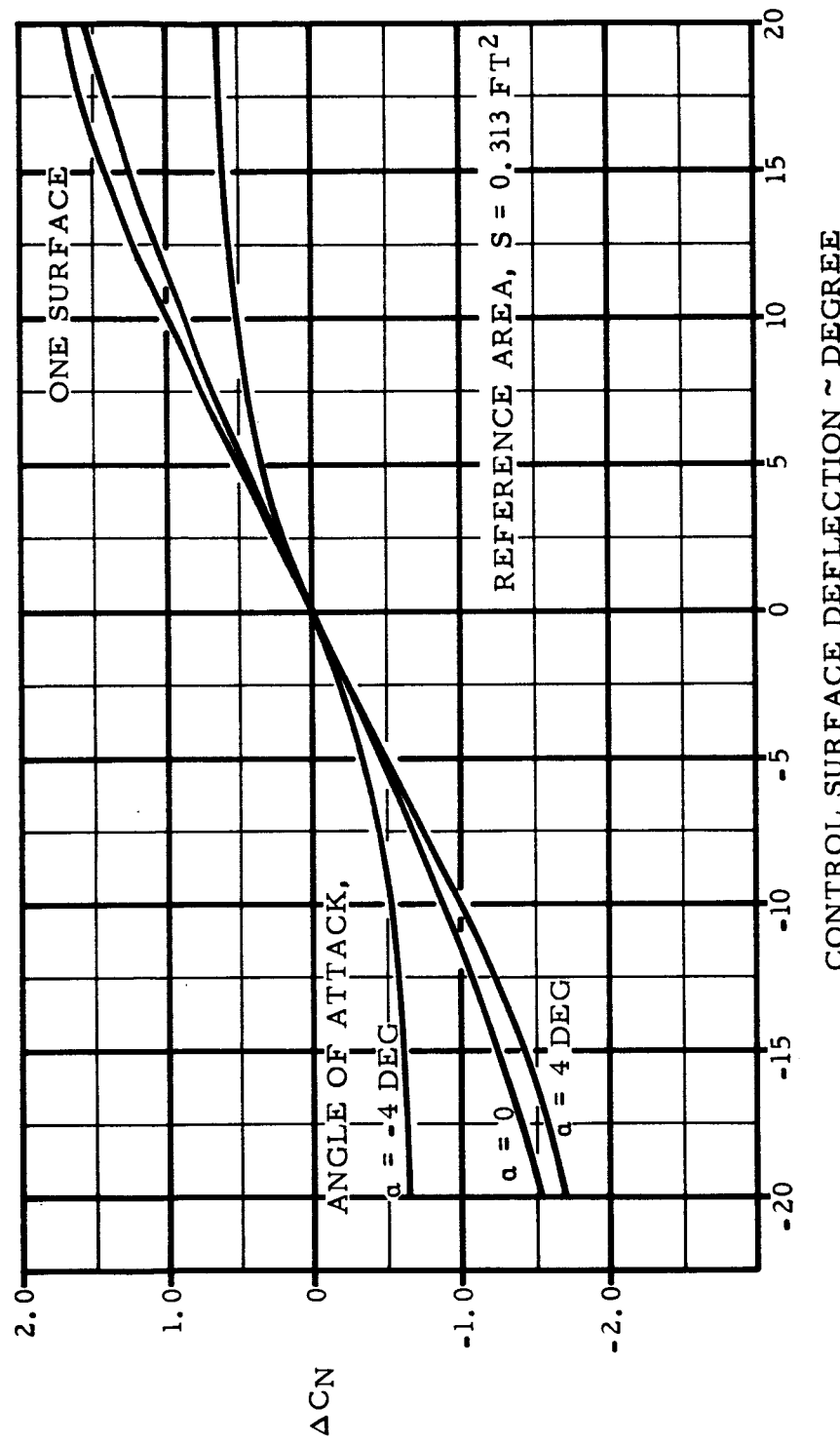


Figure VIII-15 Aerodynamic Tip-Surface Normal-Force Coefficient
V Deflection at Mach 1.2

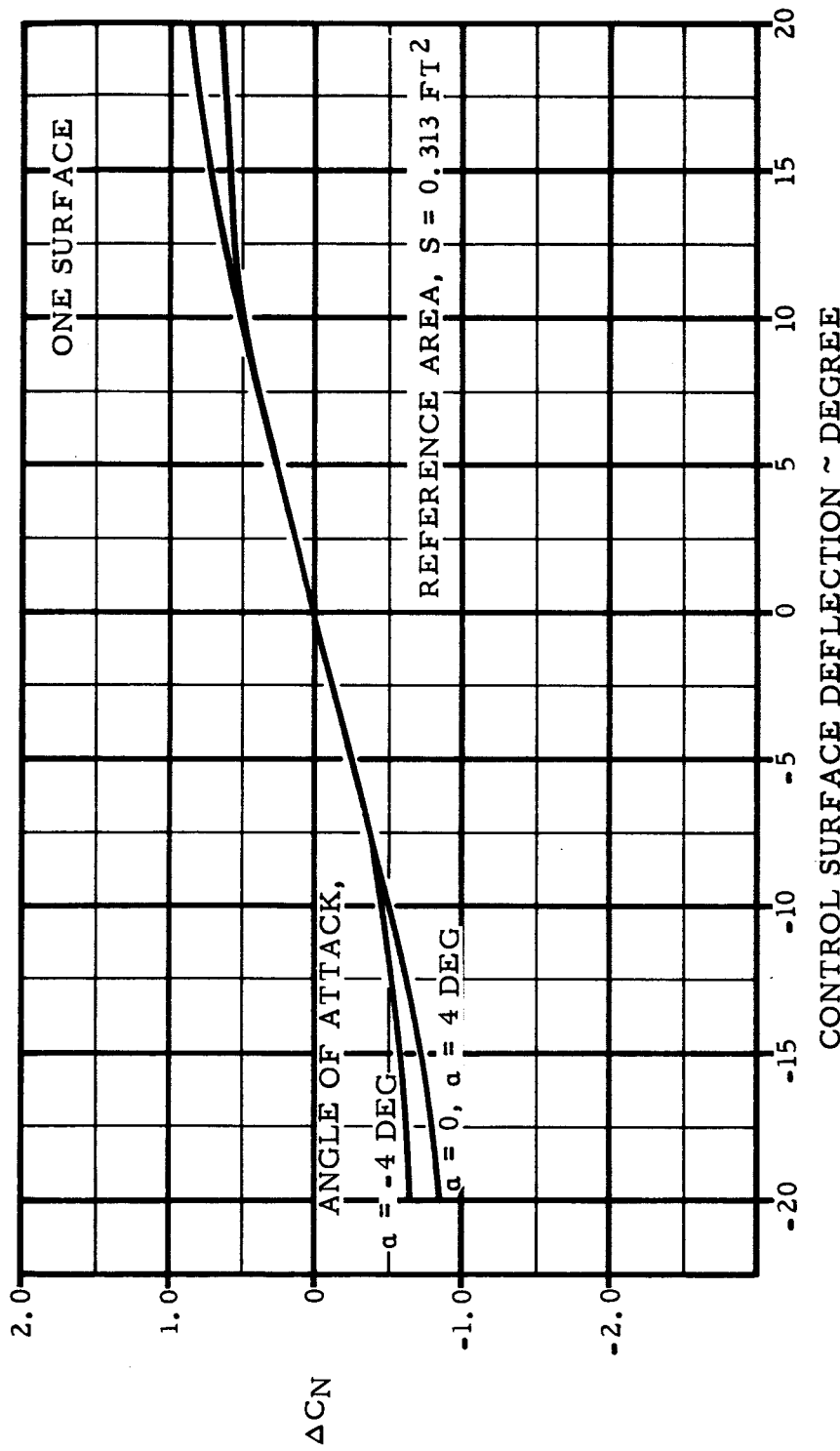


Figure VIII-16 Aerodynamic Tip-Surface Normal-Force Coefficient
Vs Deflection at Mach 2.0

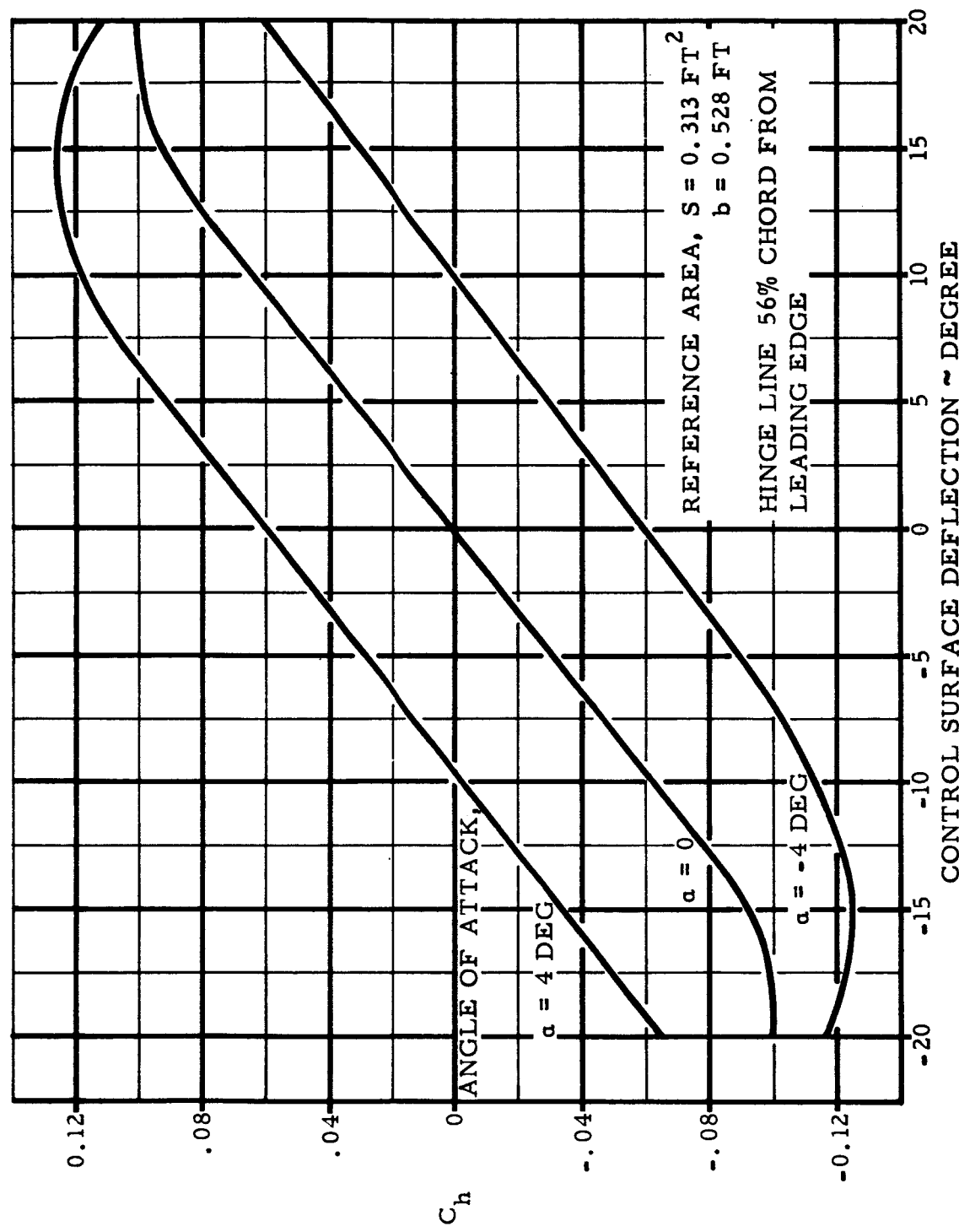


Figure VIII-17 Aerodynamic Tip-Surface Hinge Moment Coefficient
Vs Deflection at Mach 0.8

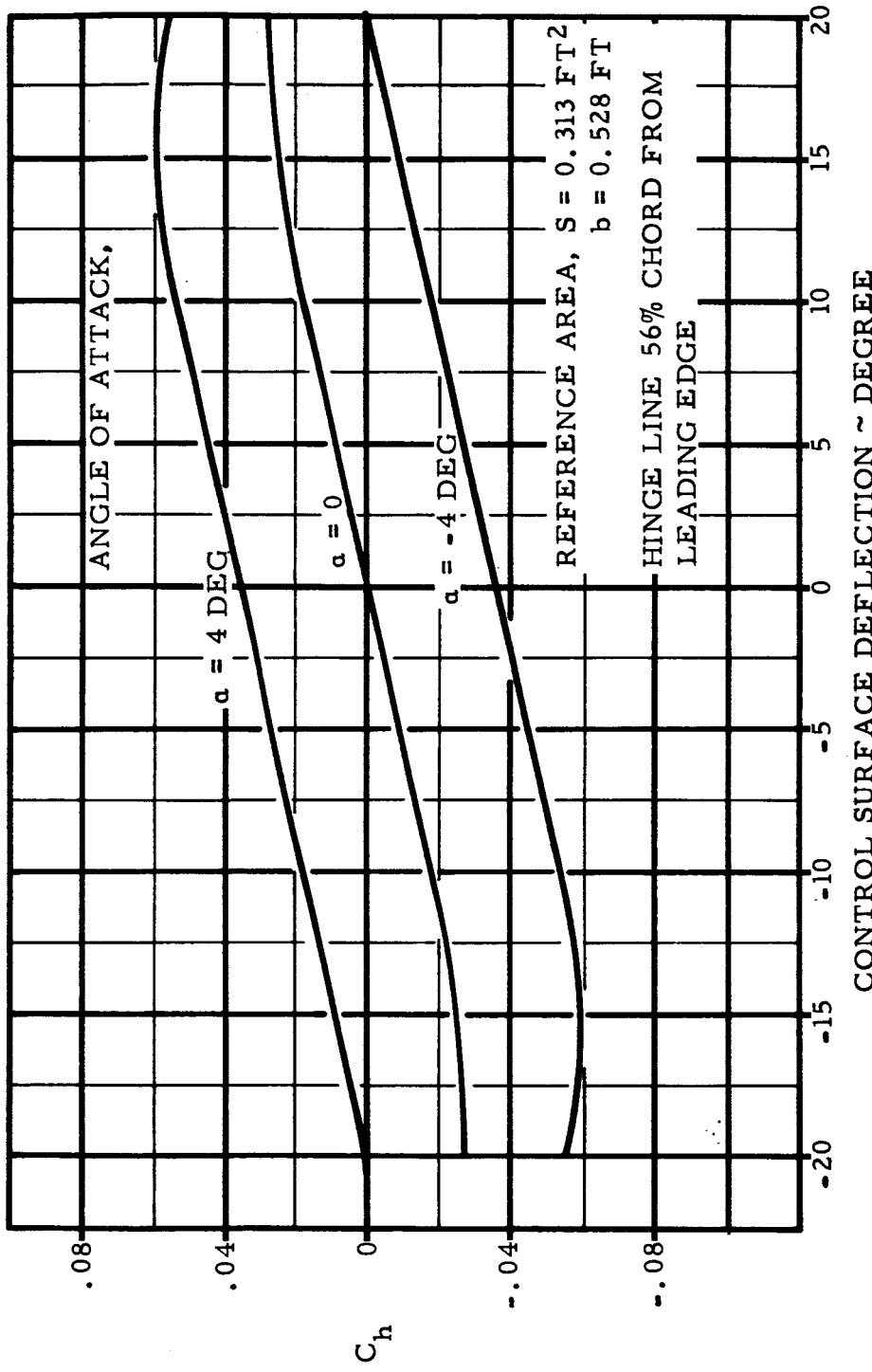


Figure VIII-18 Aerodynamic Tip-Surface Hinge Moment Coefficient
Vs Deflection at Mach 1.0

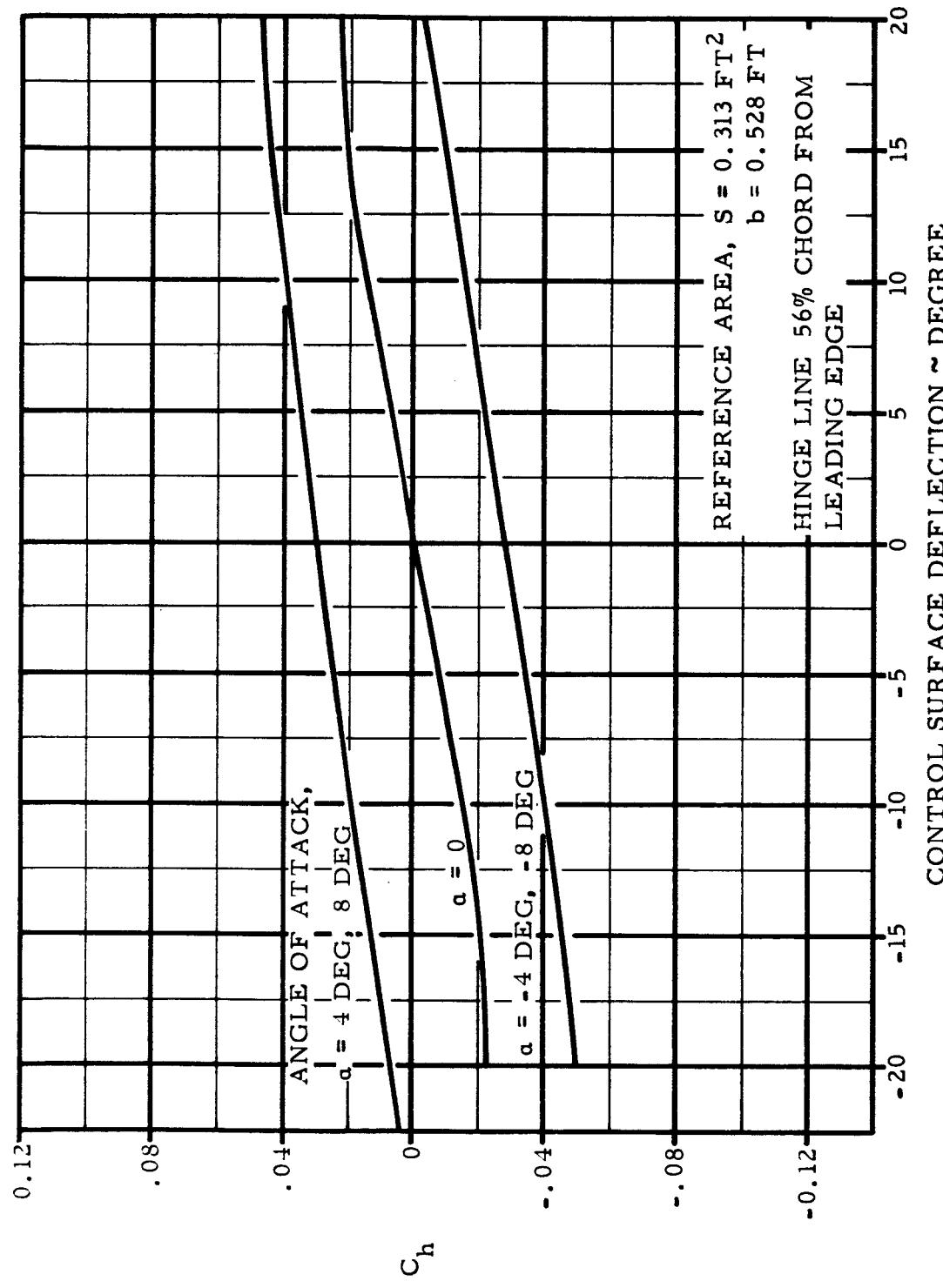


Figure VIII-19 Aerodynamic Tip-Surface Hinge Moment Coefficient
Vs Deflection at Mach 1.2

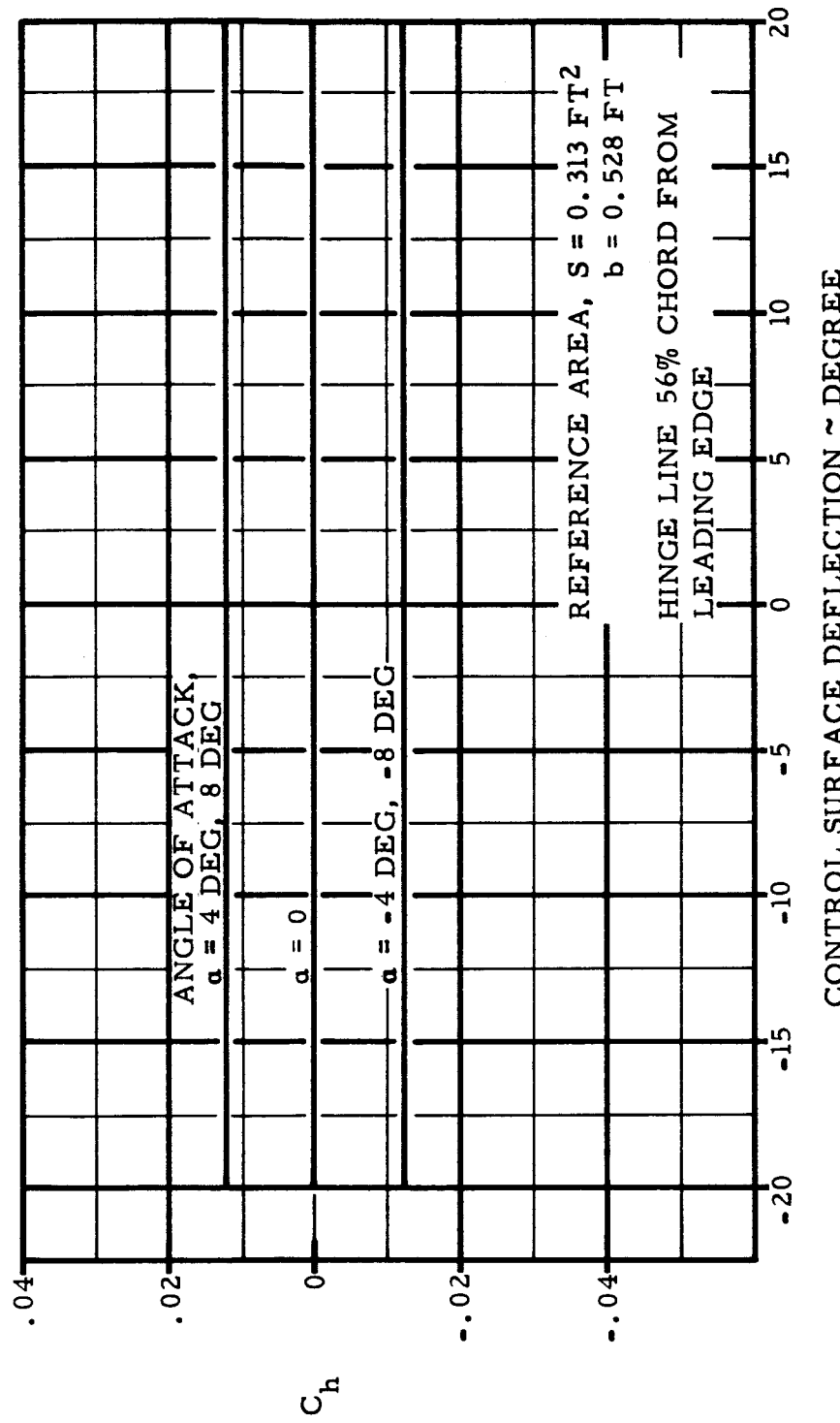


Figure VIII-20 Aerodynamic Tip-Surface Hinge Moment Coefficient
Vs Deflection at Mach ≥ 2.0

VALVE PRESSURE DROP = 1000 PSI
OIL TEMPERATURE = 110 DEG F

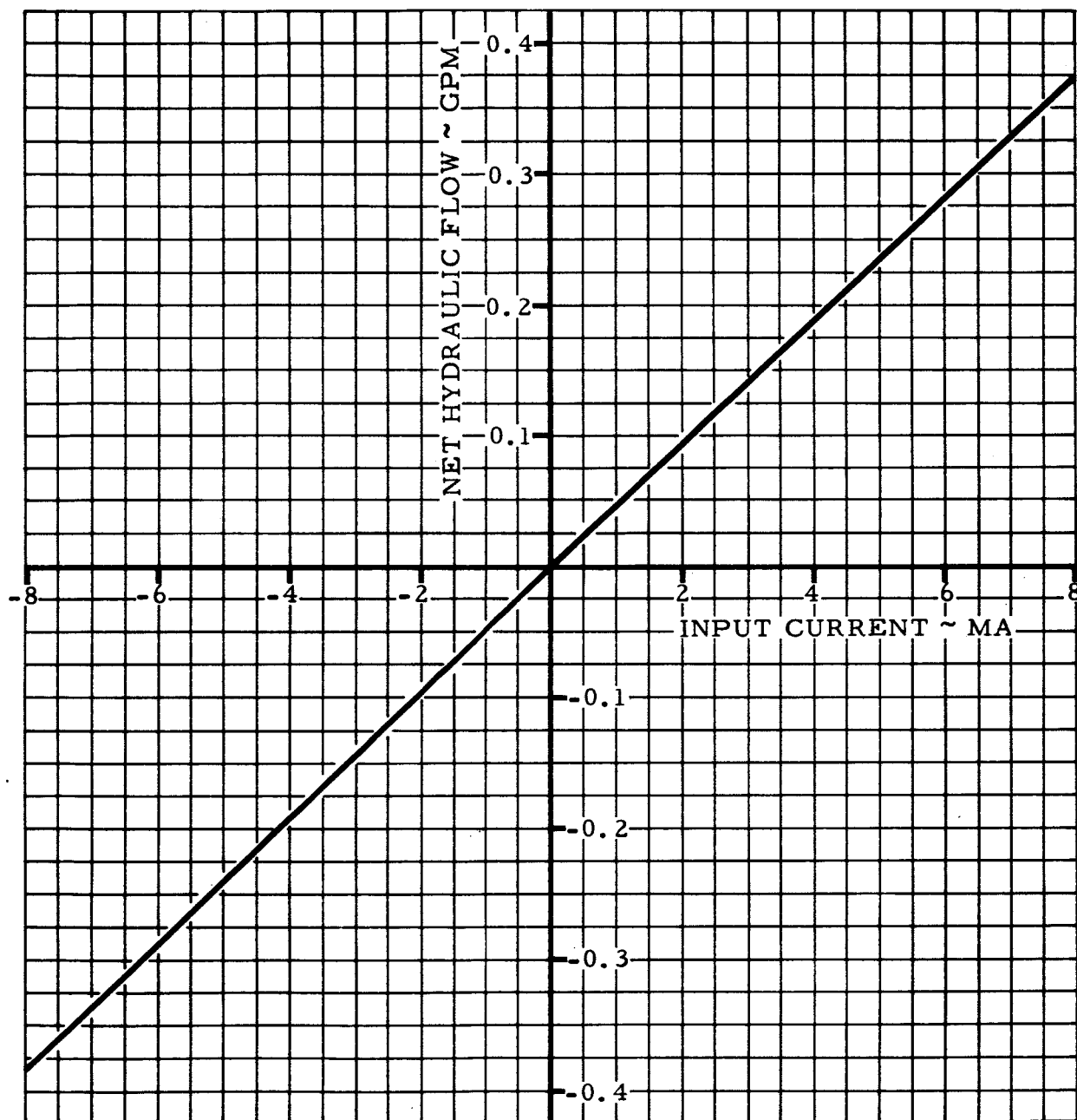


Figure VIII-21 Servo Actuator Control Valve Flow Vs Input Signal

SECTION IX

FLIGHT PROFILE

R-ED 11122
IX-1

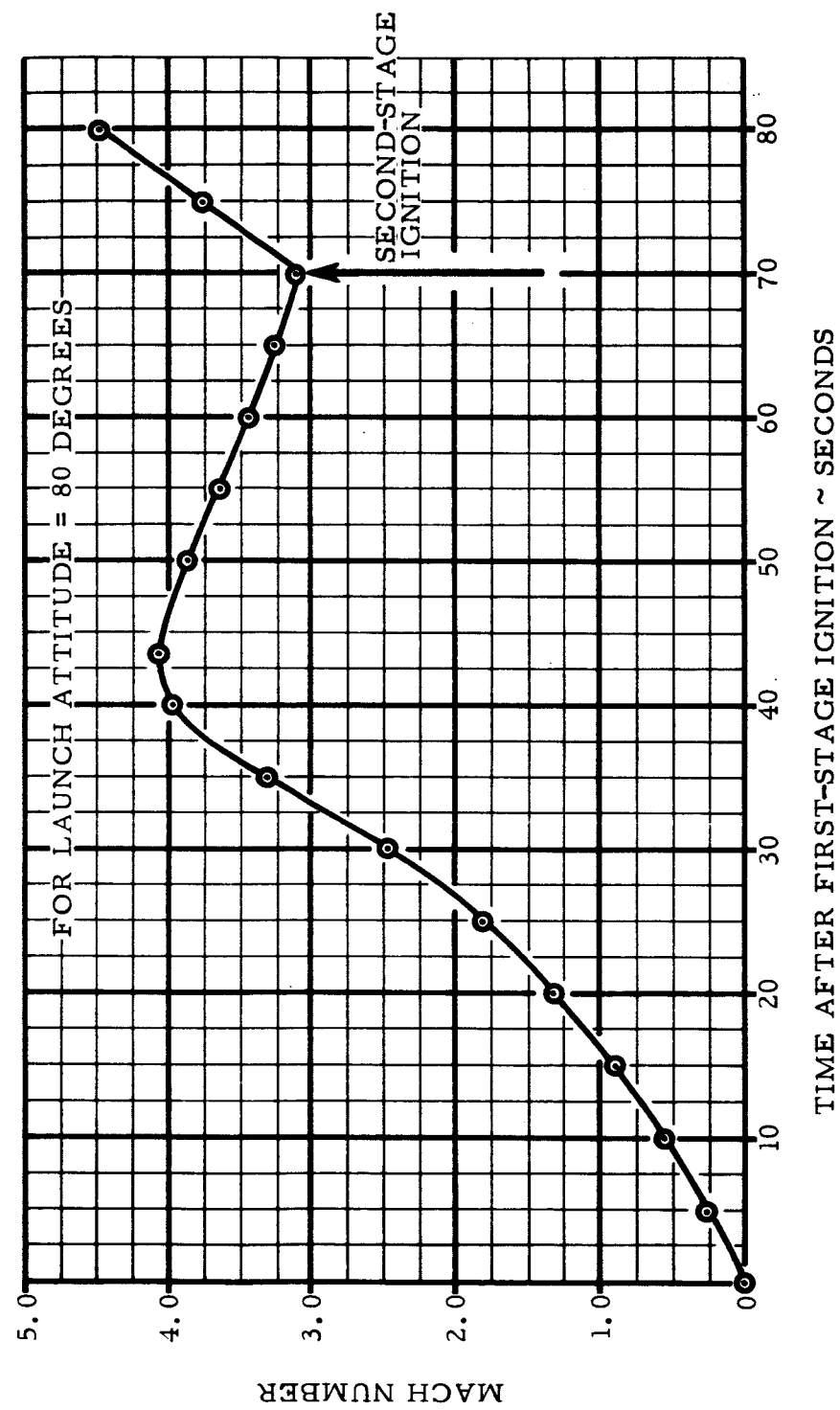


Figure IX-1 First-Step Mach Number Vs Time
IX-2

R-ED 11122
IX-2

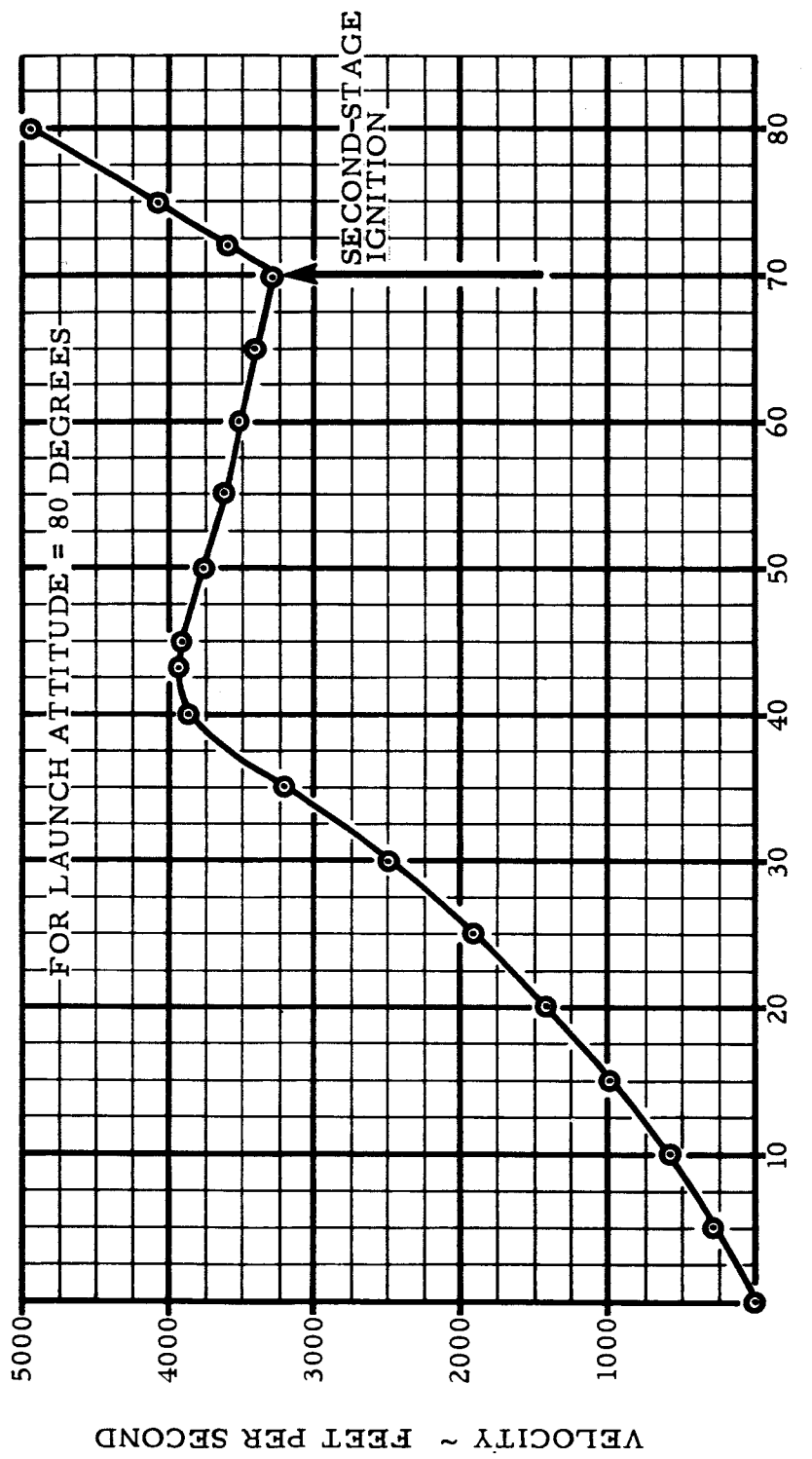


Figure IX-2 First-Step Velocity Vs Time
IX-3

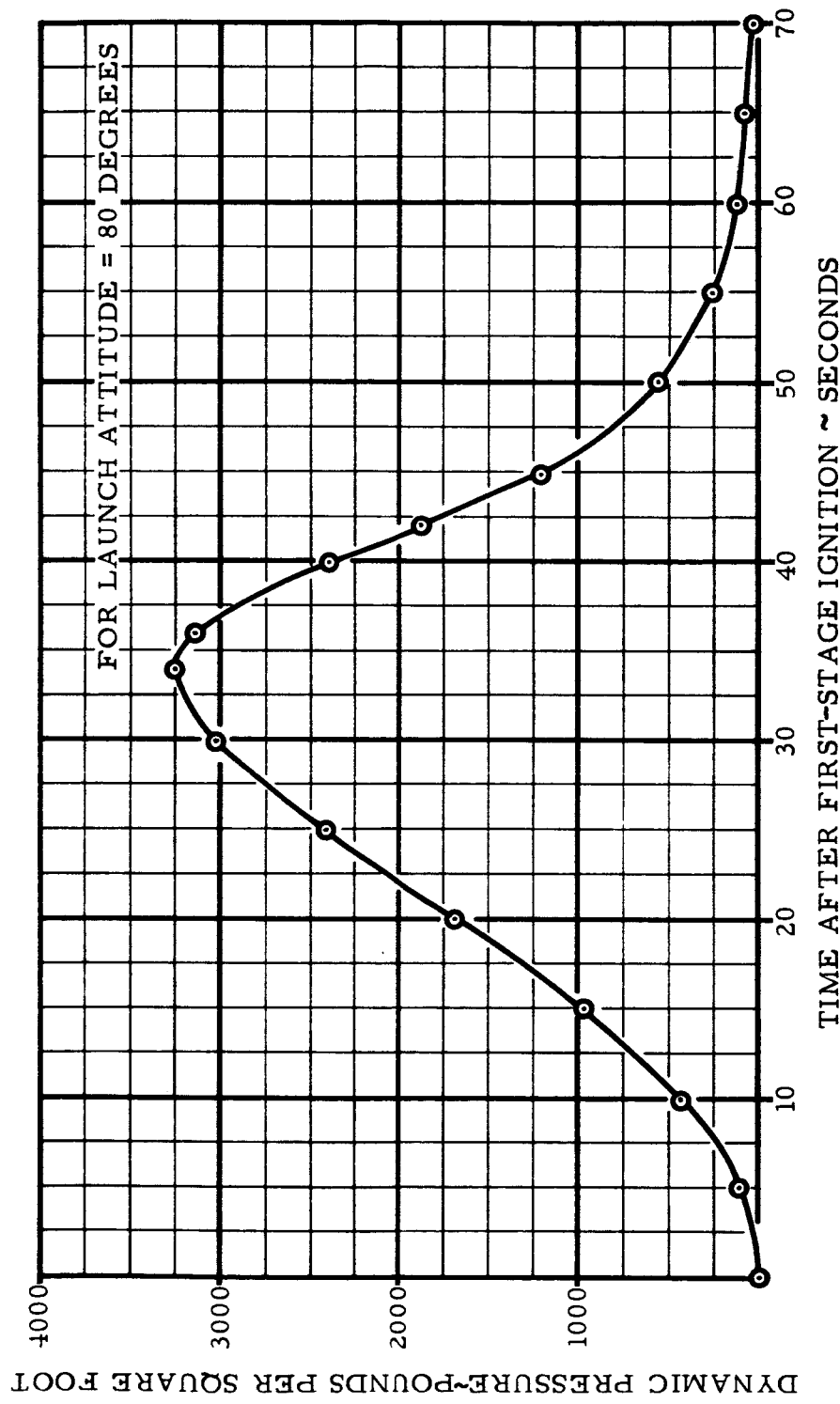


Figure IX-3 First-Step Dynamic Pressure Vs Time
IX-4

R-ED 11122
IX-4

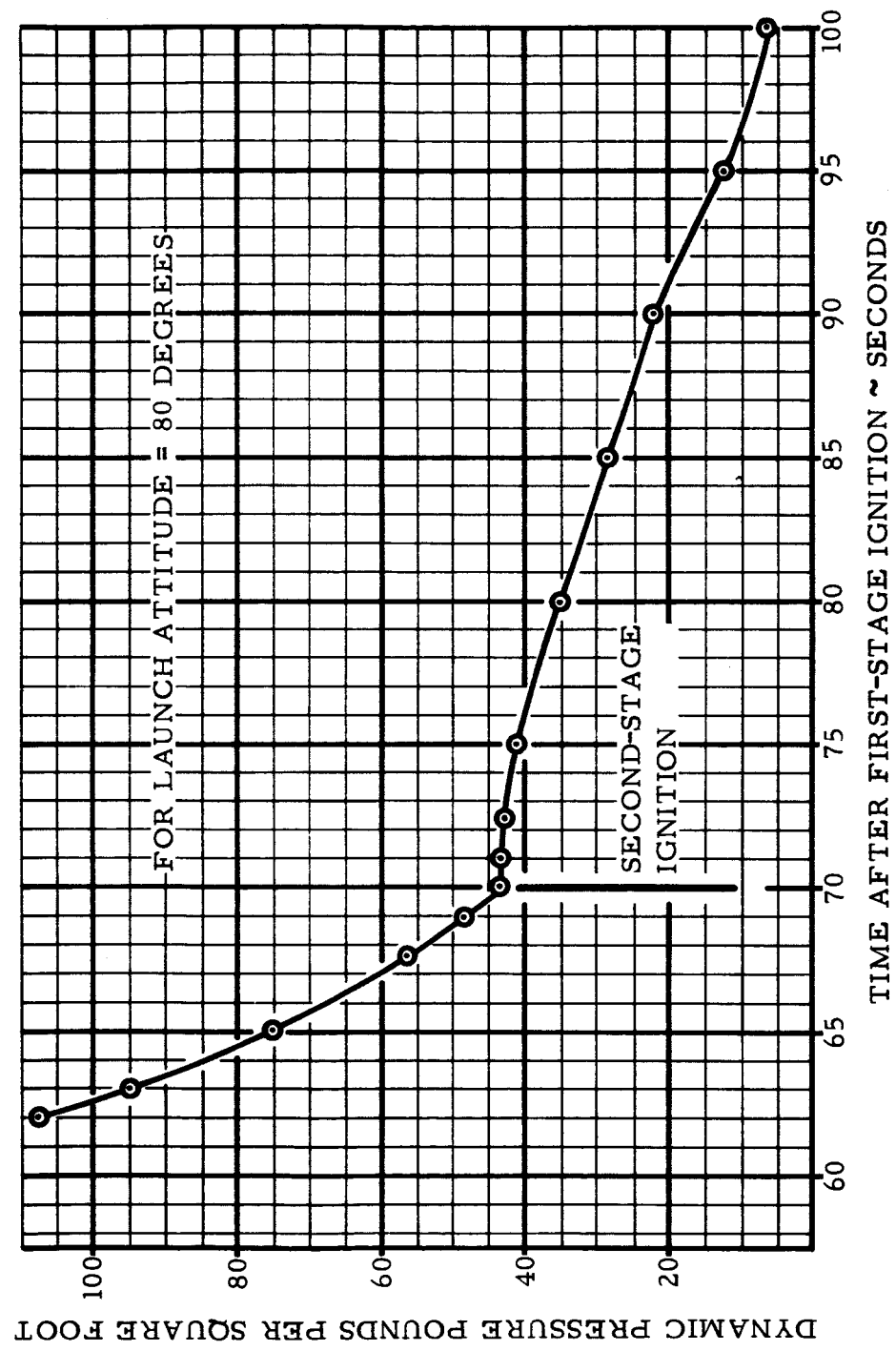


Figure IX-4 First and Second-Step Dynamic Pressure Vs Time

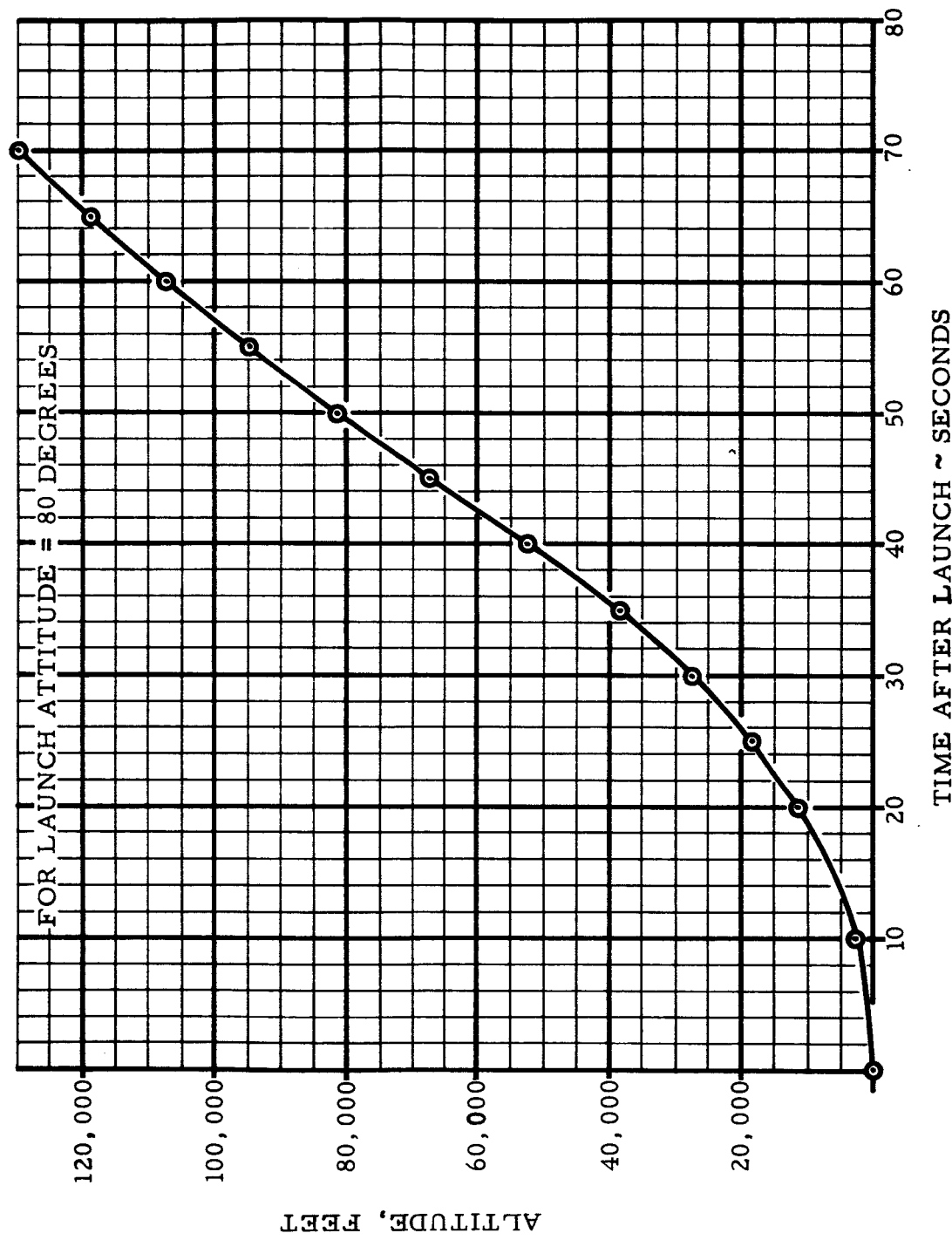
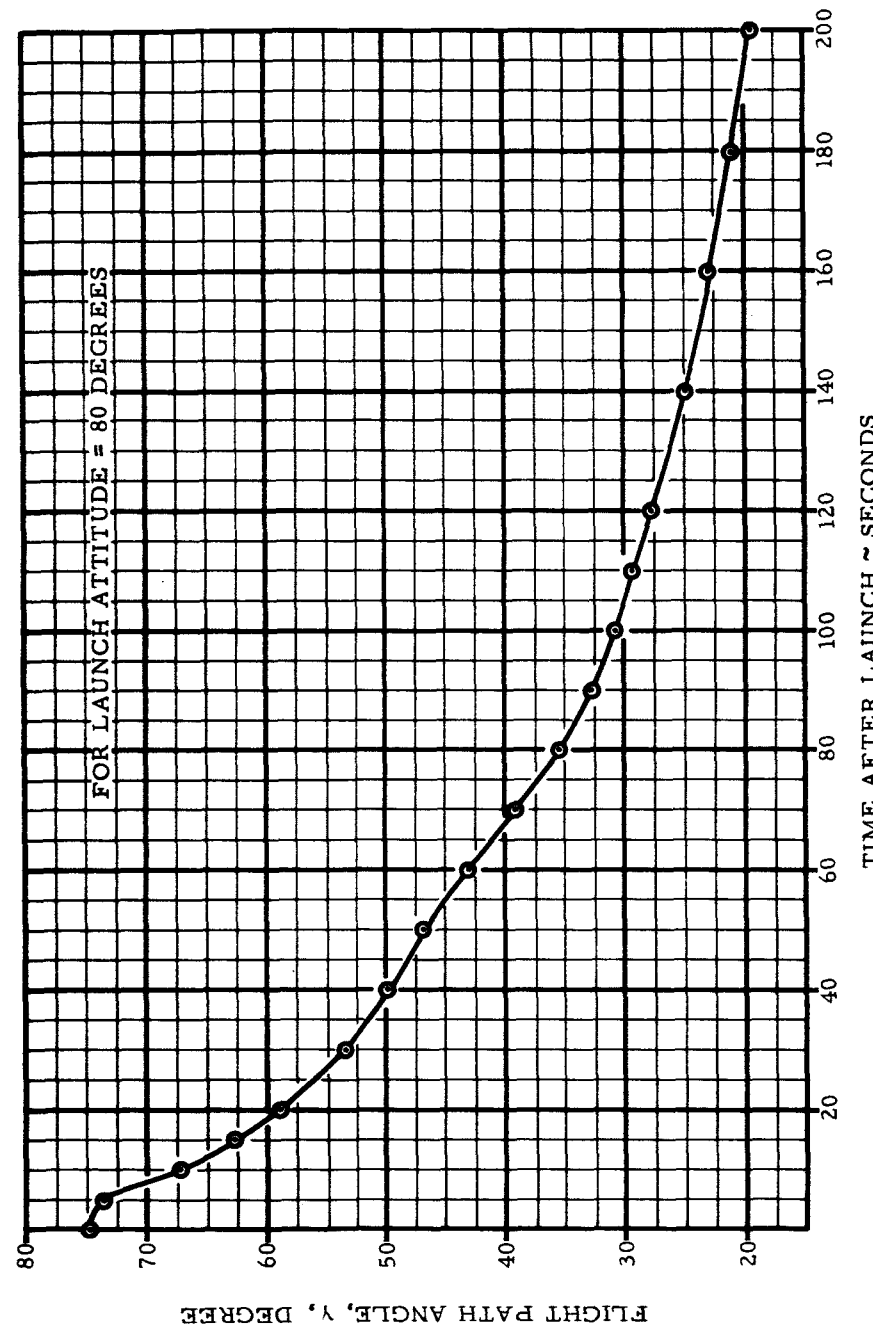


Figure IX-5 First-Step Altitude Vs Time
IX-6

Figure IX-6 First-Step Flight Path Angle Vs Time



R-ED 11122
IX-7

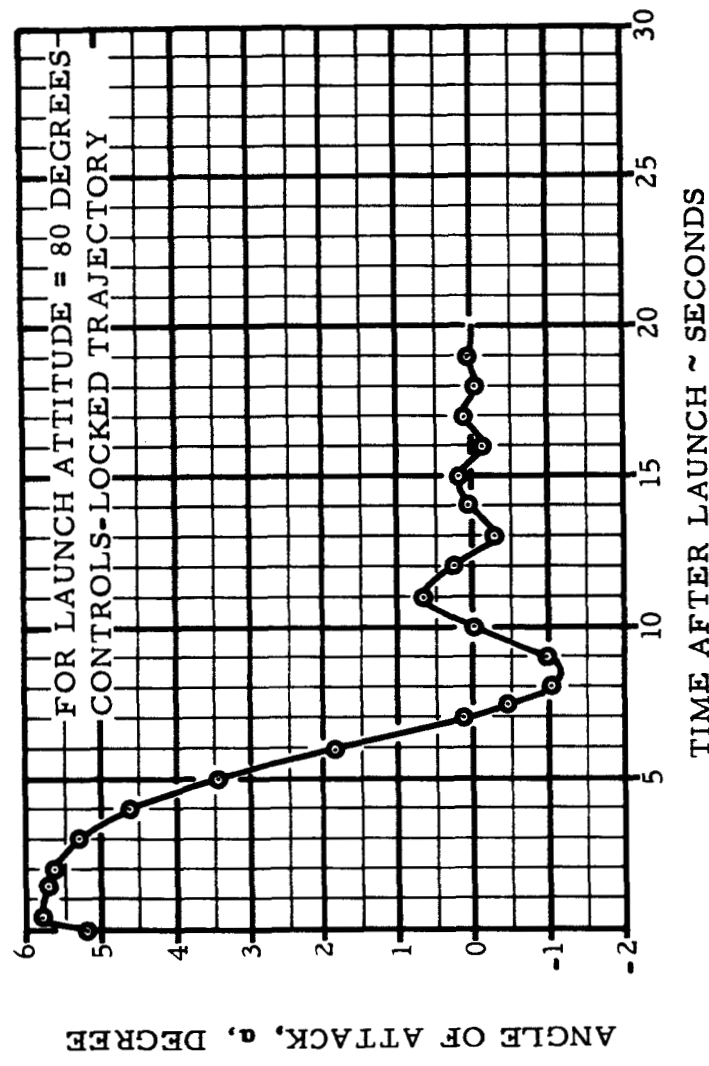
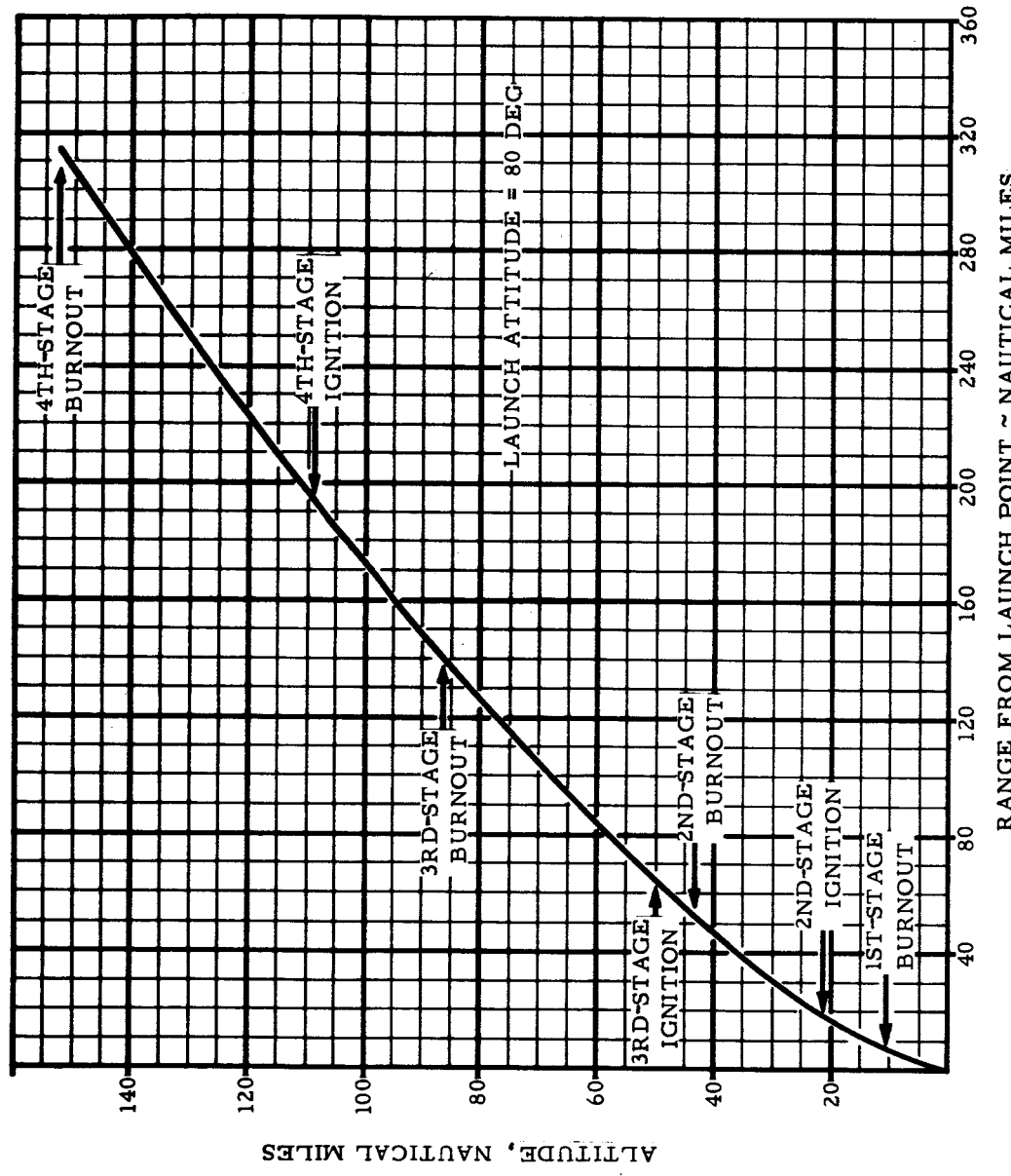


Figure IX-7 First-Step Angle of Attack Vs Time

Figure IX-8 Trajectory Plot Showing Stage Ignition, Burnout, and Coast



R-ED 11122
IX-9

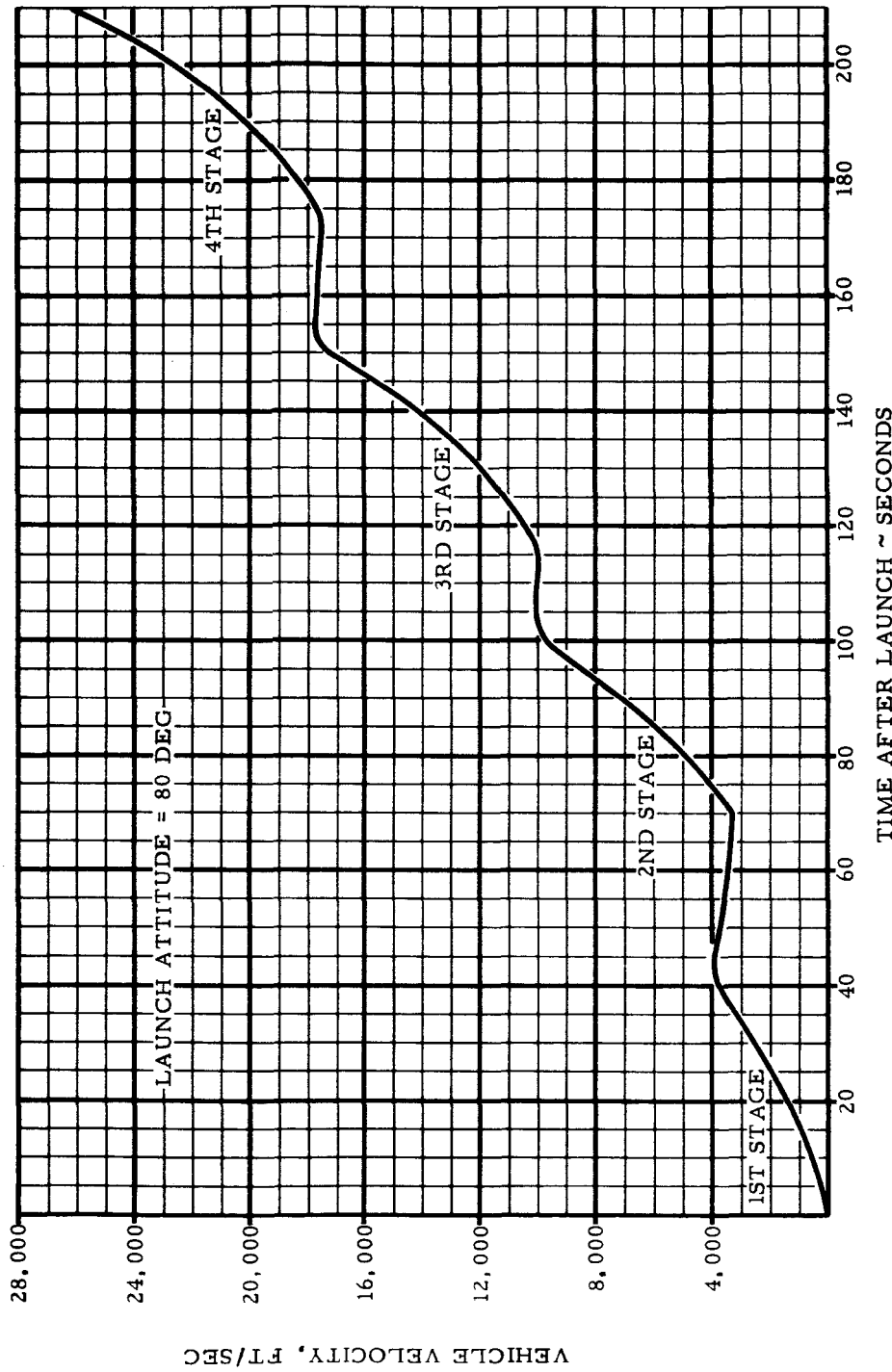


Figure IX-9 Vehicle Velocity Vs Time for the Entire Trajectory

R-ED 11122
IX-10